

**APPLICATION OF NATURE-INSPIRED ALGORITHMS
AND ARTIFICIAL INTELLIGENCE FOR OPTIMAL
EFFICIENCY OF HORIZONTAL AXIS WIND TURBINE**

MD. RASEL SARKAR

**FACULTY OF ENGINEERING
UNIVERSITY OF MALAYA
KUALA LUMPUR**

2019

**APPLICATION OF NATURE-INSPIRED
ALGORITHMS AND ARTIFICIAL INTELLIGENCE
FOR OPTIMAL EFFICIENCY OF HORIZONTAL AXIS
WIND TURBINE**

MD RASEL SARKAR

**DISSERTATION SUBMITTED IN FULLFILLMENT OF
THE REQUIREMENT FOR THE DEGREE OF MASTER
OF ENGINEERING**

**FACULTY OF ENGINEERING
UNIVERSITY OF MALAYA
KUALA LUMPUR**

2019

UNIVERSITY OF MALAYA
ORIGINAL LITERARY WORK DECLARATION

Name of Candidate: Md Rasel Sarkar

Matric No: KGA140057

Name of Degree: Master of Engineering Science (M. Eng. Sc.)

Title of Project Paper/Research Report/Dissertation/Thesis ("this Work"):

Application of Nature-Inspired Algorithms and Artificial Intelligence for
Optimal Efficiency of Horizontal Axis Wind Turbine

Field of Study: Engineering Design

I do solemnly and sincerely declare that:

- (1) I am the sole author/writer of this Work;
- (2) This Work is original;
- (3) Any use of any work in which copyright exists was done by way of fair dealing and for permitted purposes and any excerpt or extract from, or reference to or reproduction of any copyright work has been disclosed expressly and sufficiently and the title of the Work and its authorship have been acknowledged in this Work;
- (4) I do not have any actual knowledge nor do I ought reasonably to know that the making of this work constitutes an infringement of any copyright work;
- (5) I hereby assign all and every right in the copyright to this Work to the University of Malaya ("UM"), who henceforth shall be owner of the copyright in this Work and that any reproduction or use in any form or by any means whatsoever is prohibited without the written consent of UM having been first had and obtained;
- (6) I am fully aware that if in the course of making this Work, I have infringed any copyright whether intentionally or otherwise, I may be subject to legal action or any other action as may be determined by UM.

Candidate's Signature

Date: 17/07/2019

Subscribed and solemnly declared before,

Witness's Signature

Date:

Name:

Designation:

ABSTRACT

Since wind power is directly influenced by wind speed, long-term wind speed forecasting (WSF) plays an important role for wind farm installation. WSF is essential for controlling, energy management and scheduled wind power generation in wind farm. With this aim, a number of forecasting methods have been proposed in different studies till now, among many soft computing-based approaches are the most successful ones as they offer high accuracy as well as application simplicity. Among them, artificial neural networks (ANN) have drawn a major attention and ANNs can make any complex nonlinear input-output relationship by just learning from datasets given to it regardless any discontinuity and without any extra mathematical model.

It is found that past studies used Nonlinear Autoregressive (NAR) and Nonlinear Autoregressive Exogenous (NARX) Neural Network (NN) for wind speed forecasting. There have two most uses activation function namely tansig and logsig. The essence of this study is that it compares the effect of activation functions (tansig and logsig) in the performance of time series forecasting since activation function is the core element of any artificial neural network model.

On the other hand, blade design of the horizontal axis wind turbine (HAWT) is very significant parameter that determines the reliability and efficiency of a wind turbine. It is important to optimize the capture of the energy in the wind that can be correlated to the power coefficient (C_p) of HAWT system. Several researchers have reported different optimization methods for blade parameters such as Blade Element Momentum theory (BEM), Computational Fluid Dynamics (CFD) and Supervisory Control and Data Acquisition (SCADA) system. There is no particular study which focuses on the optimization and prediction of blades parameters using natural inspired algorithms namely Ant Colony Optimization (ACO), Artificial Bee Colony (ABC) and Particle Swarm Optimization (PSO) and Adaptive Neuro-fuzzy Interface System (ANFIS)

respectively for optimal power coefficient (C_p). In this study, the performance of these three algorithms in obtaining the optimal blade design based on the C_p are investigated and compared. In addition, ANFIS approach is implemented to predict the C_p of wind turbine blades for investigation of algorithms performance based on Coefficient Determination (R^2) and Root Mean Square Error (RMSE).

Instead, in order to produce maximum wind energy, controlling of various parts are needed for medium to large scale wind turbines (WT). This study presents robust pitch angle control for the output wind power model in wide range wind speed by proportional-integral-derivative (PID) controller. In addition, ACO algorithm has been used for optimization of PID controller parameters to obtain within rated smooth output power of WT from fluctuating wind speed. The proposed system is simulated under fast wind speed variation and its results are compared with conventional PID controller and Fuzzy-PID to verify its effectiveness. The proposed approach contains several benefits including simple implementation, tolerance of turbine parameter or several nonparametric uncertainties. Robust control of the generator output power with wind-speed variations can also be considered as a big advantage of this strategy.

ABSTRAK

Oleh kerana kuasa angin secara langsung dipengaruhi oleh kelajuan angin, ramalan kelajuan angin jangka panjang (WSF) memainkan peranan penting untuk pemasangan ladang angin. WSF adalah penting untuk mengawal, pengurusan tenaga dan penjanaan kuasa angin yang dijadualkan di ladang angin. Dengan matlamat ini, beberapa kaedah ramalan telah dicadangkan dalam kajian yang berbeza sehingga sekarang, di antara pendekatan berasaskan pengkomputeran yang lembut adalah yang paling berjaya kerana mereka menawarkan ketepatan yang tinggi serta kesederhanaan aplikasi. Antaranya, rangkaian saraf buatan (ANN) telah menarik perhatian utama dan ANN boleh membuat sebarang hubungan input-output bukan linear kompleks dengan hanya belajar dari dataset yang diberikan kepadanya tanpa mengira apa-apa kekurangan dan tanpa sebarang model matematik tambahan.

Difahamkan bahawa kajian lepas menggunakan Rujukan Neural Network (NN) Nonlinear Autoregressive (NAR) dan Nonlinear Autoregressive Exogenous (NARX) untuk ramalan kelajuan angin. Terdapat dua fungsi pengaktifan yang paling banyak digunakan iaitu tansig dan logsig. Inti dari kajian ini adalah membandingkan kesan fungsi pengaktifan (tansig dan logsig) dalam prestasi ramalan siri masa kerana fungsi pengaktifan adalah elemen teras bagi mana-mana model rangkaian neural tiruan.

Sebaliknya, reka bentuk bilah kipas turbin angin paksi mendatar (HAWT) adalah parameter yang sangat penting yang menentukan kebolehpercayaan dan kecekapan turbin angin. Adalah penting untuk mengoptimumkan penangkapan tenaga dalam angin yang boleh dikaitkan dengan pekali kuasa (C_p) sistem HAWT. Beberapa penyelidik telah melaporkan kaedah pengoptimuman yang berbeza untuk parameter bilah kipas seperti teori Blade Element Momentum (BEM), Dinamik Fluida Dinamik (CFD) dan Sistem Kawalan Pengawasan dan Pemerolehan Data (SCADA). Tidak ada kajian khusus yang

menumpukan kepada pengoptimuman dan ramalan parameter bilah yang menggunakan algoritma semulajadi yang diilhamkan iaitu Pengoptimuman Ant Colony (ACO), Buatan Bee Colony (ABC) dan Pengoptimuman Swarm Partikel (PSO) dan Interface Neuro-Fuzzy Interface (ANFIS) untuk pekali kuasa optimum (C_p).

Dalam kajian ini, prestasi ketiga-tiga algoritma dalam mendapatkan reka bentuk bilah kipas optimum berdasarkan C_p diselidiki dan dibandingkan. Di samping itu, pendekatan ANFIS dilaksanakan untuk meramalkan C_p bilah turbin angin untuk penyiataan prestasi algoritma berdasarkan Penentuan Kestabilan (R^2) dan Ralat Kesalahan Maksimum Root (RMSE).

Sebaliknya, untuk menghasilkan tenaga angin maksimum, mengawal pelbagai bahagian diperlukan untuk turbin angin skala sederhana dan besar (WT). Kajian ini membentangkan kawalan sudut pitch yang kuat untuk model kuasa angin keluaran dalam pelbagai kelajuan angin dengan alat pengawal-terikat-derivatif (PID). Di samping itu, algoritma ACO telah digunakan untuk mengoptimumkan parameter pengawal PID untuk memperolehi dalam keluaran nilai lancar WT dari kelajuan angin yang turun naik. Sistem yang dicadangkan disimulasikan dalam variasi laju angin pantas dan keputusannya dibandingkan dengan pengawal PID konvensional dan Fuzzy-PID untuk mengesahkan keberkesanannya. Pendekatan yang dicadangkan ini mengandungi beberapa manfaat termasuk pelaksanaan mudah, toleransi parameter turbin atau beberapa ketidakpastian nonparametrik. Kawalan kuat kuasa output penjana dengan variasi laju angin juga boleh dianggap sebagai kelebihan besar strategi ini.

ACKNOWLEDGEMENTS

First of all, I would like to express my gratitude to the almighty Allah who has created the whole universe.

I would also like to express my gratitude to my father, mother and wife to encourage and give hope throughout my research period in University of Malaya.

Foremost, I would like to thank my supervisors Dr. Sabariah Binti Julai and Associate Prof. Dr. Chong Wen Tong for the continuous support into me, for their patience, motivation, enthusiasm, and immense knowledge. Their guidance has helped me in all the time of this work. I am glad that I have been their student.

I am especially grateful to my colleagues for providing his helpful advice and support which help me a lot to accomplish my research. I am likewise thankful to my friend Md. Mahmudur Rahman, Md Sazzad Hossain, Md. Arafat Hossain, and Tam Jun Hui who have encouraged me continuously. Finally, I would like to acknowledge gratefully the University of Malaya for providing me the financial support from its (ERGS No. ER0142013A, RP015C-13AET) and High Impact Research Grant (HIR-D000006-16001)) to accomplish this work. Thanks also go to all the staffs in University of Malaya who directly or indirectly helped me to carry out this work.

TABLE OF CONTENTS

Abstract	iii
Abstrak	v
Acknowledgements	vii
Table of Contents	viii
List of Figures	xi
List of Tables.....	xiv
List of Symbols and Abbreviations	xv
CHAPTER 1: INTRODUCTION	1
1.1 Background	1
1.2 Problem Statement.....	8
1.3 Research Gap	10
1.4 Objectives	11
1.5 Research Flow	12
1.6 Thesis Outline	12
CHAPTER 2: LITERATURE REVIEW.....	14
2.1 Wind Turbine Modeling	14
2.1.1 Profile of Wind Speed	19
2.2 Wind Turbine Controlling	20
2.2.1 Proportional Integral Derivative Controller	20
2.2.1.1 Actuator Model.....	24
2.3 Nature-Inspired Algorithms	24
2.3.1 Ant Colony Optimization	25
2.3.2 Particle Swarm Optimization	29

2.3.3	Artificial Bee Colony	32
2.4	Artificial Intelligence	37
2.4.1	Adaptive Neuro-Fuzzy Interface System	39
2.4.2	Nonlinear Autoregressive Neural Network	43
2.4.3	Nonlinear Autoregressive Exogenous Neural Network	46
2.4.4	Performance Analysis Criteria	47
2.4.4.1	Root Mean Square Error.....	47
2.4.4.2	Coefficient of Determination.....	48
2.4.4.3	Mean Absolute Error	48
2.4.4.4	Mean Absolute Percentage Error.....	48
CHAPTER 3: METHODOLOGY.....		50
3.1	Methodology Overview	50
3.2	Modeling and Simulation Parameters Setting	51
3.2.1	Optimization and Prediction Process.....	51
3.3	Wind Speed Forecasting	53
3.4	Pitch Angel Control of Wind Turbine	55
CHAPTER 4: RESULTS AND DISCUSSION.....		57
4.1	Optimization of Blade Parameters Using ACO, PSO, and ABC	57
4.1.1	Convergence Graph.....	57
4.1.2	Optimized Parameters of the Wind Turbine Blade	62
4.1.3	Computational Time	64
4.1.4	Prediction of Power Coefficient Using ANFIS	68
4.1.5	Validation of Power Coefficient Optimization and Prediction	74
4.2	Long-Term Wind Speed Forecasting.....	75
4.3	Pitch Angle Controlling	85

CHAPTER 5: CONCLUSIONS AND RECOMMENDATIONS	90
5.1 Conclusions.....	90
5.2 Recommendations.....	94
References	95
List of Publications.....	106

University of Malaya

LIST OF FIGURES

Figure 1-1: Wind power installed capacity in world market (GWEC, 2013).	3
Figure 1-2: Horizontal and vertical axis wind turbine (Chopade & Malashe, 2014).	5
Figure 1-3: Research flow of the present study.	12
Figure 2-1: Power coefficient versus tip-speed ratio for different pitch angle (Duong et al., 2014).	18
Figure 2-2: Wind power curve versus rotor speed for different wind speed.	18
Figure 2-3: Wind power curve versus wind speed (Bianchi et al., 2006).	19
Figure 2-4: Wind speed profile (Tran et al., 2010).	20
Figure 2-5: A typical block diagram of PID controller with feedback loop.	20
Figure 2-6: State space graph of ACO (Julai et al., 2009).	27
Figure 2-7: Flow chart of ACO algorithm.	29
Figure 2-8: Particle swarm optimization algorithm.	30
Figure 2-9: Flow chart of PSO.	32
Figure 2-10: Flow chart of ABC algorithms.	36
Figure 2-11: The structure of ANFIS.	42
Figure 2-12: Nonlinear autoregressive neural network.	44
Figure 2-13: The NARX neural network.	47
Figure 3-1: Block diagram of blades parameters optimization and prediction methodology.	52
Figure 3-2: Average wind speed in three regions.	54
Figure 3-3: LT wind speed forecasting using NARNN and NARXNN.	55
Figure 3-4: Wind turbine MATLAB/Simulink model.	55
Figure 4-1: Convergence curve of different algorithms (ABC, ACO and PSO) with 20 populations.	59

Figure 4-2: Convergence curve of different algorithms (ABC, ACO and PSO) with 50 populations.	60
Figure 4-3: Convergence curve of different algorithms (ABC, ACO and PSO) with 100 populations.	61
Figure 4-4: The computational time in seconds for natural inspired algorithms where number of populations 20 with different iterations.	65
Figure 4-5: The computational time in seconds for natural inspired algorithms where number of populations 50 with different iteration.	66
Figure 4-6: The computational time in seconds for natural inspired algorithms where number of populations 100 with different iteration.	67
Figure 4-7: Power coefficient prediction by ANFIS and optimized (ACO)	70
Figure 4-8: Power coefficient prediction by ANFIS and optimized (PSO)	70
Figure 4-9: Power coefficient prediction by ANFIS and optimized (ABC)	71
Figure 4-10: Predicted (ANFIS) versus optimized (ACO) of power coefficient.	71
Figure 4-11: Predicted (ANFIS) versus optimized (PSO) of power coefficient.	72
Figure 4-12: Predicted (ANFIS) versus optimized (ABC) of power coefficient.	72
Figure 4-13: Prediction of ACO, PSO, and ABC.	73
Figure 4-14: Comparison of wind speed forecasting from proposed activation functions of NARNN methods at Kuala Lumpur, Kuantan and Melaka.	76
Figure 4-15: Comparison of wind speed forecasting from proposed activation functions of NARXNN methods at Kuala Lumpur, Kuantan and Melaka.	77
Figure 4-16: Correlation of coefficient of wind speed forecasting at Kuala Lumpur, Kuantan, and Melaka using both activation functions (tansig and logsig) of NARNN.	78
Figure 4-17: Correlation of coefficient of wind speed forecasting at Kuala Lumpur, Kuantan, and Melaka using both activation functions (tansig and logsig) of NARXNN.	79
Figure 4-18: Success rate of test wind speed data for Kuala Lumpur, Kuantan, and Melaka using both activation functions (tansig and logsig) of NARNN.	80
Figure 4-19: Success rate of test wind speed data for three different areas in Malaysia using both activation functions (tansig and logsig) of NARXNN.	81

Figure 4-20: Convergence curve of ACO. 87

Figure 4-21: Pitch angle of wind turbine blade. 87

Figure 4-22: (a) Optimized wind turbine output power of PID-ACO in comparison with conventional PID and Fuzzy-PID; (b) zoomed figure region. 88

University of Malaya

LIST OF TABLES

Table 3-1: Variable input parameters for optimization process.	52
Table 3-2: Geographical coordinate and altitude of three wind station	54
Table 3-3: Parameters of wind turbine system (Civelek et al., 2016).	56
Table 4-1: The best inputs combination for optimal power coefficient using ABC.	62
Table 4-2: The best inputs combination for optimal power coefficient using ACO.	63
Table 4-3: The best inputs combination for optimal power coefficient using PSO.	63
Table 4-4: Optimal value of input parameters of ACO, PSO and ABC algorithms.	64
Table 4-5: Computation time of different algorithms (ACO, PSO, and ABC) with different population size (20, 50, and 100).	68
Table 4-6: Performance of the established training and testing of ANFIS models for power coefficient based on statistical indicators.	73
Table 4-7: Validation of this present investigation with related literatures.	75
Table 4-8: Model parameters of NARNN and NARXNN with tansig and logsig functions.	82
Table 4-9: Performance indicators of WSF.	83
Table 4-10: Supportive outcome other studies.	85
Table 4-11: K_p , K_i and K_d parameters of conventional PID with Fuzzy logic and ACO.	89
Table 4-12: Root mean square error (RMS) error of proposed PID-ACO to compare with PID and Fuzzy-PID.	89
Table 5-1: Optimization of power coefficient using ACO, PSO, and ABC.	93

LIST OF SYMBOLS AND ABBREVIATIONS

NOMENCLATURE

Symbols

a	: Acceleration (ms^{-2})
v_u	: Upstream Wind Velocity (ms^{-1})
v_d	: Downstream Wind Velocity (ms^{-1})
v_w	: Wind Velocity (ms^{-1})
F	: Force (Nm^{-1})
E	: Kinetic Energy (<i>Joules</i>)
m	: Mass (<i>kg</i>)
W	: Work (<i>Joule</i>)
A	: Swept Area of Blade (m^2)
r	: Radius (m)
D	: Diameter (m)
C_p	: Power Coefficient
ρ	: Air Density (kgm^3)
σ	: Solidity Ratio
λ	: Tip-Speed Ratio
C_L	: Lift Coefficient
C_D	: Drag Coefficient
ε	: Sliding Ratio
B	: Number of Blade
c	: Chord Length (m)
ω_r	: Rotational Speed ($rads^{-1}$)
P_w	: Wind Power

P_m	: Mechanical Power
k	: State Vector
P	: Node
CP	: Cumulative Probability
n	: Number of Parameters
i	: Travel Index
N_{ant}	: Number of Ant
P_{ij}	: Ant Probability
Q	: Quantity of Pheromone
X_i	: Velocity vector
p_i	: pbest
p_g	: gbest
X_j^{min}	: Lower Boundary
X_j^{max}	: Upper Boundary
f_i	: Cost Value
p_i	: Nectar Amount
P_{ip}	: Predicted Values
P_{im}	: Measured Values
n	: Delay of Input
$\epsilon(t)$: Error Tolerance
$y(t)$: Time Series
$x(t)$: External Time Series

Abbreviation

ABC	:	Artificial Bee colony
ACO	:	Ant Colony Optimization
AI	:	Artificial Intelligence
ANFIS	:	Adaptive Neuro-fuzzy Interface System
ANN	:	Artificial Neural Network
FSWT	:	Fixed Wind Speed Turbine
GRNN	:	Generalized Regression Neural Networks
HAWT	:	Horizontal Axis Wind Turbine
LMBP	:	Levenberg-Marquardt Backpropagation
LT	:	Long-Term
MABE	:	Mean Absolute Bias Error
MAPE	:	Mean Absolute Percentage Error
MSE	:	Mean Squared Error
MT	:	Medium-Term
ARIMA	:	Autoregressive Integrated Moving Average
NARNN	:	Nonlinear Autoregressive Neural Network
NARXNN	:	Autoregressive Exogenous Neural Network
EMD-ANN	:	Empirical Mode Decomposition and Artificial Neural Networks
PID	:	Proportional integral derivative controller
PSO	:	Particle Swarm Optimization
R ²	:	Coefficient of Determination
RBFN	:	Radial Basis Function Network
RMSE	:	Root Mean Square Error
ST	:	Short-Term
VST	:	Very Short-Term

VSWT	:	Variable Speed Wind Turbine
RE	:	Renewable Energy
RVFLNN	:	Random vector functional link neural network
RNN	:	Recurrent Neural Network
MMD	:	Malaysian Meteorological Department
KL	:	Kuala Lumpur
SREP	:	Small renewable energy power program
tansig	:	hyperbolic tangent sigmoid
logsig	:	logistic sigmoid
TNB	:	Tenaga Nasional Berhad
v-SVM	:	Variant Support Vector machine
ϵ -SVM	:	Epsilon Support Vector machine

CHAPTER 1: INTRODUCTION

1.1 Background

Over the last few decades, the demands of energy have been gradually increasing, especially for electrical power and environmental issues and this has become a challenging issue for the world. Furthermore, pollution is growing parallel with the energy demand while sources of conventional energy such as fossil fuels are rapidly depleting. In the past decade, researchers have been conducting studies to improve the energy efficiency (Boroumand Jazi et al., 2012). This has led to the discovery of various alternatives for renewable energy that is a combination of natural sources and that used for electrical power generation. These natural sources are in the form of wind, sunlight, geothermal heat, tide, water, and various forms of biomass. These sources are free of cost and reduces the greenhouse effect. Power generation from renewable energy, especially from wind energy is rapidly growing. Wind energy is one of the most widespread sources of an environmental-friendly energy source and has become an important part of the distribution of power in the world. It is produced from wind turbines where kinetic energy is converted into the electrical energy using natural wind. Wind has been used for various purposes such as wind mills for mechanical power and water pump by wind power. It is a substitution of fossil fuels because of no effect upon the environment.

The World's total consumption of electricity is not only rapidly increasing but also the greenhouse gas (GHG) emission increasing by the power generation from fossil fuels. Moreover, the World electricity generation rate (2.7% average annual) is increasing from 2003 to 2015 and it will continue until 2030 (Shafiullah et al., 2013) . However, approximately 40% GHG emissions of World's total emissions are from electricity generation where most of the industries uses fossil fuels namely coal and oil. (Shafiullah, 2016). GHG emission is considered to be hazardous for the human race, and fortunately

fossil fuels can be omitted by renewable energy sources namely wind, solar, biomass, and rain to name a few. Demand of wind energy is increasing to overcome the greenhouse effect and make efficient usage of surrounding energy resources. Because of the free cost nature and availability, the wind energy is considered to be the most efficient and technologically advanced renewable energy sources accessible (Shafiullah et al., 2013)

Gradually, the windmill has been developed. At this present moment, the windmill has reached the modern era. Wind turbines are manufactured by new technology in a wide range. Rapid development of wind turbine is with both, horizontal and vertical axis types. There are different sizes of wind turbines available nowadays. A small sized wind turbine can be used for battery charging, caravans, board and power traffic warning, while medium-sized wind turbines are used for domestic power supply. These days, the wind farm has become an important source of renewable energy as well as electric power. Recently, many countries have come to depend on wind power. There are also several countries that are concerned about the changing of the global climate as well as wind energy. Installation of wind farms is increasing and the contribution of wind turbines is remarkable. Presently, wind energy is the faster growing source among the other alternatives sources of renewable energy (Ponta et al., 2007).

A survey in 2010 has stated that wind power has produced 197 GW which is about 2.5% of the world's electricity. In the same year, China has surpassed the wind capacity of the United States of America (USA) and China has become one of the world's big players in the field. The Denmark Government has produced a remarkable 28.1% of total power from wind farms (Jureczko et al., 2005). In the world, approximately 80% of wind energy is produced from among five countries which are Germany, USA, Denmark, India and Spain (Ackermann & Söder, 2000). The United Nations (UN) hosted Sustainable Energy Report in 2014 stated that these five countries have produced more than about

8 % of the total world power from 2013. The wind capacity has reached a higher level of more than 318 GW at the end of 2013. This is the indication that this type of energy is increasing every year. About 103 countries are producing wind power that helps to improve the current commercial growth rating. The evaluation from The World Energy Association stated that the wind power will be increased up to 700GW by the year 2020 (Huang & McElroy, 2015). Wind energy is a rapidly growing renewable source and the capacity of wind energy is dramatically increasing at present. Figure 1-1 shows the capacity of the installed wind power from 2013 to 2018 (GWEC, 2013).

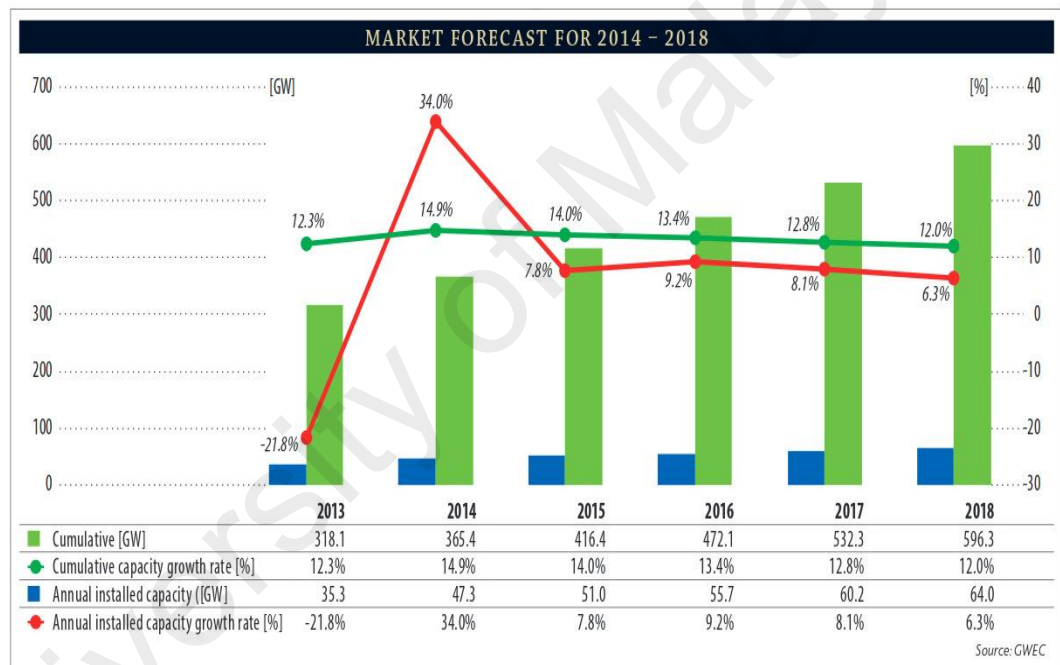


Figure 1-1: Wind power installed capacity in world market (GWEC, 2013).

In the past few years, the Malaysian Government has endeavoured developing renewable energy. The Government concern is to utilize the onshore wind energy at potential area in Malaysia. In Malaysia, wind energy was introduced in the early 1990s at Mersing, Kuala Terengganu, Petaling Jaya, Melaka and Cameron Highland (Sopian et al., 1995). From the investigation, it was observed that Mersing and Kuala Terengganu are possible areas in Malaysia for wind power production. In November 1995, the hybrid of 150kW system was established at Terumbu Layang-Layang (Swallow Reef) by the

Tenaga Nasional Berhad (TNB) (Tenaga Nasional Berhad, 2014). Numerous studies on the wind power and pump water power generation have been done successfully by The Universiti of Kebangsaan Malaysia (UKM) in 2005 (W. T. Chong et al., 2013; Oh et al., 2010; Shafie et al., 2011).

In the world, most of the wind turbines have been inspired by Europe and United State of America (USA). High wind speed ($V_w > 6\text{ m/s}$) is required for most of the wind turbine modelling, simulation and manufacturing for prevail regions. In Malaysia, the wind speed is very low, i.e., in the range of 2.0 m/s to 12 m/s and it is not enough to produce more power. Due to this reason, a rotor must be designed for to produce wind with the wind speed of less than 4 m/s and lower rotational speed of blades (W.T Chong, 2006)

Wind turbine is a complex system consists of various components such as blades, generator, rotor transmission line, tower and electro-mechanical subsystems. The blade of rotor is the most important component in the wind turbine system that will convert wind energy to mechanical power. It has classified into various types of systems such as constant and variable speed system, power controlling system, and off grid or on grid system (Marques et al., 2003). Based on the rotation of axis, there are two types of wind turbines, namely Vertical Axis Wind Turbine (VAWT) and Horizontal Axis Wind Turbine (HAWT). HAWT is the most popular choice for large amounts of power production (Eriksson et al., 2008). The blades for HAWT rotate in a horizontal axis. It was the first innovation of wind industry. HAWT produces more electricity with respect to the applied amount of wind. It is capable of self-starting and does not need the external mechanism. The comparison between HAWT and VAWT has described by Thomas and Urquhart (1996). Younsi et al. (2001) developed the behavior of the dynamic wind blades of a HAWT with various model analysis. The performances of wind turbines are depending on two factors i.e., aerodynamic design and wind speed. Wind speed is

dependent on the location of the wind turbine installation areas and the surrounding weather. The blades of VAWT is rotate with perpendicular to the ground. At first, VAWT is used in residential areas as a small wind energy production. Nowadays, the application of VAWT is growing due to its low cost and easy mechanism. The electricity produced from the VAWT comes from the wind when it is directed to turbine blades in 360 degrees, whereas for some wind turbines power is produced when the blowing of the wind is from top to the bottom. In this system, the external sources are needed for rotation of turbine blades. The efficiency of VAWT is not satisfactory in comparison to HAWT (Schubel & Crossley, 2012). Both HAWT and VAWT have shown in Figure 1-2.

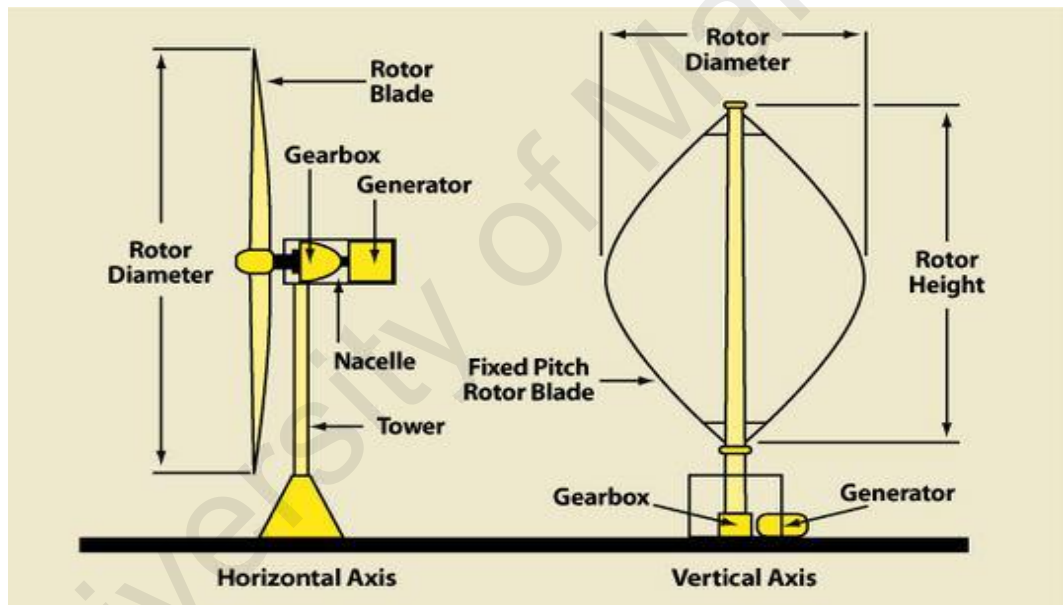


Figure 1-2: Horizontal and vertical axis wind turbine (Chopade & Malashe, 2014).

The power coefficient of the wind blades, which can be defined as the capture capability of efficiency and it is the most basic index of wind energy (Lanzafame & Messina, 2010). Design parameters selections are critical for optimization of wind turbine performance. There are various parameters that influence the energy production of wind turbine, such as, rotor rotational velocity, wind speed and blade pitch angle (Petković et al., 2014; Rajakumar & Ravindran, 2012). For power coefficient optimization of wind turbine blades, the influence of lift to drag ratio, blade radius, tip-speed ratio, solidity ratio

and chord length of blade have been widely investigated. The nature-inspired algorithms such as ant colony optimization (ACO), particle swarm optimization (PSO), and artificial bee colony (ABC) have been used in various wind turbine applications. In other aspect, the prediction of power coefficient of the wind turbine is obtained by ANFIS.

The site selection for wind turbine installation is very crucial to obtain maximum wind energy production, and the maximum wind power generation can be achieved when the available wind speed is higher than the wind turbine's cut-in wind speed. In addition, the relation between wind speed and wind power is cubic proportional; therefore, slight change of wind speed will give much higher wind power (cubic). Consequently, progress in wind speed prediction for wind energy conversion system will help lessen the risks to install wind turbines in low-effective places.

Although, the wind speed is the most challenging factor for wind power generation, the variation of wind speed found in nature is chaotic. Sometimes, wind turbine can be affected by high cut-out wind speed, i.e., the production of wind power generation is stopped when wind speed is very high. The WSF plays a very important role for optimum planning and wind energy applications. Time series forecasting of the wind speed is defined by wind data over time. One-month-ahead wind speed forecasting data can be developed by historical weather or wind data (Tasnim et al., 2014). Basically, forecasting of wind speed can be divided into four-time categories: very short-term (VST), short-term (ST), medium-term (MT), and long-term (LT) forecasting. Where, VST refers to less than 30-minutes-ahead of WSF. In real time, wind turbine can be controlled by ST wind speed forecasting; moreover, less than 72 hours to 1 hour resides in ST forecasting (Chang et al., 2017), and planning of load dispatch can be employed by ST forecasting. On the other hand, 6 hours to 1-day-ahead resides in MT wind speed forecasting, which helps to manage power system and secure operation of wind turbines. Lastly, LT forecasting is useful to optimize the operation cost and schedule maintenance. It can also be applied to

save cost when operators need to schedule wind project maintenance and construction. Wind projects often require the turbines to be taken down during the commissioning of new turbines, and this can take from hours to weeks depending on the weather. LT forecasting of wind speed can minimize the scheduling errors and in turn increase the reliability of the electric power grid and reduce the power market ancillary service costs (Azad et al., 2014; Z. Guo et al., 2012; Zhao et al., 2016). The forecasting process of wind speed is very difficult as wind speeds are chaotic depending on the earth's rotation and properties of topographical condition such as temperature and pressure. Methodologically, wind speed prediction can be classified into four groups, i.e., physical, statistical, artificial intelligence (AI) and hybrid methods (Azad et al., 2014; Zheng et al., 2011). In this study, AI namely NAR and NARX neural network has been chosen for wind speed forecasting due to higher forecasting accuracy and no mathematical model required.

A variable speed wind turbine (VSWT) can be reached at peak value of efficiency over any kind of wind speed. Whereas, a fixed wind speed turbine (FSWT) is not able to reach maximum energy efficiency. To compare between VSWT and FSWT, the VSWT is most suitable for maximum efficiency pick-up. The maximum efficiency of VSWT can be reached by wind speed control between cut-in speed to rated wind speed (Assareh & Biglari, 2015; Chen & Shiah, 2016). By controlling wind speed, the generator output is kept to rated power. If wind speed reaches above the rated wind speed, the pitch angle of WT blade should be controlled to keep output power within the rated power (Leithead & Connor, 2000). The change of blade angle position with longitudinal axis is kept by pitch angle controlling. For wind power limit, pitch angle controlling methods is recommended to kept the interior rated speed. The PID controller is very common method to control pitch angle.

Pitch angle control systems have normally been employed in medium to large wind turbines for keeping the captured wind power close to the rated value above the rated wind speed. It can also bring the advantages of power quality as well as improved control flexibility. The structural wind loads can be alleviated by such systems that can defend the wind turbine from fatigue damage. This damage can happen for the strong wind gusts. An immediate influence around the regulation of wind power can be observed by these systems which also have the great importance for the variable pitch wind turbine. However, Modern turbine can perform consistently and it can assist to meet the over increasing requirements for performance of reliability oriented advanced pitch control systems (Dueñas-Osorio & Basu, 2008; Yin et al., 2015).

1.2 Problem Statement

Artificial intelligence and nature-inspired algorithms had become more popular throughout the years. There exists a need to look into different ways to improve the performance of the HAWT using soft computing techniques and making it easier to be implemented in more areas especially with optimization, prediction, forecasting and controlling of WT.

Wind speed plays an important role for wind farm installation since wind power is directly influenced by wind speed. Before wind farm installation, it should be concerned of wind speed in that area because some place is low wind speed and some place are high wind speed. By the wind speed forecasting, it can be identified wind condition. NARNN and NARXNN both AI which can be effective forecasting of wind turbine in Malaysia areas.

Wind turbine blades parameters are very crucial that determines the reliability and efficiency of a wind turbine. According to Betz's law, wind turbine is not able to capture

kinetic energy more than 0.59 (power coefficient) from wind speed. Researchers are trying to reach near Betz's coefficient. In addition, the power coefficient of modern HAWT is reached at 0.51. Therefore, there is a good possibility to reach maximum power coefficient through to optimize blade parameters of wind turbine using algorithms and prediction employed through ANFIS with best input parameters combination and AI.

The fluctuating wind speed is the reason to damage of large wind turbine as well as lower output power. Pitch angle is increased by fluctuating wind speed which is above of rated wind speed of WT. By the pitch angle controlling, it is good possibility to overcome the wind turbine damage as well as control the output power within rated power of wind turbine. PID controller is far common and flexible method to control pitch angle. The optimization of PID control parameters using ACO are considered more effective controller over conventional PID controller for pitch angle of wind turbine.

This research has outline to overcome the following objectives to improve the existing design and to find optimal performance of by AI and nature-inspired algorithms which yields higher performance.

1.3 Research Gap

Research Gap	Proposed Study
<p>The wind speed forecasting has been investigated using different neural networks namely NAR, NARX, support vector machine, conventional neural network. There is no any particular study which focuses on to find out more efficient activation function neural network for forecasting</p>	<p>The essence of this study is that it compares the effect of activation functions (namely tansig and logsig) in the performance of time series forecasting since activation function is the core element of any artificial neural network model.</p>
<p>Blades parameters optimization have been investigated with different theories and algorithms used such as Blade element theory, Computational fluid dynamics (CFD), Genetic algorithms (GA) and support vector machines (SVM) for optimal efficient of horizontal axis wind turbine.</p>	<p>The effectiveness of the proposed algorithm in wind turbine blades optimization design identification is investigated as compared to, such as Artificial Bee Colony (ABC), Ant Colony Optimization (ACO) and Particle Swarm Optimization (PSO) using ANFIS for optimal efficiency of wind turbine</p>
<p>The PID controller gains are generally tuned with trial and error methods. Also, for tuning process, step input excitation is used for tracking the error between the reference and actual input. Therefore, tuning process using ACO for pitch angle control has not been investigated</p>	<p>The optimum controller gains are achieved using PID-ACO process which is an automatic process to find desired control pitch angle. Sine input is used to find the controller gains to ensure optimal control pitch angle to ensure maximum fluctuating reduction under chaotic. The proposed controller (PID-ACO) provides optimal control parameters can overcome the fluctuating wind turbine power</p>

1.4 Objectives

By focusing on the limitations found in previous researches, the objectives of this study have been made as follow:

1. To propose an effective activation functions of NAR and NARX Neural Network for wind speed forecasting in Malaysia
2. To optimize wind turbine blade (Airfoil S822) parameters using ACO, PSO and ABC algorithms and to find out effectiveness of proposed algorithms using ANFIS.
3. To optimize of PID controller parameters using ACO for pitch angle controlling of wind turbine for stable wind power.

University of Malaya

1.5 Research Flow

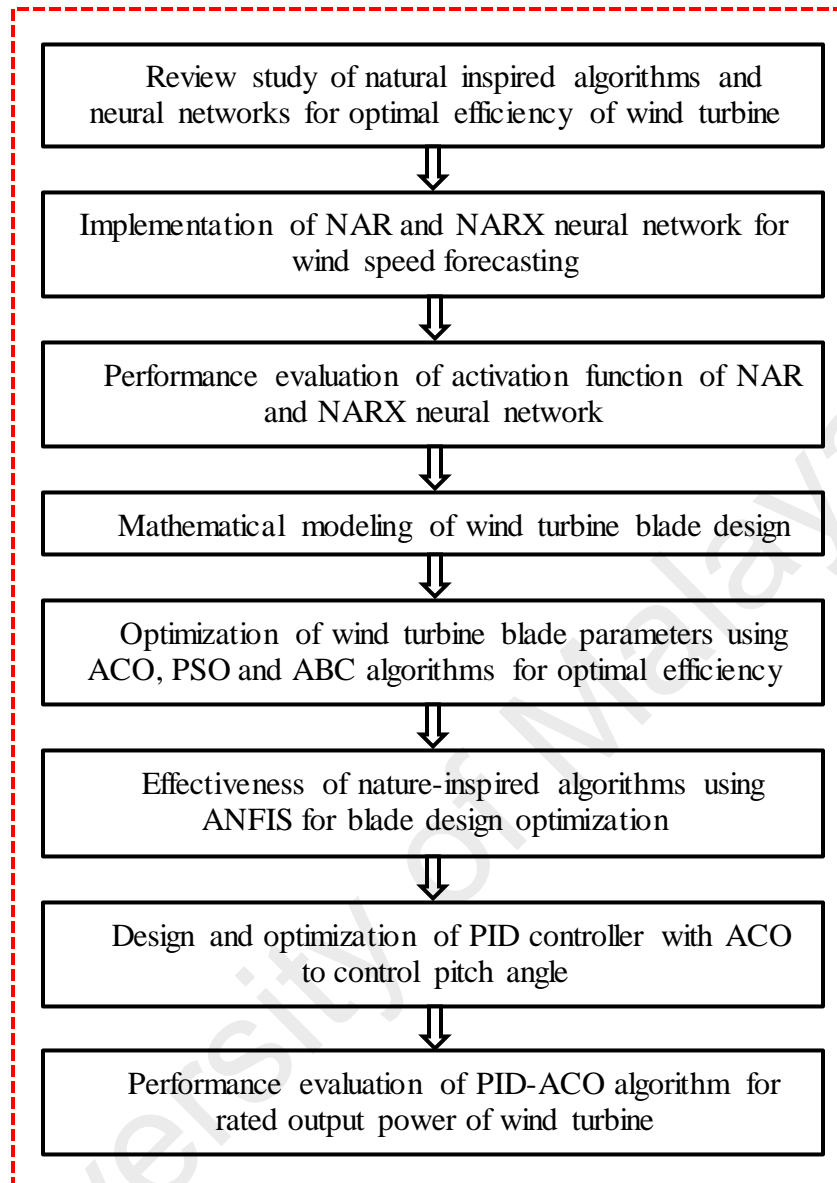


Figure 1-3: Research flow of the present study.

1.6 Thesis Outline

This thesis consists of five chapters. Brief descriptions of each chapter are presented as follows:

CHAPTER 1: This is the introductory chapter that represents an overall view of the importance of optimal efficiency of wind turbine using AI and nature-inspired algorithms

in respect of the present and future energy crisis. Finally, objectives and scope of this work of the study are illustrated.

CHAPTER 2: This is the chapter where required information related to the study has been extensively reviewed. Information regarding availability of the effectiveness of NAR and NARX neural networks for wind speed forecasting, blade parameters optimization and prediction, and pitch angle controlling of wind turbine blades influence of PID controller which parameters are optimized ACO algorithm yield, forecasting, optimization, prediction and controlling using neural networks and algorithms from related literature results of others researchers has been expiated. Lastly, the research gap has been found out according to previous study.

CHAPTER 3: Overall procedure to conduct the forecasting, optimization, prediction, controlling and forecasting have been explained in this chapter parameters selection and simulation procedure and method have been discussed briefly. A brief discussion about the MATLAB software that is used for the simulation has been given.

CHAPTER 4: This is the chapter for presenting for the simulation result and discussion. Firstly, the power coefficient optimization and prediction are showed by the natural inspired algorithms and ANFIS respectively. Secondly, wind speed forecasting by NAR and NARX neural network, the results found from the simulation are discussed. Thirdly, pitch angle control is showed by the optimization of PID controller parameters using ACO algorithm.

CHAPTER 5: In this chapter, the essences of the results are presented and also some recommendations for possible future studies have been described briefly.

CHAPTER 2: LITERATURE REVIEW

2.1 Wind Turbine Modeling

Renewable energies such as wind, bioenergy and solar energy conversion systems have determined during the last decade with the intention of the environmental concerns. The most promising sources of renewable energy is wind energy due to low cost in comparison to other energies such as solar energy, biomass energy etc. (Eltamaly & Farh, 2013; Oghafy & Nikkhajoei, 2008). Wind energy utilization is an improvisation on technology of wind turbine. It is estimated that, within the next two to three decades, wind energy technology will be durable for power generation. In the last few years, wind energy has been amplified around 30–40 times. It is recognized all over the world as an inexpensive with environmentally friendly system which may cover the shortage of energy. The number of wind power plants is increasing every year. The United States of America (USA) takes a target at least 20% power produce within 2030 from total power. Wind energy is the most accessible sources in renewable energy sources.

Wind power conversion system consists of the wind turbine rotor mounted to a nacelle, generator, tower and control system. The system of a wind turbine is complex. The wind energy conversation system converts kinetic energy to electric or mechanical energy. The behavior and performance of wind turbine operation and control need to be understood before the development of mathematical modelling. Firstly, under constant acceleration a , the kinetic energy E of the wind having a mass m , the velocity v is equal to the work done W in displacing that wind from rest to a distance, s under a force F (Ochieng et al., 2010), So

$$E = W = Fs \quad (2.1)$$

Law of motion according to the Newton's

$$F = ma \quad (2.2)$$

The kinetic energy E

$$E = mas \quad (2.3)$$

$$a = \frac{v^2 - u^2}{2s} \quad (2.4)$$

where, the initial objective velocity is $u = 0$ so

$$a = \frac{v^2}{2s} \quad (2.5)$$

From the Eq. (2.2)

$$E = \frac{1}{2}mv^2 \quad (2.6)$$

The wind power is obtained by the rate of change of kinetic energy of the wind.

$$P_w = \frac{dE}{dt} = \frac{1}{2} \frac{dm}{dt} v_w^2 \quad (2.7)$$

where $\frac{dm}{dt} = \frac{1}{2}\rho A v_w^3$ is obtained from the mass flow rate where ρ is the wind density of air, A is the area of blades through wind passing. Eq. (2.6) becomes

$$P_w = \frac{1}{2}\rho A v_w^3 \quad (2.8)$$

The mechanical power equation of HAWT can be written as

$$P_{mechanical} = 0.5 \rho C_p A_s V_w^3 \quad (2.9)$$

where air density is expressed by ρ in (kg/m^3), wind velocity in $V_w(ms^{-1})$ and C_p is known as the rotor efficiency or power coefficient (C_p). Wind energy conversion is directly depending on the C_p of the aerodynamic system which is converted from wind energy to electrical power. The progress of present commercial wind power generator has been continuously moving forward to the latest megawatt (MW) turbine. For HAWT, parameters selection is challenging. The production of wind turbine power is influenced by various fixed parameters, such as, wind velocity, chord length of blades, rotor diameter and lift to drag ratio etc. (Lanzafame & Messina, 2010). There are two goals of the design

of a HAWT, i.e., optimizing and estimating the power coefficient (Arifujjaman, 2010). Recently, attentions have been placed on rotor of wind turbine design for maximum aerodynamic performance (Jureczko et al., 2005; Khalfallah & Koliub, 2007; Selig & Coverstone-Carroll, 1996). The mechanical power equation of HAWT can be written as

$$C_{opt.}\left(\lambda, \frac{C_L}{C_D}, \sigma, r, c\right) = \left(\frac{16}{27}\right) \lambda \left[\lambda + \frac{1.32 + \left(\frac{\lambda - 8}{20}\right)^2}{\left(\frac{\sigma A_s}{c}\right)^{\frac{2}{3}}} \right]^{-1} - \frac{(0.57)\lambda^2}{\frac{C_L}{C_D} \left(\lambda + \frac{1}{\frac{2\sigma(2\pi R)}{c}} \right)} \quad (2.10)$$

where the swept area of turbine rotor is A_s in (m^2) and λ is the tip-speed ratio. R , C_D and C_L are the blades radius, drag, and lift coefficient blade airfoil, respectively. Wind turbine coefficient strongly depends on the rotor blade performance and airfoil section. The blade is very important part of the HAWT. For HAWT designing, blade design is very important part of HAWT. Basically, there are two types design of blades such as, aerodynamic and structural design. Both designs are important for HAWT performance (Zhu et al., 2016). The aerodynamic efficiency, annual energy production (AEP), and power performance are those aspects accounted in aerodynamic design. On the other hand, the structural design is concerned by material, mass, fatigue load, stability etc. (Kim et al., 2013). The theoretical maximum power coefficient is $C_{max} = 0.59$. The power coefficient of modern wind turbine reaches up to 0.51 which is close to Betz limit (Manwell et al., 2010). The power coefficient directly depends on lift to drag ratio of HAWT blades. The power coefficient is varying with tip speed ratio as well lift to drag ratio (Burton et al., 2001). For each aerodynamic airfoil, C_L and C_D depends on attack angle and Reynolds number. Solidity ratio of blades can be defined as (C.-J. Bai et al., 2016; Rajakumar & Ravindran, 2012)

$$\sigma = \text{solidity ratio} = \frac{\text{Number of blades}(B) \times \text{area of each blades}(A)}{A_s} \quad (2.11)$$

Lift and drag coefficients are dimensionless numbers that are used for measurement of aerodynamic lift and drag forces. It can be defined as,

$$C_L = \frac{L}{.5\rho V_w^2 A_s} \quad (2.12)$$

$$C_D = \frac{D}{.5\rho V_w^2 A_s} \quad (2.13)$$

Therefore, the lift to drag ration can be defined as. The lift to drag ratio is also called sliding ratio.

$$\varepsilon = \frac{C_L}{C_D} \quad (2.14)$$

where ω_m is the rotational speed of rotor in (rad/s) and V_w (m/s) is the wind velocity. The radius of blade is R . For the optimization and prediction, range the tip-speed ratio is 3 to 10. The power coefficient of WT can be written as following Eq. (2.15)

$$C_p(\lambda, \beta) = c_1 \left(\frac{c_2}{\lambda_i} - c_3 \beta - c_4 \right) e^{-c_5/\lambda_i} + c_6 \lambda \quad (2.15)$$

where, $c_1 = 0.5176$, $c_2 = 116$, $c_3 = 0.4$, $c_4 = 5$, $c_5 = 21$ and $c_6 = 0.006$

$$\frac{1}{\lambda_i} = \frac{1}{\lambda + 0.08\beta} - \frac{0.035}{\beta^3}$$

Wind energy conversion is directly depending on the C_p of aerodynamic system which is converted from mechanical energy into electrical energy. The nonlinear parameters are λ, β defined by tip-speed ratio and pitch angle respectively. In addition, the tip-speed ration has expressed by (M. Singh & Chandra, 2011)

$$\lambda = \frac{\omega_r r}{V_w} \quad (2.16)$$

where r is the rotor radius, ω_r is the angular velocity of wind turbine rotor. A nonlinear function power coefficient and tip-speed ration have been changed by angular speed of rotor of turbine and wind speed. From the Eq. (2.15), the power coefficient is changed by the pitch angle of WT blade as shown in Figure 2-1.

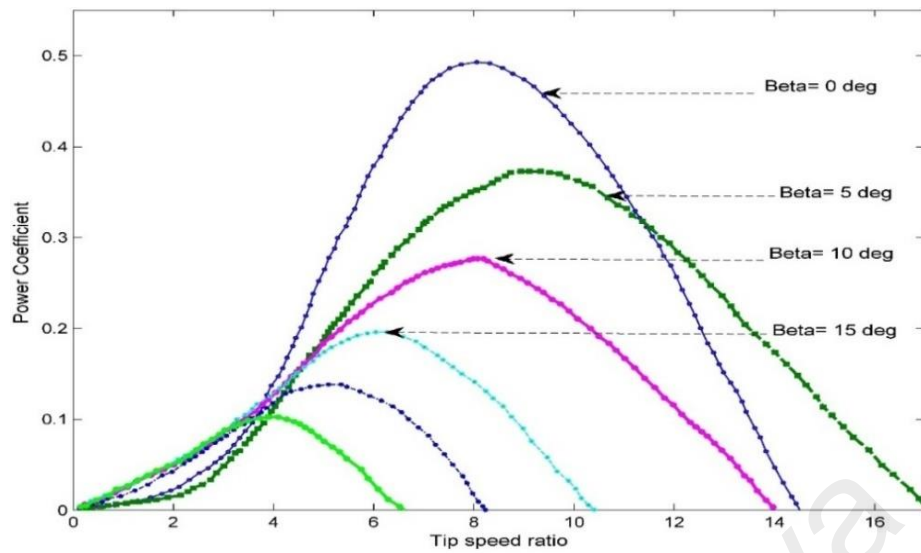


Figure 2-1: Power coefficient versus tip-speed ratio for different pitch angle (Duong et al., 2014).

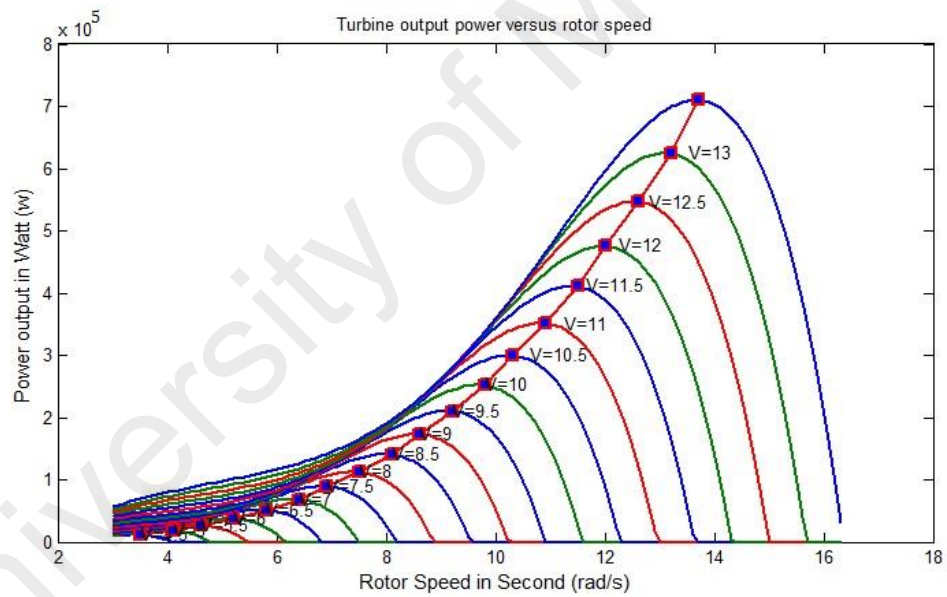


Figure 2-2: Wind power curve versus rotor speed for different wind speed.

In general, the wind turbine generator power has been changed by wind speed and rotor speed that shown in Figure 2-2. The WT operating region has been divided into four areas which are shown in Figure 2-3. In the first region, the wind speed reaches 0 to cut-in where output power is zero because the WT does not execute the operation. The second region is indicated that the wind speed is cut-in to rated speed. The third region shows the wind speed is between rated to cut-out speed. For the WT protection, the fourth region is

beyond the cut-in speed, when output wind power reaches its rated power. At this moment, if wind speed increases, output wind power will cross the rated WT power. For the steady WT output power within rated power, pitch angle controlling is needed for output power maintained within rated power.

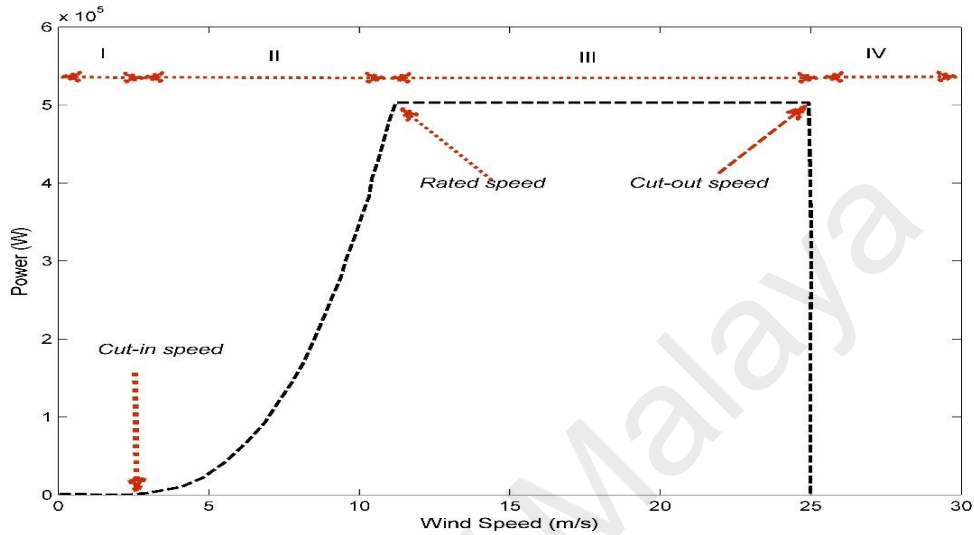


Figure 2-3: Wind power curve versus wind speed (Bianchi et al., 2006).

2.1.1 Profile of Wind Speed

The WT power is influenced by chaotic and fluctuating wind speed. It is changing continuously. The magnitude of wind speed is randomly over any interval. For this study, the simulated wind speed is defined by the following equation (Tran et al., 2010).

$$V_w = x + \sin(0.1047t) + 5\sin(0.02665t) + \sin(1.293t) + 1\sin(3.664t) \quad (2.17)$$

where, x is the user define number based on WT mean wind speed. Based on Eq. (2.17) the simulated wind gusts, the magnitude and frequency of the sinusoidal fluctuations which are increased, are shown in Figure 2-4.

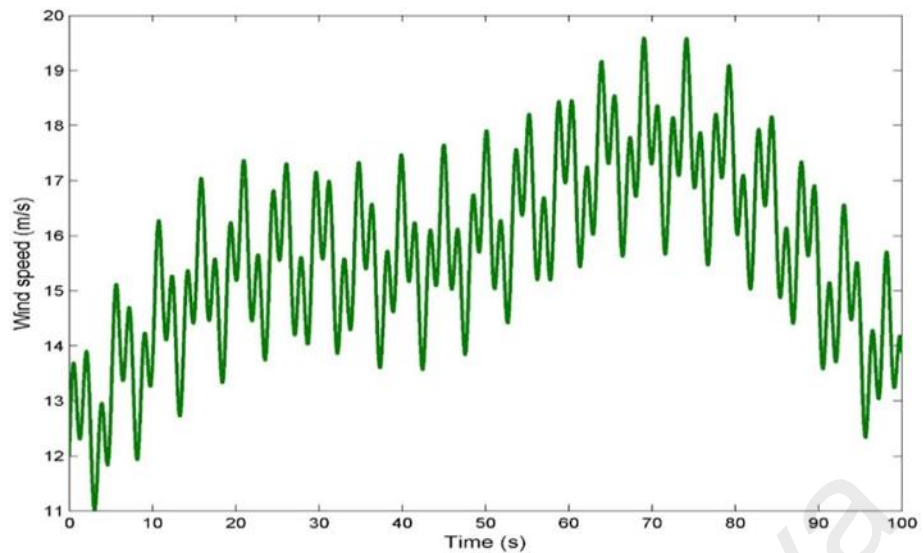


Figure 2-4: Wind speed profile (Tran et al., 2010).

2.2 Wind Turbine Controlling

2.2.1 Proportional Integral Derivative Controller

PID controller has selected in this study for some of its characteristics, such as flexibility, reliability and easy operating system. It consists of three control parameters namely proportional (K_p), integral (K_i) and derivative (K_d). Each controller parameter has an individual contribution for controlling any kind of system. A typical block diagram of the PID controller with a feedback loop is shown in Figure 2-5.

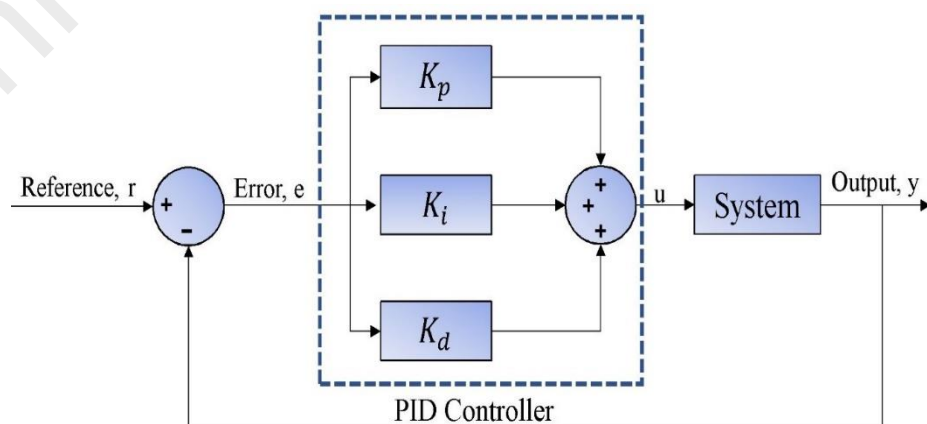


Figure 2-5: A typical block diagram of PID controller with feedback loop.

From the Figure 2-5 the sum of the control parameters is $u(t)$. The function of tracking error's $e(t)$ can be referred by each and every control parameter and these parameters are working independently. The mathematical equation of PID control can be written as,

$$u(t) = K_p e(t) + K_i \int_0^t e(t) dt + K_d \frac{de(t)}{dt} \quad (2.18)$$

The PID control parameters can be tuned by several methods namely trial and error, Ziegler- Nichols (Z-N), Tyreus-Luyben, Cohen-Coon and auto tuned. In this study, trial and error method has been adopted for controlling parameters tuning. In the trial and error method, a critical gain value is measured by increasing K_p at which the system provides sustained oscillations and the corresponding period is computed to calculate three control parameters of PID controller. Nevertheless, the tuning of the PID controller reaches a new era.

Several methods are being used for PID tuning such as auto tuning (Z-N), fuzzy logic, AI, and some nature-inspired algorithms. Those techniques are getting preference. In the study, ACO has been used for PID parameter tuning in the optimization process.

The technique of optimization for PID controller parameter tuning is common for pitch angle control of a large wind turbine. ACO algorithm is simple and effective for PID parameters tuning. By the discrete search space method, it was implemented by Dorigo and Gambardella (1997a). The concept of algorithm is inspired by natural ant behavior of food searching by a shortest path which is shown in Figure 2-6.

Researchers have used a number of control techniques to control the pitch angle of WT. The generalized predictive control (GPC) has been applied for pitch angle controlling with wide range of wind speed. GPC can also minimize the error of the control signal in each interval and the minimization of performance index assists to eliminate its divergence. Nevertheless, the GPC control system can't be able to stay stable output

power of WT if the output power's error is large. If the large interval is between cut-in to cut-out wind speed, the output power fluctuates heavily. The linear quadratic Gaussian (LQG) has been applied for pitch angle control to design wind turbine. But the robustness of the LQG has imperfectness for extremely nonlinear wind turbine (Ekelund, 1994; Shaked & Soroka, 1985). In recent few years, researchers have focused to control the pitch angle for effective and smooth wind power outcome through AI, fuzzy logic method and natural inspired algorithms for PID controller parameter optimization. In this study, conventional PID controller has used for pitch angle control. Kong et al. (2006) have provided the combination of set theory of fuzzy to control a nonlinear sliding mode for steady wind power of MW range wind turbines. Amendola and Gonzaga (2007) employed the two FLC methods, i.e., first one controlled the pitch angle control and the second one controlled the generator speed of WT to achieve stable output power. Gao and Gao (2016) have proposed novel Proportional Integral (PI) and a PID control system of pitch angle of three WTs. Direct search optimization was used for PI and PID control the parameters optimization. The hybrid algorithm, PSO-RBFNN, was proposed by Perng et al. (2014) that was also used for optimal PID parameters tuning in WT control design. Another investigation was conducted based on fuzzy-proportional-derivative for large WTs operating above-rated power to investigate a blade pitch control (Zhang et al., 2008). Self-tuning of PID parameters has been carried out by FLC for adjustable control of the pitch of large WT power by Dou et al. (2010). In addition, they found optimum torque with pitch angle control by some blade parameters. Civelek et al. (2016) proposed a new intelligence genetic algorithm (IGA) for PID controller parameters tuning for pitch angle control of medium scale WT. They found a decent result which was compared to the conventional genetic algorithm.

Conventional blade pitch angle controller along with the outstanding part of these wind turbines are only equipped. This functional system can maintain the output power of wind

generator at its rated level. It is possible when the wind speed is higher than rated speed but below the cut-out speed. Therefore, it is very important to design a suitable controller which can provide an optimal desired power. The natural inspired algorithms such as Ant colony optimization (ACO), particle swarm optimization (PSO) and genetic algorithm (GA) have been developed with promising results in optimization applications. For the pitch angle of wind turbine, PSO and GA are implemented by Gaing (2004) and Civelek et al. (2016). To deal with control problem, PID controller is designed to provide required pitch angle control that can control the actuator. Previous studies have showed that PID controller is well known in pitch angle control but it has been tuned with trial and error method or classical method in the most studies. These methods are extremely time consuming and difficult to get optimal values in most cases. PID controller is investigated with promising ACO algorithm and it is not investigated previously to optimize PID controller for pitch angle control. ACO algorithm has been developed after inspired by real ants' behavior and it has proved its effectiveness in application of optimization because ants can construct shortest path when searching for food in short time. ACO method automatically optimizes PID parameters by minimizing error between desired and actual output.

Pitch angle control of WT has been considered a very well accepted method to improve the power quality of the wind turbine generator (WTG). A proposed pitch angle control strategy based on PID controller parameter's optimization thought ACO algorithm is almost completed smoothing the WT output power in the full load region. PID controller is designed in this study for pitch angle control because of its simplicity and effectiveness. PID controller parameters are optimized using nature-inspired optimization method, i.e. ACO and its effectiveness are compared with trial and error method of PID and Fuzzy-PID.

2.2.1.1 Actuator Model

An actuator is machine component which can be accountable for controlling and moving mechanism. It can be electrical and hydraulic operated. The accuracy of electrical actuator for speed control and position precision is satisfied. The blade of WT can be set by DC servo motor. DC servo motor can be used as an actuator for wind turbine pitch angle control (Qi & Meng, 2012). The transfer function of DC servo motor can be expressed by Eq. (2.19).

$$G_s(s) = \frac{\alpha}{\tau s + \beta} \quad (2.19)$$

where, τ is the time constant. Both α and β are motor constants.

$$G_p(s) = \frac{\alpha}{s(\tau s + \beta)} \quad (2.20)$$

The position control of transfer function of DC servo motor can be expressed by Eq. (2.20). The value of motor parameter is 1. Therefore, the Eq. (2.20) can be expressed by Eq. (2.21).

$$G_p(s) = \frac{\alpha}{s(s + 1)} \quad (2.21)$$

2.3 Nature-Inspired Algorithms

Nature-inspired algorithms are the algorithms inspired by nature. ACO, PSO, and ABC are used for aerodynamic optimization. The aerodynamic optimization of HAWT is a complex technique characterized by many trade-off decisions intended at finding the ideal overall performance. The researcher designs the WT in enormous ways and more often it is difficult to make ideal decision. Commercial turbines have been derived from both theoretical and empirical methods, but there is no clean evidence on which of these is optimal.

The optimization method of ACO, PSO, and ABC are finding best solution for specific problem by the soft computing solution of maximization of power coefficient. In wind

turbine system, power maximization is very important for effective efficiency. For the optimization, the power coefficient optimization parameters are determined by airfoil S822 of National Renewable Energy Laboratory (NREL).

2.3.1 Ant Colony Optimization

From last few years, the researchers have been using ACO to optimization problem of wind turbine system. Eroğlu and Seçkiner (2012) determined the wind farm layout using ACO. They found maximum energy output that considered wake loss, wind turbine location and wind direction. Fuchs and Gjengedal (2011) applied ACO for the necessary time step resolution in a transmission expansion and wind power integration in Nordic area. They determined the average and peak values for power production from wind technology. Jovanovic et al. (2016) focused on maximum segregating of computed graphs of supply and demand. For the optimization, they used ACO and found that the error was less than 5% in comparison with the optimal solutions. Abd-Allah et al. (2015) investigated the lightning point in wind turbine farm as lightning is harmful for wind turbine farm. They used ACO to search for the sensitive points in wind farm. Mustafar et al. (2007) studied the loss of reduction of transformer tap setting to control reactive power using ACO technique.

ACO approach performs “intelligent” randomization using suitable procedure for the problem of attention (Dorigo & Gambardella, 1997b). ACO is based on the foraging behavior of actual ant colonies that are looking for food. ACO is first expressed by Dorigo and Gambardella (1997a), and later has been modified and presenting as a optimization techniques by Shen et al. (2005) and Dorigo et al. (2006). If the ants have found a food source, they will carry out some evaluation about size of the source and carrying a percentage of the food to the nest of ant, while send off some pheromone on the way back

that is known as the pheromone trail. This pheromone trail gives the opportunity to the other ants of the same nest to hint the found source and same way follow the other ants of the same nest to reach the food source. The total amount of the pheromone collected on the ground is directly proportional to the quantity and quality of the base source they were discovered (Socha & Dorigo, 2008). Since the pheromone is like vaporizable substance, the quantity of pheromone will be decreased over the time (Kiran et al., 2012). Therefore, the indication path of the ants for food collection and pheromone trails staying on the path. Based on the methodology, the shorter path is the priority to the pheromone trail. Indeed, ants are collecting their food by the shortest path. The optimization method is based on updating pheromone path of better solution. The researchers have been done ACO technique for difference purpose such as energy optimization and estimation. In this study, continuous ACO used (He & Han, 2007; Wang & Xie, 2002) for optimization problem. The problem of optimization can be solved by the support of artificial ant colony by using information through pheromone deposited on graph edges.

Assume the vector $X = [x_1, x_2, \dots, x_n]$ are the parameters of optimization, where total number of parameters is n , the lower and upper bounds is to be $x_i \in D(x_i) = [x_{i_{low}}, x_{i_{up}}]$ with $i = 1, 2, \dots, n$. The field definition $D(x_i)$ is divided by the subspace M and node is defined the middle of each subspace. A single artificial ant $k = 1, 2, \dots, N_{ant}$, where the maximum ant numbers is defining N_{ant} , the ants move from one node to another node where P is the total node in each field definition $D(x_i)$. Each subspace

$$h_i = \frac{x_{i_{up}} - x_{i_{low}}}{M} \quad (2.22)$$

For each level, which has P nodes on it, there are $M \times n$ nodes in total. k is the state vector of ant that entire tour shown in Figure 2-6 with travel index $[i_8, i_7, i_6, \dots, i_4]$. The travel index directly depends on the cumulative probability (CP) from the probability

P_{ij} of the ant k to move the i^{th} node on the j^{th} level. For example, if $M = 10$, $CP = [0.1, 0.2, 0.3, 0.4, 0.5, 0.6, 0.7, 0.8, 0.9, 1.0]$ and the generated random number lies between 0.8 and 0.9, the first travel index, i_8 , is chosen as 8 (eighth column of the CP). Those processes have continued until found the all travel index. The values of the parameters X , held by ant, are as

$$[x_1, x_2, \dots, x_n] = [x_{1 \text{ low}} + i_8 \times h_1, x_{2 \text{ low}} + i_7 \times h_2, x_{3 \text{ low}} + i_6 \times h_3, \dots, x_{n \text{ low}} + h_n \times i_n] \quad (2.23)$$

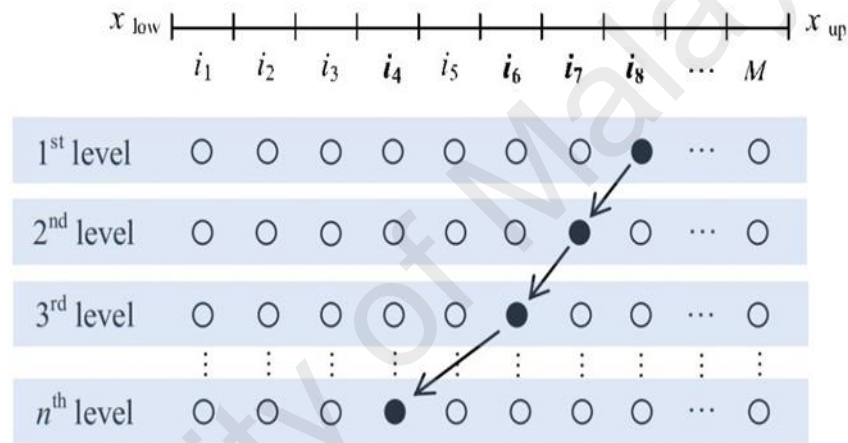


Figure 2-6: State space graph of ACO (Julai et al., 2009).

The rule of state transition of the ant k is defined as

$$P_{ij} = \frac{\tau_{ij}}{\sum_{i=1}^n \tau_{ij}} \quad (2.24)$$

Where, the ant probability P_{ij} move to the i^{th} node on the j^{th} level. The pheromone at the node is τ_{ij} . The pheromone is updated by using the following equation, when all ants finished their tours.

$$\tau_{ij} = (1 - \rho)\tau_{ij} + \frac{Q}{f_{best}} \quad (2.25)$$

Where, the pheromone decay parameter range is $0 < \rho < 1$, Q is the quantity of pheromone laid by an ant per cycle, τ_0 is a constant for the initial value of τ_{ij} (for

initialization τ_{ij} on the right-hand-side is set to be τ_0), and f_{best} is function of objective. From the objective function, the best value is given by ant in each searching period.

As shown in Figure 2-6, the algorithm starts with the initialization of the pheromone track. The desired optimization power coefficient (C_p) is calculated for each ant and the maximum value is stored as f_o (Galdi et al., 2008). Each and every iteration, an ant makes a complete solution of objective function according to the Eq. (2.24) of probabilistic state transition rule. The quantity of pheromone at the third step is a global pheromone updating role applied in two phases. First, an evaporation phase where a fraction of the pheromone evaporates, and a reinforcement phase where each ant deposits an amount of pheromone which is proportional to the power coefficient (C_p) of its solution. The process is continuing until the stopping criterion is satisfied. The optimization process is shown in Figure 2-7.

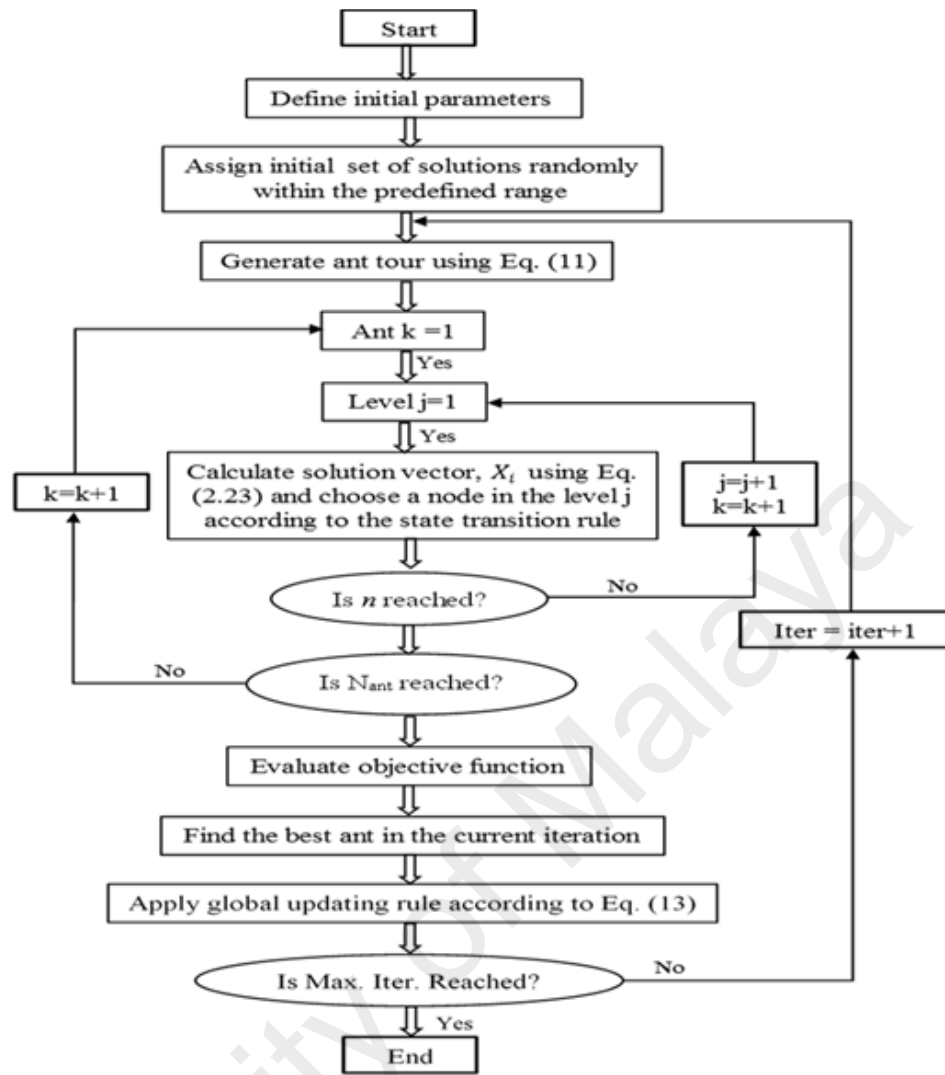


Figure 2-7: Flow chat of ACO algorithm.

2.3.2 Particle Swarm Optimization

The explicit mathematical model can be represented as the optimization processes. In complex optimization problems, it is difficult to use the mathematical model with nonlinear of optimization. While the simulation system can be processing any problem by the tool for evaluating the performance. the simulation and optimization can find optimum solution (Sharafi & ELMekkawy, 2014).

PSO is the meta-heuristics approach. Basically, meta-heuristics are used in which problem where the optimization problem not able to solve those problems. As PSO is the meta-heuristics type therefore it can solve more complex problem (Q. Bai, 2010; Dufo-

López et al., 2007). PSO algorithm was established by Kennedy and Eberhard in the year of 1995 (R. Eberhart & Kennedy, 1995; Kennedy et al., 2001). PSO is the multi-parallel searching techniques to obtain the optimum results. PSO is inspired by the natural “bird flocking” or fish schooling. In this algorithm, the set of swarms or particle that are described by their position and velocity vector fly through the search space.

The particles motion of PSO is defined by the velocity vector its direction. The best solution achieved by all particles is called the best global particle. All swarm position and velocity are updated by best global particle their obtained experience. The experience sharing between particle and swarm is the vital reason behind PSO success (R. C. Eberhart & Shi, 2000).

At starting period, the random population of swarms is generated with random position vectors and velocity of vectors $X_i = (x_{i1}, x_{i2}, \dots, x_{id})$ and $V_i = (v_{i1}, v_{i2}, \dots, v_{id})$ respectively. Each particle best position is $P_i = (p_{i1}, p_{i2}, \dots, p_{id})$ according to the best fitness value obtained by the particle time t . After each iteration, the new positions and velocities to the particle for the next fitness evolution are calculated by the following Eq. (2.26) (Y. Shi & R. Eberhart, 1998) (Y. Shi & R. Eberhart, 1998).

$$v_{id}(t+1) = \omega \times v_{id}(t) + c_1 \times \varphi_1 \times (p_{id} - x_{id}(t)) + c_1 \times \varphi_2 \times (p_{gd} - x_{id}(t)) \quad (2.26)$$

$$x_{id}(t+1) = x_{id}(t) + v_{id}(t+1) \quad (2.27)$$

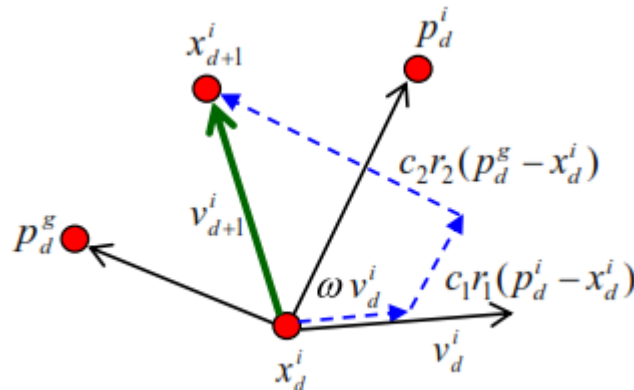


Figure 2-8: Particle swarm optimization algorithm.

Where $\omega \geq 1$ play a vital role to ensure the convergent behavior φ_1 and φ_2 are uniform random number with interval (0,1), c_1 and c_2 are constants of acceleration, $p_i(pbest)$ is the personal best particle, $p_g(gbest)$ and i is the best position of particle i.e. the best position of the particle in the population so far (Y. Shi & R. C. Eberhart, 1998). The first part of Eq. (2.26) represents the previous velocity, which provides the necessary momentum for particles to roam across the search space. The second part, known as the “cognitive” component, represents the personal thinking of each particle. The cognitive component encourages the particles to move towards their own best positions found so far. The third part is known as the “social” component, which represents the collaborative effect of the particles, in finding the global optimal solution. This part always pulls the particles towards the global best particle found so far. The flow chart of PSO is shown in Figure 2-9.

Many researchers have also been using PSO algorithm for location optimization. Safaei et al. (2016) proposed the new two-step PSO algorithm for placement of WTG for maximum allowable capacity and minimizing the power losses of wind turbine. The wind turbine placement at wind farm was optimized by Wan et al. (2010). Pookpant and Ongsakul (2013) used the binary PSO for wind turbine optimum placement at wind farm. The size optimization of hybrid system was determined by PSO (Maleki et al., 2015).

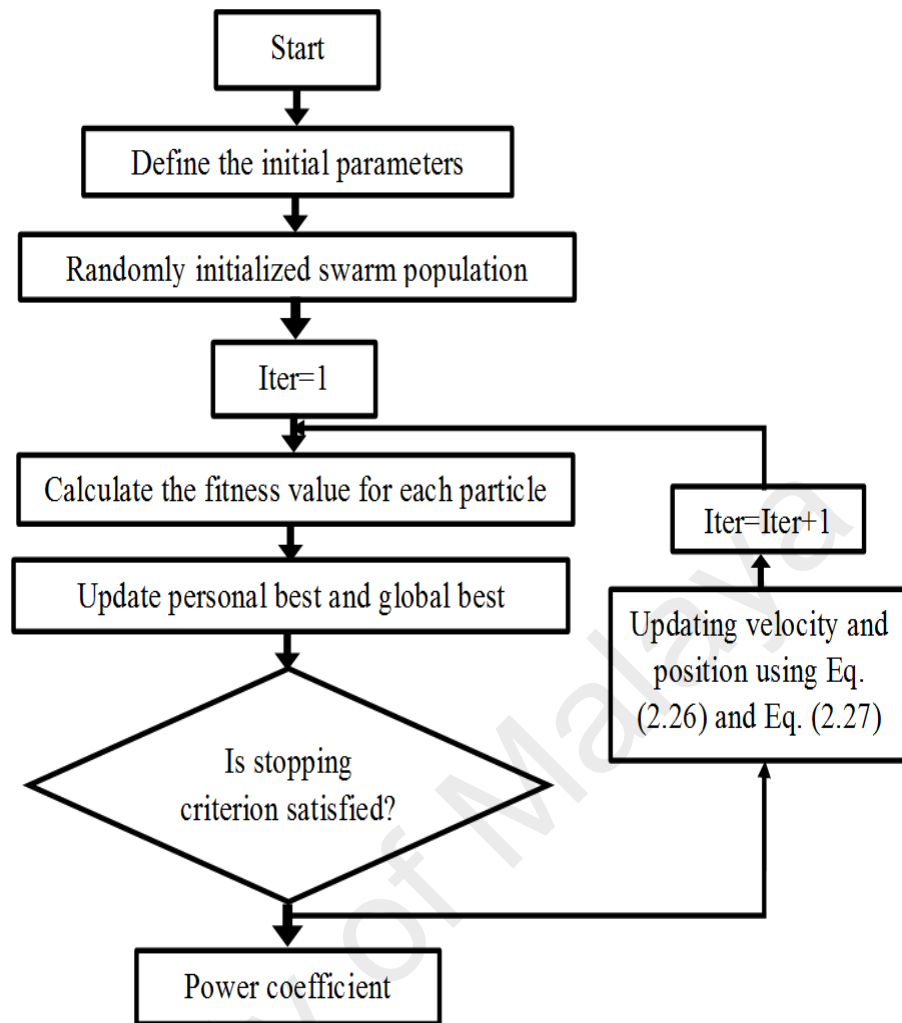


Figure 2-9: Flow chat of PSO.

2.3.3 Artificial Bee Colony

ABC is based on the swarm intelligence optimization algorithm which is proposed and developed by Karaboga (2005), and Karaboga and Basturk (2007) respectively. ABC algorithm is a bionic simulation algorithm that is executed from bees foraging behavior. In this algorithm, there are three types of bees devoted such as employed, onlooker and scouts. The half of colony bees are onlooker and other half of bees are employed. The number of employed bees is equal to the number of food source (S. Singh & Kaushik, 2016). The optimization problem solution is represented by the position of food sources. The employed bees pass information to onlooker bees about food sources. According to

the obtain information from employed bees, the onlooker bees select the food sources and find out new food sources near to the selected one food sources (Akay & Karaboga, 2012). When the selected food sources mined out, the employed bees are become a scout bee. Those scout bees randomly find out new food sources to replace the one which is mined out (Karaboga & Akay, 2011; S. Singh & Kaushik, 2016; X. Song et al., 2015)

$$X_{ij} = X_j^{min} + rand(0,1)(X_j^{max} - X_j^{min}) \quad (2.28)$$

where $i = 1, 2, \dots, SN, j = 1, 2, \dots, D. SN = CS/2$ is the number of food sources is equal to the number of employed bees (X. Song et al., 2015). In addition, employed bees are equal to the onlooker bees. X_j^{min} and X_j^{max} are the lower and upper boundary of parameters of optimization problem. D is the number of problem parameter $rand(0,1)$ is the random number distribution within $[0,1]$. After initialization, employed bees try to detect new food sources with the nearest areas. They saved in memory until creating new food sources to following the equation

$$v_{ij} = X_{ij} + \varphi_{ij}(X_{ij} - X_{kj}) \quad (2.29)$$

where, $j = 1, 2, \dots, D$ and $k = 1, 2, \dots, SN$ are the random selected indices. X_{ij} give randomly different solution form to X_{kj} . In addition, a random integer number represented by φ_{ij} within $[-1,1]$. The parameter's value can be acceptable when if a parameter value produced by operation exceeds its predetermined boundaries. So, the set boundaries if $X_i > X_i^{max}$ then $X_i = X_i^{max}$; if $X_i < X_i^{min}$ then $X_i = X_i^{min}$

After producing, v_i within the boundaries, a fitness value for a maximization problem can be assigned to the solution to following equation

$$fitness_i = \left\{ \begin{array}{l} \frac{1}{1 + f_i} \text{ if } f_i \geq 0 \\ 1 + abs(f_i) \text{ if } f_i < 0 \end{array} \right\} \quad (2.30)$$

where, f_i is the cost value of the solution v_i . For maximization problems, the cost function can be directly used as fitness function. A greedy selection is applied between X_i and v_i , then the better one is selected depending on fitness values presenting the nectar amount of the food sources at X_i and v_i . If the sources at X_i and v_i is greater than X_i in terms of profitability. The onlooker bees memorize the latest position and forget the old one. While, onlooker bees kept in memory previous one. If X_i cannot be improved, its counter holding the number of trails is incremented by 1, otherwise the counter is resets to 0.

After all the employed bees complete their searches, they share their information related to the nectar amounts and the positions of their sources with the onlooker bees on the dance area. This is the multiple interaction features of the artificial bees of ABC. An onlooker bee evaluates the nectar information taken from all employed bees and chooses a food source site with a probability value related to its nectar amount (fitness) P_i , by Eq. (2.29).

$$p_i = \frac{fitness_i}{\sum_{i=1}^{SN} fitness_i} \quad (2.31)$$

The probabilistic selection depends on the fitness values of the solutions in the population. A fitness-based selection scheme might be a roulette wheel, ranking based, stochastic universal sampling, tournament selection or another selection scheme. In basic ABC, roulette wheel selection scheme in which each slice is proportional in size to the fitness value is employed. In this probabilistic selection scheme, as the nectar amount of food sources (the fitness of solutions) increases, the number of onlookers visiting them increases, too. This is the positive feedback feature of ABC.

In the ABC algorithm, a random real number r_i within the range $[0,1]$ is generated for each source. If the probability value p_i Eq. (2.29) associated with that source is greater than this random number, $r_i < p_i$ then the onlooker bee produces a modification on position of this food source site by Eq. (2.28) as in the case of the employed bee. After

the source is evolution, greedy selection scheme is applied and the onlooker bee either memorizes the new position by forgetting the old one or keeps on the old one. If the solution X_i cannot be improved, then the counter holding trials are incremented by 1. Otherwise, the counter is reset to 0. This process is repeated until all onlookers are distributed onto food source sites

In a cycle, after all employed bees and onlooker bees complete their searches, the algorithm checks to see if there is any exhausted source to be abandoned. In order to decide if a source is to be abandoned, the counters which have been updated during search are used. If the value of the counter is greater than the control parameter of the ABC algorithm, known as the "limit", then the source associated with this counter is assumed to be exhausted and is abandoned.

The food source abandoned by its bee is replaced with a new food source discovered by the scout, which represents the negative feedback mechanism and fluctuation property in the self-organization of ABC. This is simulated by producing a site position randomly and replacing it with the abandoned one. Assume that the abandoned source is X_i , then the scout randomly discovers a new food source to be replaced with X_i . This operation can be defined as in Eq. (2.28). In basic ABC, it is assumed that the only one source can be exhausted in each cycle, and only one employed bee can be a scout. If more than one counter exceeds the "limit" value, one of the maximum ones might be chosen programmatically. The flow chart of ABC is shown in Figure 2-10.

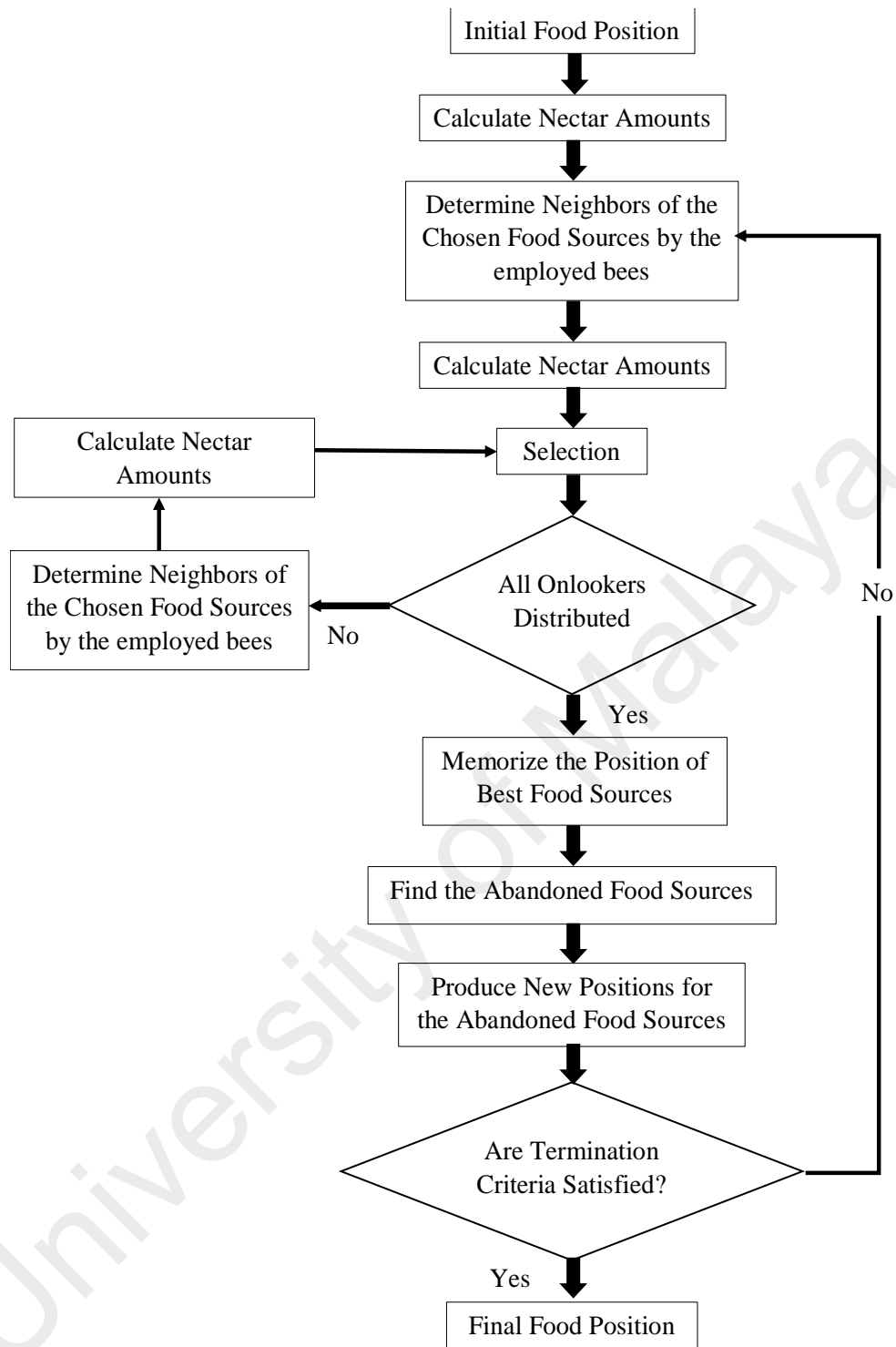


Figure 2-10: Flow chart of ABC algorithms.

In last few years, ABC has massively been studied for complex problem, modelling, and optimization. ABC algorithm is not only used in optimization but also for prediction and control. Delgarm et al. (2016) determined the performance of energy building using multi-objective and optimization approach. In addition, J. Song et al. (2016) used the

improved ABC algorithm to optimize the combustion of boiler to consider NO_x emission. Ebrahim (2014) has used ABC algorithm for proportional integral derivative (PID) controller parameters optimization for speed control of AC driver. Derakhshan et al. (2015) optimized the wind turbine blade shape to determine the performance of aerodynamic of blades. Habbi et al. (2015) proposed a fuzzy logic system that was self-generated by ABC algorithm. Based on the above reviews, ABC algorithm is vastly used for complex problem solving due to its excellent search capability.

2.4 Artificial Intelligence

ANN is the most promising artificial intelligence. Neural network not only emulated the human brain but also knowledge gain through a learning process (Afroz et al., 2018). Last few years, ANN has been proven to be a promising technique for time series prediction, assessment of energy, and pattern reorganization. For the application of time series forecasting, several ANN types are used, for instance, NARXNN, Nonlinear NARNN, Recurrent Neural Network (RNN). In this paper, NARNN and NARXNN has been used to execute wind speed forecasting for the chosen areas in Malaysia. Since the real-world happenings are dynamic and depends on their current state, only non-linear system can properly depict them. In such dynamic and non-linear cases, neural network structure such as: the dynamic recurrent neural network (RNN), the NAR, and the NARX with exogenous inputs are very advantageous. One of the major benefits of such that they can accept dynamic inputs represented by time series sets. In order to achieve the knowledge of the process that generates time series in not indispensable, non-parametric methods are used. Time series forecasting using NN is such non-parametric method. Although the NAR and NARX model uses the past values of the time series to predict

future values, but the RNN model does not need past time series values as inputs nor delays (Cao et al., 2012; Ruiz et al., 2016).

Several researchers have reported different ANN model for WSF ranging from few seconds to more than one-year ahead. Z.-h. Guo et al. (2011) proposed the hybrid back propagation neural network for WSF one-year-ahead in order to remove seasonal effects of wind speed from 2001 to 2016 in Minqin, China, and their proposed BPNN shows lower mean absolute percentage error (MAPE) of 28.16% in comparison to single BPNN. H. Liu et al. (2012) have employed a hybrid Empirical Mode Decomposition and Artificial Neural Networks (MED-ANN) to forecast and eliminate randomness of wind speed. For WSF, a highly-satisfied result was obtained with ANN than that of the Autoregressive Integrated Moving Average (ARIMA) method. Masseran et al. (2012) have considered 10 wind stations to find out the most potential areas in Malaysia for wind speed forecasting. Although the existing wind speed in Malaysia is quite low compared to other countries, Mersing has found considerably higher wind speed than other wind station places in Malaysia, which is around 18.2% power produces from Mersing wind station. One-day-ahead WSF have been done by Li and Shi (2010) using three ANN in North Dakota, United State of America (USA). Azad et al. (2014) considered two meteorological stations in Malaysia for long-term WSF using ANN. They found lower mean absolute error (MAE) of 0.8 ms^{-1} using their proposed algorithm. Short-term WSF at La Venta, Oaxaca in Mexico was practiced by Cadenas and Rivera (2009) using ANN. The accuracy of proposed ANN is satisfactory based on their error level, i.e. MAE (0.0399) and MSE (0.0016). In addition, Cadenas and Rivera (2010) have proposed a hybrid ARMIA-ANN model for average WSF in Mexico in 2010 for three places in Mexico. The accuracy of hybrid model was higher than that of single ARMIA and ANN. Jiang et al. (2017) applied v-SVM model for WSF to overcome the similar fluctuation information between the adjacent wind turbine generators. The proposed Variant Support

Vector machine (v -SVM) has showed better accuracy in comparison to Epsilon Support Vector machine (ϵ -SVM) model. Men et al. (2016) applied mixture density neural network (MDNN) for ST wind speed and wind power forecasting in Taiwan using wind farm data. The MDNN had three-layer architecture where different number of hidden layers and nodes were used for each layer, and this method was effective for multi-step ahead wind power and wind speed forecasting.

In several aspects of the proposed study expands upon Karlik and Olgac (2011) proposed the five activation functions namely Uni-Polar Sigmoid, Hyperbolic Tangent (tansig), Radial Basis and Conic Section those applied in Multi-Layer Perceptron (MLP) NN. In addition, tansig achieved more accuracy to other four activation functions at 100 and 500 iterations. Regression problem can be solved by Random Vector Functional Link Neural Network (RVFLNN) where statistically tansig function prefer superior result than other two function (logsig, tribas) (Vuković et al., 2018). Activation function of ANN applied to forecast flows at the outlet of a watershed that is located in Khosrow Shirin watershed in Iran. They found superior result with tansig- ANN to compare logsig- ANN and conventional hydrological model (Rezaeianzadeh et al., 2013). Moreover, tansig- ANN provided 94% accuracy than logsig- ANN 84% for psychological variables in ascertaining potential archers (Musa et al., 2019). Vafaeipour et al. (2010) investigated wind velocity prediction using neural network with two activation functions in Tehran, Iran and found tansig activation function works better than logsig activation function. Their suggestions were based on mean square error (MSE) root mean square error RMSE, and correlation coefficient (R) performance indicators.

2.4.1 Adaptive Neuro-Fuzzy Interface System

ANFIS is one kind of neural network that shows better learning and estimation capabilities (Jang, 1993). ANFIS can be categorized to discrete control system by online

identification, approximation of highly nonlinear function and predict a chaotic time series. Basically, for the fuzzy 'IF THEN' rules, predetermined inputs and outputs are used to construct the ANFIS. The membership function (MFs) of ANFIS is created by input and output parameters. ANFIS obtains the fuzzy interface system (FIS) through the input and output and algorithm of backpropagation. FIS is executed by the combination of rule base, database, and reasoning mechanism. Firstly, fuzzy logic finds the rule base. The database allocates the MFs that work in the rules of fuzzy logic. Finally, reasoning mechanism is reduced from the rules and input data those come to a feasible outcome. It can be adjusted to better perform for changing environment. An ANFIS system is conducted like intelligence of human within certain field (Petković & Shamshirband, 2015).

The ANFIS (training and evaluation) systems have been employed in the MATLAB. In ANFIS system, there are five input parameters to influence the power coefficient of HAWT in as shown in Table 3-1. The 'IF THEN' rules of Takagi and Sugeno's class of fuzzy logic with two inputs for the first order Sugeno is employed for the purpose of this study (Mamdani & Assilian, 1975) (Al-Hmouz et al., 2012).

If x is P and y is R , then

$$f_1 = p_1x + q_1y + r_1 \quad (2.32)$$

The input parameters of MFs are made up by first layer and providing the input values to the following layer. Each node considers as adaptive node having a node function $0 = \mu_{PQ}(x)$ and $0 = \mu_{RS}(x)$ where $\mu_{PQ}(x)$ and $\mu_{RS}(x)$ are MFs. The maximum value of Triangle MFS is (1.0) and (0.0) is the minimum value. Like as,

$$\mu(x) = \text{triangle}(x; p_i, q_i, r_i) = \begin{cases} 0, & x \leq p_i \\ \frac{x - p_i}{q_i - p_i}, & p_i \leq x \leq q_i \\ \frac{r_i - x}{r_i - q_i}, & q_i \leq x \leq r_i \\ 0, & r_i \leq x \end{cases} \quad (2.33)$$

where set of parameters set are $\{p_i, q_i, r_i\}$ and x and y are the inputs to nodes and it signifies to tip-speed ratio, blade radius, lift and drag ratio, solidity, and chord length and power coefficient.

In ANFIS system, the second layer of ANFIS is called MFs. It looks for the weights of each function of membership. The first layer send signal to MFs. The performance of MFs is represented by the input variable fuzzy set shown in Figure 2.6. The nodes of MFs are referred as a non-adaptive. The MFs layer refers as multiplier to receive to signal and send out the outcome in $w_i = \mu_{PQ}(x) * \mu_{PQ}(y)$ form. Output nodes are represented the firing strength of a rule.

The third layer is known as rule layer. In this layer, all neurons perform as the precondition to match the fuzzy rules. Each rule's activation level is calculated by the number of fuzzy rules, that is equal to the quantity of layers. This layer's node calculates the weights of normalized and it is considering as non-adaptive. Each node calculates the value of the rule's firing strength over the sum of the rules firing strengths in the form of

$w_i^* = \frac{w_i}{w_1 + w_2}, i = 1, 2$. The results are mentioned to as the normalized firing strengths.

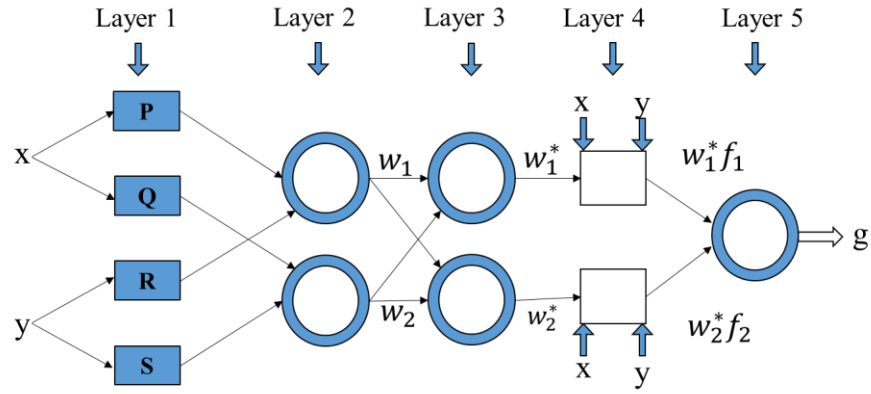


Figure 2-11: The structure of ANFIS.

The fourth layer is called as the defuzzification layer. It is countable for providing the outcomes values as the result of the inference of rules. Every node of the layer is an adaptive node having following the node function $0_i^4 = w_i^* x f = w_i^* (p_i x + q_i y + r_i)$. Here, $\{p_i, q_i, r_i\}$ are the set of variables. This set variable is nominated as the consequent parameters as

$$0_i^5 = \sum_i w_i^* x f = \frac{\sum_i w_i f}{\sum_i w_i} \quad (2.34)$$

The final layer is called output layer of ANFIS. The final layer obtains the inputs from the previous layer. After that, this layer is converted the fuzzy classification outputs into a binary (crisp) but this is not non-adaptive layer. The structure of ANFIS is showed in Figure 2.7. The total output is calculated by summing all signal received from the nodes.

ANFIS is one kind of neural network that shows better learning and estimation capabilities (Jang, 1993). In the power coefficient prediction or estimation, there are various artificial intelligences. Artificial neural networks (ANN) are user-friendly tools which are able to learn the mathematical mapping between input and also output variable of nonlinear system. Petković et al. (2013) applied adaptive neuro-fuzzy for power coefficient estimation. Tip-speed ratio and pitch angle were considered for power coefficient estimation. They found that the optimal power coefficient was around 0.36.

Rajakumar and Ravindran (2012) determined the power coefficient and lift and drag coefficient for various airfoil (NASA) using computational fluid dynamics. They showed that the power coefficient level was higher when the drag coefficient was set to zero and correction of tip loss factor was set to be a constant. Shamshirband et al. (2014) used support vector regression (SVR) based on kernel function for estimating power coefficient and minimizing the generalization error bound. They found similarities in the results of ANFIS and ANN. Sedaghat and Mirhosseini (2012) implemented Blade Element Momentum theory (BEM) for power coefficient of 300kW HAWT technology in the province of Semnan in Iran. They obtained the maximum power coefficient of 0.51 when tip-speed ratio was up to its optimum value of 10.

2.4.2 Nonlinear Autoregressive Neural Network

The application of time series has been characterized by chaotic wind speed. The linear mathematical model is very complex to determine the wind prediction as wind varies randomly in real environment. So, the fleeting transient and the higher variation wind speed needs to be predicted by nonlinear model as Eq. (2.35). For this, Nonlinear Autoregressive Neural Network (NARNN) can be used for effective nonlinear time series forecasting. The NARNN can be defined as given in Refs. (López et al., 2012; Nyanteh et al., 2013).

$$y(t) = f [y(t-1), y(t-2), y(t-3), \dots, y(t-n)] + \epsilon(t) \quad (2.35)$$

Where y is the data series of wind speed at time, the input delay of wind speed series n and f denotes a transfer function. The training of the neural network aims to estimate the function by means of the optimization of the network weights and neuron bias. The y series of wind speed has been determined by approximation of the term $\epsilon(t)$ which stands

for error tolerance. With endogenous input of NARNN can be expressed as Eq. (2.36) given in Refs. (Al-allaf & AbdAlKader, 2011; Ruiz et al., 2016)

$$\hat{y}(t) = f [y(t - 1), y(t - 2), y(t - 3), \dots, y(t - 72)] + \epsilon(t) \quad (2.36)$$

where delay of input $n = 72$. NARNN consists of one input layer, one or more hidden layer(s) and one output layer. NARNN is dynamic and recurrent with connection of feedback as shown in Figure 2-12. Both hyperbolic tangent (tansig), Eq. (2.37) and sigmoid (logsig), Eq. (2.38) function have been implemented using MATLAB to compare the network accuracy for wind speed forecasting. To obtain better performance from the network, topology of NARNN was optimized by trial and error. It should be noted that, the system will be complex by an increased number of neurons. Levenberg-Marquardt Backpropagation (LMBP) has been chosen as the only training algorithm of NARNN as it is fast and more accurate than other training algorithms (MathWorks®, 2016). In this study, ‘trainlm’ function of MATLAB has been used with defaults setting for the LMBP (Beale et al., 2010).

$$O_{tansig} = \frac{e^u - e^{-u}}{e^u + e^{-u}} \quad (2.37)$$

$$O_{logsig} = \frac{1}{1 + e^{-u}} \quad (2.38)$$

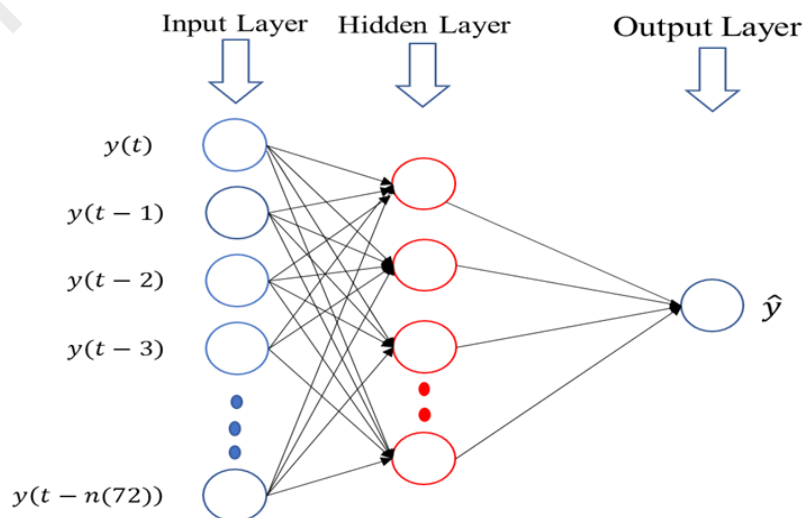


Figure 2-12: Nonlinear autoregressive neural network.

The wind speed is the most challenging for wind power generation by the wind turbine. The variation of wind speed is chaotic. Sometimes, wind turbine can be affected by high wind speed due to the production of wind power generation is stopped when wind speed is very high. The WSF is very important role for optimum planning and wind energy application. Basically, forecasting of wind speed can be divided into four time series categories: very short-term (VST), short-term (ST), medium-term (MT), and long-term (LT) forecasting. VST refers to less than 30-minutes-ahead of WSF. In real-time, wind turbine can be controlled by ST wind speed forecasting. Less than one-week to 1-day-ahead resides in ST forecasting. Planning of load dispatch can be employed by ST forecasting. 6 hours to 1-day -ahead resides in MT wind speed forecasting, which helps to manage power system and secure operation of wind turbine. Lastly, LT forecasting is useful to optimize the operation cost and schedule maintenance (Azad et al., 2014; Z. Guo et al., 2012; Zhao et al., 2016). The wind speed forecasting is very difficult as the wind speeds are chaotic depending on the earth rotation and properties of topographical condition (temperature and pressure). Methodologically, wind speed prediction can be classified into four groups defined as: physical, statistical, AI, and hybrid methods (Azad et al., 2014; Zheng et al., 2011). Among them, AI has been chosen for wind speed prediction in this study. This is due to no extra mathematical model needed for prediction, but instead it provides higher accuracy.

Over the last number of years, ANN has been proved to be a promising technique for pattern reorganization, assessment of energy and time series prediction. There are several ANN types for the application of time series forecasting such as NARXNN, NARNN, and Recurrent Neural Network (RNN). In this study, NARNN has been used to execute wind speed forecasting for three different areas: Kuala Terengganu, Melaka, and Kuantan in Malaysia.

The most effective way of long-term WSF has been found to be AI methods, because they do not require extra mathematical models other than their own universal algorithm for future time series prediction. To authors' best collection of information, usage of NARNN with two different transfer functions is unreported till date in the field of wind speed forecasting. Thus, this study analyses the potentiality of NARNN with different statistical analysis. Although implementation of NARXNN was found in several studies, NARNN has been adopted here, because it predicts the time series without any exogenous variable. Therefore, NARNN and NARXNN with two different transfer functions namely "tansig" and "logsig" have been used in this study to find the most suitable settings of the NARNN, since both transfer functions are greatly used for backpropagation neural network types.

2.4.3 Nonlinear Autoregressive Exogenous Neural Network

The nonlinear autoregressive with exogenous input is predict time series which is proposed by Lin et al. (1996). For this, NARXNN can be used for effective nonlinear time series forecasting. The time series of NARXNN can be defined as in Eq. (2.39) (Ruiz et al., 2016).

$$y(t) = h(x(t-1), x(t-2), \dots, x(t-k), y(t-1), y(t-2), \dots, y(t-p)) + \epsilon(t) \quad (2.39)$$

where past value p is predicted time series $y(t)$ and it has another external time series which is defined as $x(t)$. The dimension of the external time series $x(t)$ is single or multidimensional. The NARXNN prediction is based on the last output values with exogenous input for future values estimation. In this study, wind speed is used as input time series at time $t-1$, $y(t-1)$ and temperature (Di Piazza et al., 2016; Lydia et al., 2016) which is used as exogenous input at time $t-1$, $x(t-1)$. The single output is $y(t)$. The

NARXNN and NARNN are almost similar. Temperature is used as an external input in NARX. Figure 2-13 shows the architecture of NARXNN.

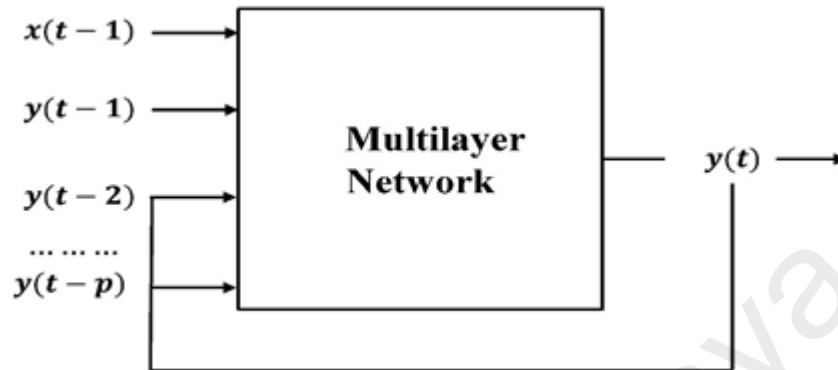


Figure 2-13: The NARX neural network.

2.4.4 Performance Analysis Criteria

For the proposed AI and nature nature-inspired algorithms model evaluation, different statistical indicators are used as shortly reviewed in the following section (W. Chong et al., 2016).

2.4.4.1 Root Mean Square Error

The root means square error (RMSE) is crucial for every model. Based on the RMSE, it can be observed for any model or design. Basically, the RMSE recognizes the model accuracy by positive value difference between predicted and measured. It is defined as

$$RMSE = \sqrt{\frac{1}{n} \sum_{n=i}^n (P_{ip} - P_{iM})^2} \quad (2.40)$$

where P_{ip} is the predicted value by the techniques of ANFIS, P_i is the measurement value of the system and the total number of testing data is represented n . Small value of RMSE represents the accuracy of the model. It can be approximated close to zero. For ideal case, it should be zero.

2.4.4.2 Coefficient of Determination

The linear relationship between measured and predicted values is provided by coefficient of determination R^2 . The R^2 is defined as

$$R^2 = 1 - \frac{\sum_{n=i}^n (P_{ip} - P_{iM})^2}{\sum_{n=i}^n (P_{ip} - P_{iM.Avg})^2} \quad (2.41)$$

where, P_{ip} and P_{iM} are the predicted/estimated and measured value respectively.

2.4.4.3 Mean Absolute Error

To obtain a satisfactory accuracy using NARNN and thus to select potential areas for further wind turbine installation. The accuracy of wind speed forecasting can be determined by Eq. (2.41) and Eq. (2.42). Here, two indicators have been used namely, MAE and MAPE for the long-term WSP of this study (Madsen et al., 2005; Santamaría-Bonfil et al., 2016).

MAE expressed as (Foley et al., 2012)

$$MAE = \frac{1}{n} \sum_{i=1}^n |R_{ws} - P_{ws}| \quad (2.42)$$

2.4.4.4 Mean Absolute Percentage Error

MAPE expressed as (D. Liu et al., 2014)

$$MAPE = \frac{1}{n} \sum_{i=1}^n \frac{|R_{ws} - P_{ws}|}{R_{ws}} \times 100 \quad (2.43)$$

where R_{ws} and P_{ws} is the real and predicted of wind speed respectively and n is defined by the number of data.

However, no study has not yet explored the effect of different activation functions in time series networks to find the most effective one. It is known that activation function is a core component in any neural network model, because they add nonlinearity and enable the network to converge during backpropagation. So, if one activation function is better

than the other, it would significantly enhance the time series prediction performance of the network by enhancing the derivative and thus the converging performance. This is why the contribution of this study is that it examined the performance of two activation functions – hyperbolic tangent sigmoid (tansig) and logistic sigmoid (logsig) when used in different time series networks such as NAR and NARX with different time series datasets but with same network parameters and architectures. Such analysis will reveal if any of the activation functions consistently perform better than the other in different conditions, so that future researchers choose the proper activation functions while conducting neural network-based time series forecasting tasks.

. To find out the best combination of blade parameters provides maximum power coefficient using ACO, ABC and PSO. An ANFIS is used to investigate the effectiveness of these nature-inspired algorithms by comparing the results predicted from ANFIS with the results obtained from nature-inspired algorithm. An endeavour is prepared for retrieving correlation between C_p and best combination of optimized blade parameters such as lift and drag ratio, blade radius, tip speed ratio, solidity ratio and chord length of blade of HAWT.

Pitch angle control of WT has been considered as a very well accepted method to improve the power quality of wind turbine generator (WTG). A proposed pitch angle control strategy based on PID controller parameter's optimization using ACO algorithm is stable output power of WT in full load region of wind speed. PID controller is designed in this study for pitch angle control because of its simplicity and effectiveness. PID controller parameters are optimised using nature inspired optimization method, i.e. ACO and its the effectiveness are compared with trial and error method of PID and Fuzzy-PID.

CHAPTER 3: METHODOLOGY

3.1 Methodology Overview

In this chapter, the research methods that were performed to obtain the desired objectives are listed here. The main objective of this research, is to find blade optimal parameters of HAWT for maximum power coefficient using ACO, PSO and ABC and ANFIS has used for power coefficient prediction. To catch on effectiveness of activation function (tansig and logsig) of NARNN and NARXNN have used long-term wind speed forecasting in Malaysia. An optimization of PID controller parameters using ACO algorithm is carried out for pitch angle controlling in WTG power obtains within rated power of WTG.

In order to achieve the above objectives, this research has mainly focused on applying computational method instead of experimental method because computational method able to verify with previous research and also able to provide decent optimization, prediction and controlling of wind turbine model. With the use of robust computational method, the research cost can be greatly reduced while maintaining the decency of the predicted results as compared to experimental work. It effectively reduces the engineering cost if different parameters were to be tested out in preliminary benchmark phase before moving into real-time prototype testing with any experimental lab work.

Throughout this research, different types of method were carried out in different phase to achieve different goals to obtain the results desired. The methods that were being applied in this research were MATLAB/Simulink modelling, numerical computational simulation analysis and data extraction and analysis.

The project is started with developing dynamic modeling of the rotor and blade section of the wind turbine, wind speed forecasting and pitch angle controlling. A simulation

algorithm characterizing the behavior of these sections is developed using finite difference methods and implemented within the MATLAB environment. Nature-inspired algorithms is used to search for a value of a certain response function of the wind turbine to develop the accurate model and controlling. These algorithms are ABC, PSO, and ACO. AI namely ANFIS, NARNN and NARXNN were apply for prediction and forecasting of power coefficient and wind speed respectively.

3.2 Modeling and Simulation Parameters Setting

3.2.1 Optimization and Prediction Process

Modeling, optimization and prediction of wind turbine blade parameters are momentous to determine the reliability and optimal efficiency of wind turbine power. The optimization process can be used to find the maximum value of the objective function, in this case is the power coefficient of the blade. The overview of the system is presented in Figure 3-1. At initial stage, the mathematical modeling of power coefficient of wind turbine has been embedded from Eq. (2.1) to Eq. (2.14). The Eq. (2.10) is the objective function which has five input variable parameters namely, blade radius, tip-speed ratio, lift to drag ratio, solidity ratio, and chord length. The parameter setting is selected from experimental database from airfoil S822 NREL for 10kW rated wind turbine model. In all simulations for power coefficient C_p , the parameter setting is as listed in Table 3-1. For the optimization, the input variables are selected from lower boundary to upper boundary.

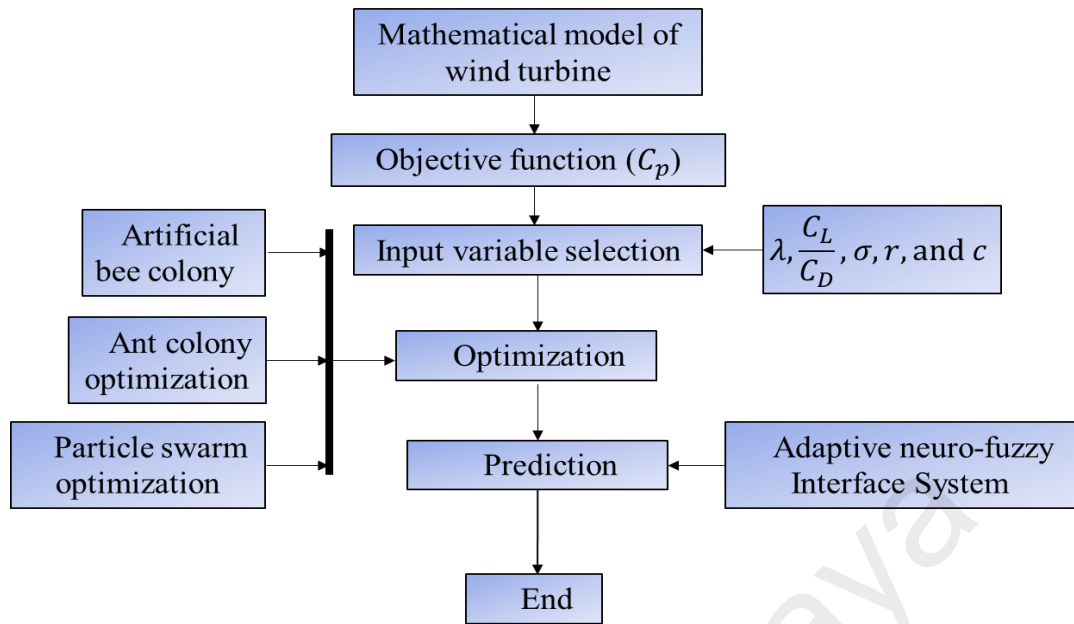


Figure 3-1: Block diagram of blades parameters optimization and prediction methodology.

Table 3-1: Variable input parameters for optimization process.

Parameters		Input values range of
Input 1	Tip-Speed Ratio	3 to 10 (Sedaghat & Mirhosseini, 2012)
Input 2	Rotor Radius	1 to 5 (Tangler & Somers, 1995)
Input 3	Lift to Drag Ratio	1 to 110 (Tangler & Somers, 1995)
Input 4	Solidity ratio	0.01 to 0.45 (C.-J. Bai et al., 2016)
Input 5	Chord Length	0.01 to 0.45 (Philippe Giguere & Selig, 1997)

The optimal efficiency of HAWT is formulated with respect to ABC, ACO and PSO algorithms to optimized blade parameters of wind turbine. Important point of optimization processing is proper input variable data selection. In this investigation, the input variable data selection has been obtained from airfoil of S822 of NREL (Tangler & Somers, 1995) (P Giguere & Selig, 1999) (Somers & Maughmer). The flow parameters for S822 airfoil are trained using natural inspired algorithms (ABC, PSO and ACO). The natural inspires algorithms code is created in MATLAB environment. The input parameters such as blades radius, tip-speed ratio, lift to drag ratio, solidity ratio and chord length is feed into the NIA code are to be optimized. Table 3-1 shows the parameters

considered as input parameters to optimize the input parameters and also used to calculate the power coefficient of HAWT blade.

In this study, ANFIS has been designed for power coefficient prediction of wind turbine. The optimization result C_p of HAWT blades has been investigated for prediction. The computational performance of ANFIS is applied in C_p optimization data and find out the effectiveness of three algorithms.

3.3 Wind Speed Forecasting

Malaysia is a country which is located in the south-east part of Asia. It is surrounded by Thailand, Indonesia and Brunei borders. In Malaysia, total coastline area is about 4675 km which is the 29th longest in the world (Ahmad & Tahar, 2014). For this reason, Malaysia concede the importance of Renewable Energy (RE) as a source of generating electricity instead of fuel. A program known as Small Renewable Energy Power program (SREP) had embraced for boosting up the evolution of RE but unfortunately the results were not acquired the way those should be. SREP scheme breakdown to grow the claim of RE in the national power generation mix by 2010. After that, Malaysian parliament passed Renewable Energy Act 2011(Act 725) (a national energy policy) in 2011 for implementation (Albani & Ibrahim, 2017) (Hashim & Ho, 2011; Khor & Lalchand, 2014; Sovacool & Drupady, 2011). In the year 2015, the wind power production target was 985 MW as reported. However, it produced around 400 MW in early year of 2015. In addition, the success percentage (50 %) was fulfilled to the original target (Mohammad, 2014) as reported that the target was impossible to achieve. Other than that, the target for year 2015 was 985 MW, while 2020 and 2030 are projected to contribute 2080 MW and 4000 MW, respectively. In Malaysia, wind energy project employed only for education research purpose.

The climate of Malaysia is categorized by four seasons: first inter monsoon (April), southwest monsoon (Mid-May to September), the second inter-monsoon (October), and northeast monsoon (November to March) (Azad et al., 2014; Masseran et al., 2012). In Malaysia, the wind flow is uniform and the maximum wind flow occurs in the afternoon and the minimum wind flow occurs before sunrise. Figure 1 shows average wind speed each month in Kuala Lumpur, Melaka, and Kuantan. The average wind speed is between 6-12 km/h of all places. The wind data with one-hour interval have been collected from the Malaysian Meteorological Department (Table 3-2) over a period of 4 months from January to April in 2017.

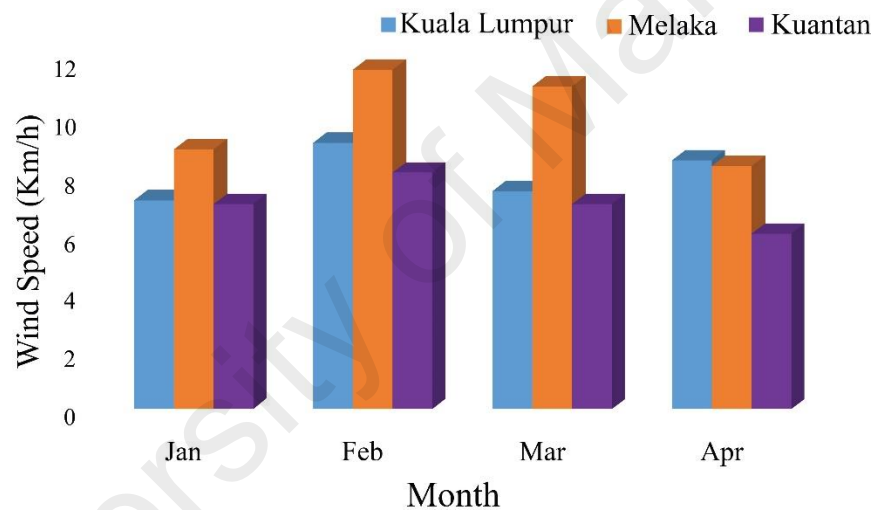


Figure 3-2: Average wind speed in three regions.

Table 3-2: Geographical coordinate and altitude of three wind station

Wind station	Latitude	Longitude	Altitude (m)
Kuala Terengganu	5°23'N	103°06'E	5.2
Kuantan	3°47'N	103°13'E	15.3
Malacca	2°16'N	102°15'E	8.5

One objective of this study is to perform 1-month-ahead WSF for three different regions in Malaysia. The first three months of wind speed data have been used for training and last one-month data have been used for testing the accuracy of NARNN. The process of WSF by NARNN is shown in Figure 3-3.

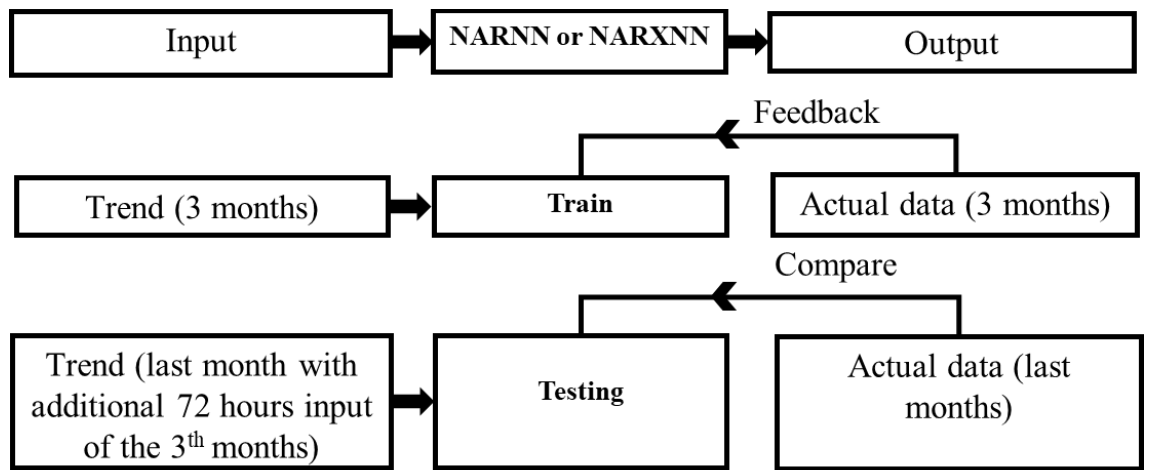


Figure 3-3: LT wind speed forecasting using NARNN and NARXNN.

3.4 Pitch Angel Control of Wind Turbine

Design and development of pitch angle control of WT system are important and these can determine the reliability and efficiency of WT power. It is to minimize overload effect of structure and power overflow of WT. Mathematical modeling of WT is important part to develop vital control system with PID controller. The overview of the system in MATLAB/ Simulink is presented in Figure 3-4.

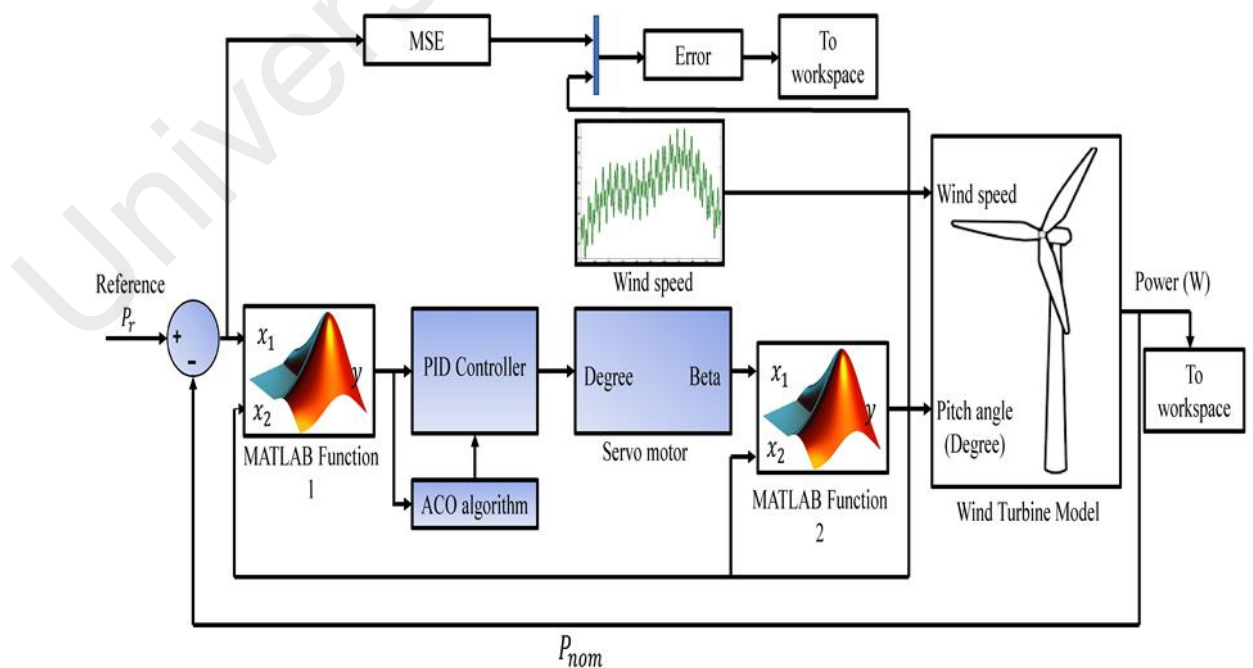


Figure 3-4: Wind turbine MATLAB/Simulink model.

At initial stage, the mathematical modeling of wind turbine and generator blades have been embedded from Eq. (2.1) to Eq. (2.9) and Eq. (2.14) to Eq. (2.17) The wind speed which is the vital input parameter in the system, is simulated by the Eq. (2.18) shown in Figure 2-4.

The parameters of wind turbine are shown in Table 3-3. The DC servo motor has been used to maintain angular position of WT blade by the Eq. (2.21). Two MATLAB/Simulink functions are used and the functions are operated for almost similar task. The MATLAB function 1 is used as conditional function so that wind speed remains between cut-in speed and nominal wind speed. On the other hand, the MATLAB function 2 control the wind speed between nominal wind speed to cut-out wind speed. The reference mechanical power P_r is the desired WT power. The error signal can be obtained from reference power to output power of WTG. PID control block obtains error signal when the wind speed is more than the nominal speed. The PID controller parameters will be optimized using ACO algorithm. The PID controller send the signal to the servo motor as a pitch angle. Pitch angle is the input for wind turbine generation system.

Table 3-3: Parameters of wind turbine system (Civelek et al., 2016).

Wind turbine parameters		
Parameters	Value	Unit
Nominal output power	500	kW
Cut-in wind speed	3	m/s
Nominal wind speed	12 m/s	m/s
Cut-out wind speed	25 m/s	m/s
Rotor diameter	48m	m
Sweep area	1840m ²	m ²
Blade number	3	
Nominal rotor speed	30 rpm	rpm
Rotor speed range	10-30rpm	rpm
Gear box rate	01:50	
Generator number	2	
Generator type	PMSG	
Generator nominal output	250	kW
Generator nominal cycle	1500	rpm
Generator voltage	690 V	V

CHAPTER 4: RESULTS AND DISCUSSION

4.1 Optimization of Blade Parameters Using ACO, PSO, and ABC

4.1.1 Convergence Graph

Convergence rate is one of the key factors that determine the reliability of an algorithm. In maximization problem, it is usually regarded as the higher the rate of convergence, the better the algorithm, if only the outcomes converge and fall within the acceptable range. As discussed before, the natural inspired algorithm produces the highest maximized objective function (C_p) values for every case, and thus, directly ascertaining its accuracy. In this section, the manner of how fast the algorithm converges and attains its highest maximized value in sequence of number of iterations is investigated and discussed.

Figure 4-1 shows the convergence progress for all algorithms with 20 populations. The maximum iteration has been varied from 100, 200, 300, 400, 500, and 600 iterations. It observed that PSO has achieved a speedy convergence at the initial stage (achieved in less than 20 iterations) for all number of iterations. However, the searching for this algorithm tend to become stagnant after less than 10 iterations, as can be seen in Figure 4-1 (b – f). Once the search is stagnant, all particles tend to gather together around the global minimum, and thus, the global best is not improved. For ACO, it can be observed the search started at the lower value of power coefficient in comparison to ABC and PSO. However, the ants kept on searching the optimum value in less than 150 iterations, which performed much better than PSO, but became stagnant or no significant changes towards the end of maximum iteration. For ABC, the searching pattern shows acceleration in the convergence speed. For all cases, the accelerated in the convergence speed can be seen in less than 250 iterations but became stagnant towards the end of maximum iteration. In terms of C_p value, ABC has performed well in obtaining the highest value for all cases

From Figure 4-2, the convergence graphs are obtained with 50 populations for all algorithms with the iteration 100, 200, 300, 400, 500 and 600. The pattern for all the convergence graphs for PSO is it is quickly stable between 10 to 20 iterations, as shown in Figure 4-2 (a-f). For the ACO, it can be noticed that the convergence graph is slightly accelerated after 50 iterations. Both PSO and ACO are not showing any significant increment from 50 iterations to really the maximum iteration. As shown in Figure 4.2, it can be observed that the PSO and ACO are performed in almost similar pattern. On the other hand, the ABC algorithm has achieved the maximum power coefficient in compare with PSO and ACO. The population in ABC is kept on searching the optimum value in less than 250 iterations. With 50 populations, the C_p obtained is almost similar to the result with 20 populations.

Figure 4-3 shows the convergence progress for all algorithms with 100 populations. The maximum iteration has been varied from 100, 200, 300, 400, 500, and 600 iterations. It can be observed that PSO has achieved a speedy convergence at the initial stage (achieved in less than 20 iterations) for all graphs. For ACO algorithm, it kept on searching for the optimum value within 100 iterations except for Figure 4-3(f). In Figure 4-3(f), the searching became constant after 250 iterations onwards. It can be noted that the value of objective function for both algorithms is almost similar, value as shown in Figure 4-3(a-f). For ABC, the searching pattern shows acceleration in the convergence graph. This acceleration pattern can be seen in less than 250 iterations for all graphs but became stagnant towards the end of maximum iteration. For ABC, it can be observed the search started at the lower value of C_p in comparison to ACO and PSO. In terms of C_p value, the consistency of the ABC algorithm in comparison to the others is presented in Table 4-1 to Table 4-2. It signifies that the proposed method is a better algorithm in terms of accuracy as well as consistency, reported with the highest maximized value (0.5295) among all the compared algorithms (ACO and PSO).

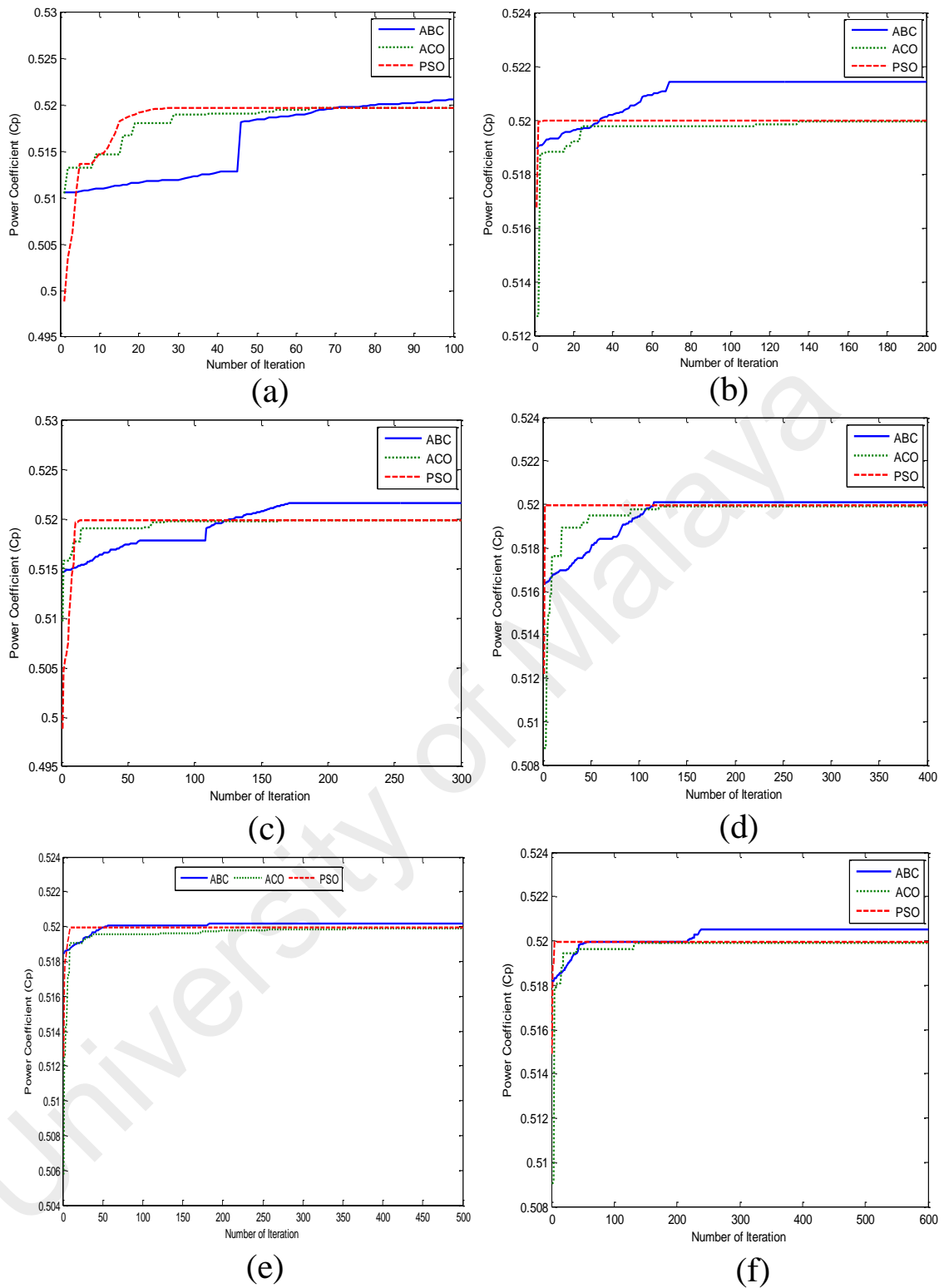
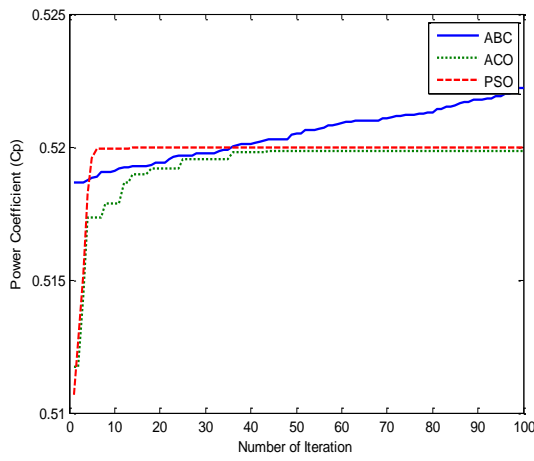
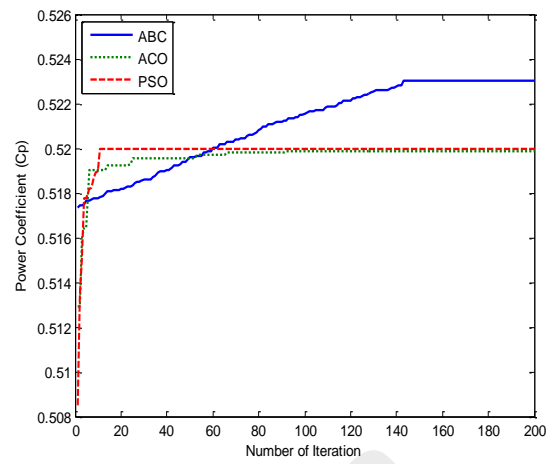


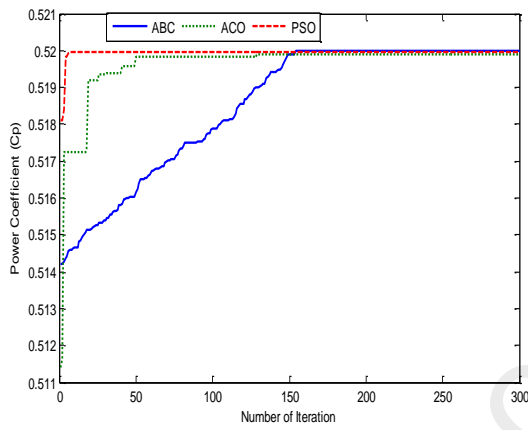
Figure 4-1: Convergence curve of different algorithms (ABC, ACO and PSO) with 20 populations.



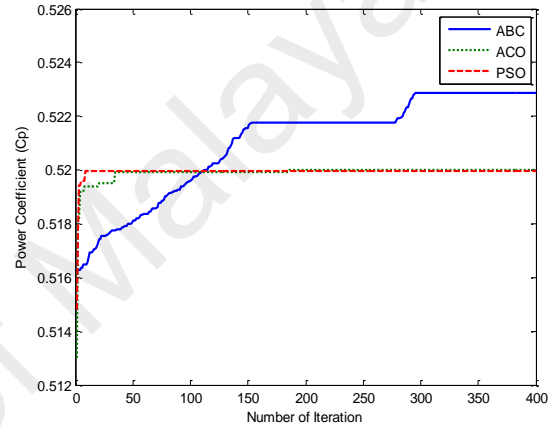
(a)



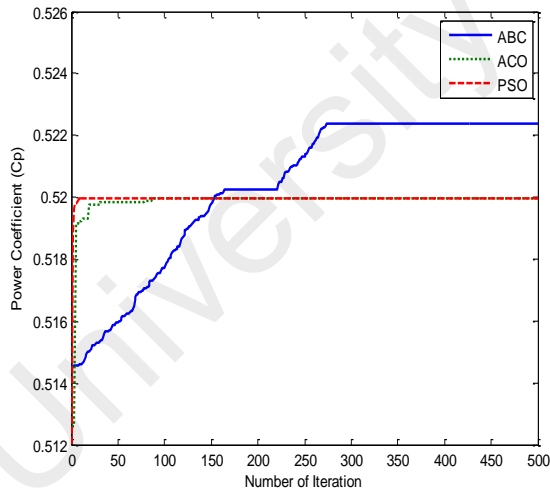
(b)



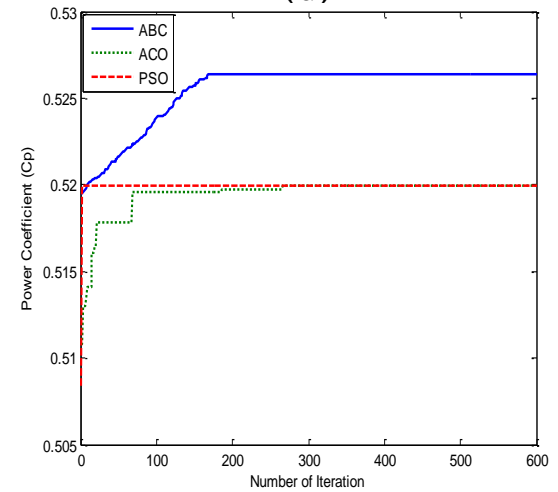
(c)



(d)

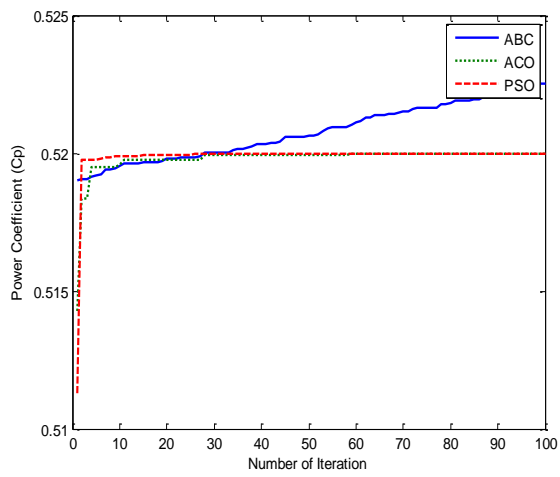


(e)

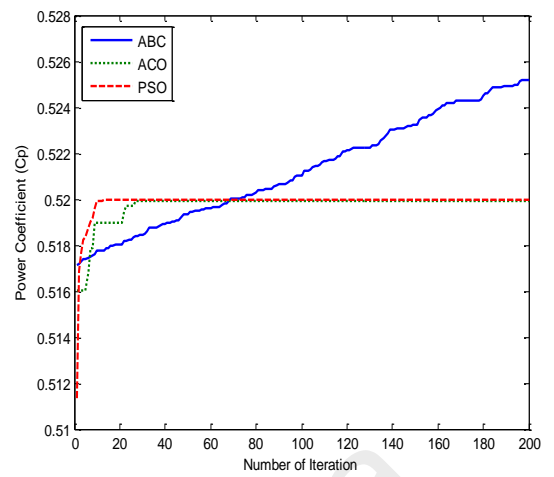


(f)

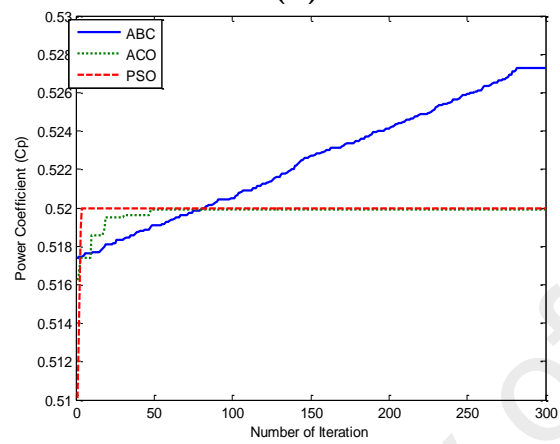
Figure 4-2: Convergence curve of different algorithms (ABC, ACO and PSO) with 50 populations.



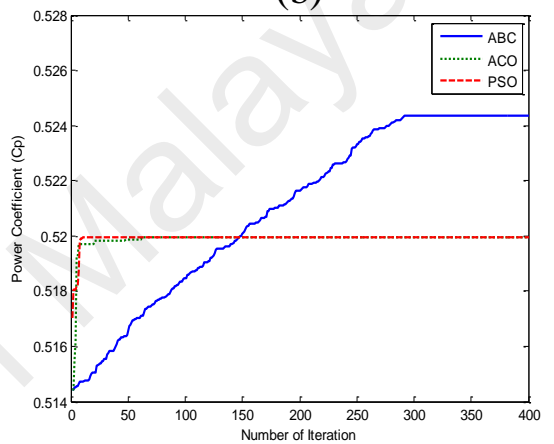
(a)



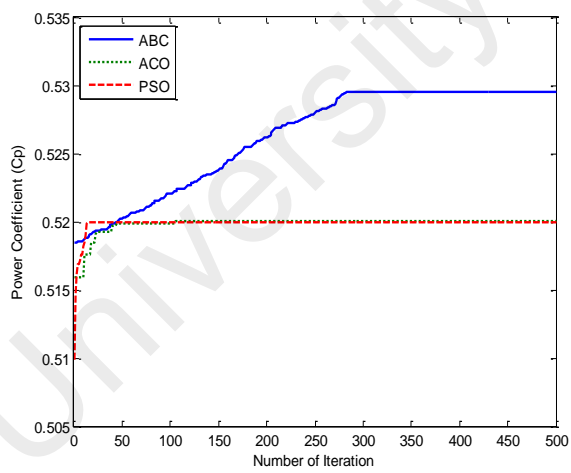
(b)



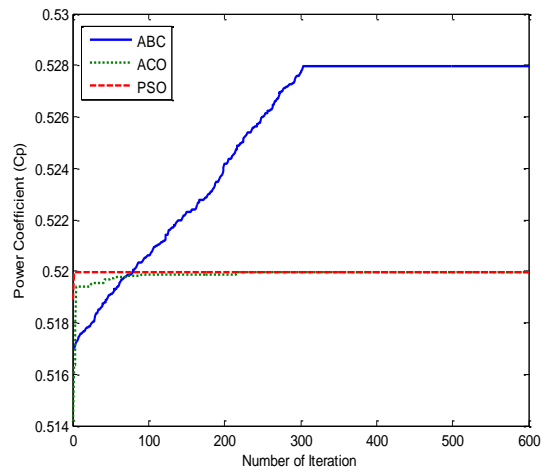
(c)



(d)



(e)



(f)

Figure 4-3: Convergence curve of different algorithms (ABC, ACO and PSO) with 100 populations.

4.1.2 Optimized Parameters of the Wind Turbine Blade

From Table 4-1 to Table 4-3, it can be observed the highest maximized objective function is obtained by the ABC algorithm. From Table 4-1 the highest value of $C_p = 0.5295$ has been obtained by ABC algorithm with the population size, maximum iteration, and the computational time is 100, 500, and 1.1 seconds, respectively. The parameters obtained for this C_p value is listed in Table 4-4.

Table 4-2 shows the maximum power coefficient is obtained by ACO algorithm, i.e. $C_p = 0.52$ with the best input parameters as shown in Table 4-4 where the population size, maximum iteration, and the computational time is 100, 500, and 2 seconds, respectively. Table 4-3 shows the maximum power coefficient is obtained by PSO algorithm, i.e. $C_p = 0.52$ with the best input parameters as shown in Table 4-4 where the population size, maximum iteration, and the computational time is 100, 500, and 2 seconds, respectively.

Table 4-1: The best inputs combination for optimal power coefficient using ABC.

Parameters Population	Tip-speed ratio	Blade radius	Lift to drag ratio	Solidity ratio	Chord length	Power coefficient
20/100	7.4172	3.1133	109.5157	0.1988	0.0263	0.5194
20/200	6.0857	3.0950	90.7939	0.3787	0.1407	0.521
20/300	5.8487	4.9986	109.6556	0.0923	0.0844	0.522
20/400	5.8397	4.3964	107.3829	0.1792	0.1554	0.5201
20/500	5.9943	4.3161	109.5036	0.3746	0.1108	0.5204
20/600	5.8928	4.5605	108.8671	0.4287	0.7379	0.5205
50/100	5.7377	2.8687	109.7278	0.4364	0.3472	0.5222
50/200	5.3950	4.8932	109.2265	0.1239	0.4086	0.5230
50/300	5.6318	4.2792	103.7974	0.3454	0.5742	0.5200
50/400	5.5327	4.3969	109.9993	0.2534	0.3456	0.5229
50/500	5.7349	4.2155	109.1837	0.1174	0.0579	0.5224
50/600	5.4482	4.3330	109.9715	0.4114	0.0882	0.5264
100/100	5.7022	4.4488	108.8699	0.3427	0.6134	0.5225
100/200	5.2578	4.2799	109.8694	0.3986	0.4413	0.5252
100/300	5.4233	3.8321	109.1304	0.3364	0.5265	0.5273
100/400	5.8911	4.7326	108.2643	0.3669	0.2716	0.5244
100/500	5.4479	4.0164	109.4848	0.3885	0.1939	0.5295
100/600	4.8203	4.9185	109.7685	0.1102	0.3148	0.5280

Table 4-2: The best inputs combination for optimal power coefficient using ACO.

Parameters	Tip-speed ratio	Blade radius	Lift to drag ratio	Solidity ratio	Chord length	Power coefficient
Population						
20/100	6.0035	4.6831	109.7894	0.2461	0.0585	0.5199
20/200	6.0066	4.5006	109.2554	0.3341	0.0348	0.5199
20/300	6.0046	4.0498	109.7711	0.4302	0.2544	0.5199
20/400	6.0001	4.6219	109.5373	0.1623	0.0486	0.5199
20/500	6.0022	4.8635	109.9023	0.3353	0.2100	0.5200
20/600	6.0048	4.0759	109.9909	0.4479	0.5094	0.5199
50/100	6.0232	2.1870	109.795	0.3245	0.0355	0.5198
50/200	6.0180	4.3231	109.8697	0.3050	0.1210	0.5199
50/300	6.0076	3.5430	109.9974	0.1563	0.1184	0.5199
50/400	6.0053	4.4361	109.961	0.3522	0.1559	0.5200
50/500	6.0046	3.8912	109.854	0.1849	0.0109	0.5199
50/600	6.0010	4.8231	109.862	0.2622	0.2556	0.5200
100/100	6.0033	4.7002	109.9547	0.3233	0.1534	0.5200
100/200	6.0022	4.7039	109.7430	0.3955	0.4027	0.5199
100/300	6.0005	3.3761	109.7601	0.2001	0.0141	0.5199
100/400	6.0053	2.9701	109.9361	0.2822	0.0583	0.5200
100/500	6.0032	4.3089	109.9935	0.0539	0.0232	0.5200
100/600	6.0067	4.8288	109.9829	0.2424	0.1600	0.5200

Table 4-3: The best inputs combination for optimal power coefficient using PSO.

Parameters	Tip-speed ratio	Blade radius	Lift to drag ratio	Solidity ratio	Chord length	Power coefficient
Population						
20/100	6.0001	4.9980	109.9996	0.3787	0.0545	0.5200
20/200	6.0003	5.0000	109.9900	0.4500	0.6918	0.5176
20/300	6.0000	5.0000	110.0000	0.3877	0.0010	0.5200
20/400	6.0000	4.9989	109.9998	0.4500	0.0010	0.5200
20/500	6.0000	5.0000	110.0000	0.4500	0.0010	0.5200
20/600	6.0000	5.0000	110.0000	0.4500	0.0010	0.5200
50/100	6.0000	4.5.0000	110.00	0.4500	0.0010	0.5200
50/200	6.0000	5.0000	110.00	0.4500	0.0010	0.5200
50/300	6.0000	5.0000	110.00	0.4500	0.0010	0.5200
50/400	6.0000	5.0000	110.00	0.4500	0.0010	0.5200
50/500	6.0000	5.0000	110.00	0.4500	0.0010	0.5200
50/600	6.0000	5.0000	110.00	0.4500	0.0010	0.5200
100/100	6.0000	4.9999	110.00	0.4500	0.0010	0.5200
100/200	6.0000	4.7290	109.997	0.4113	0.0010	0.5200
100/300	6.0000	5.0000	110	0.4500	0.0010	0.5200
100/400	6.0000	5.0000	110.00	0.4500	0.0010	0.5200
100/500	6.0000	4.9845	110.0000	0.4500	0.0010	0.5200
100/600	6.0000	5.0000	110.00	0.4500	0.0010	0.5200

Table 4-4: Optimal value of input parameters of ACO, PSO and ABC algorithms.

Optimal parameters	ACO	PSO	ABC
Tip-speed ratio	6.0032	6.00	5.4479
Blade radius	4.3089	4.50	4.016
Lift to drag ratio	109.9935	110.00	109.4848
Solidity ratio	0.0539	0.45	0.3885
Chord length	0.0232	0.0010	0.193

4.1.3 Computational Time

Computational time refers to the time taken for the algorithm to finish from the first until the maximum number of iterations. The computational time for all algorithms is in second (s). The time taken for all algorithms to complete the maximum iteration for different number of populations is shown in Figure 4-4 to Figure 4-6 and these values can be summarized in Table 4-5. It can be observed that the computational time of ABC algorithm has taken slightly higher than to ACO and PSO.

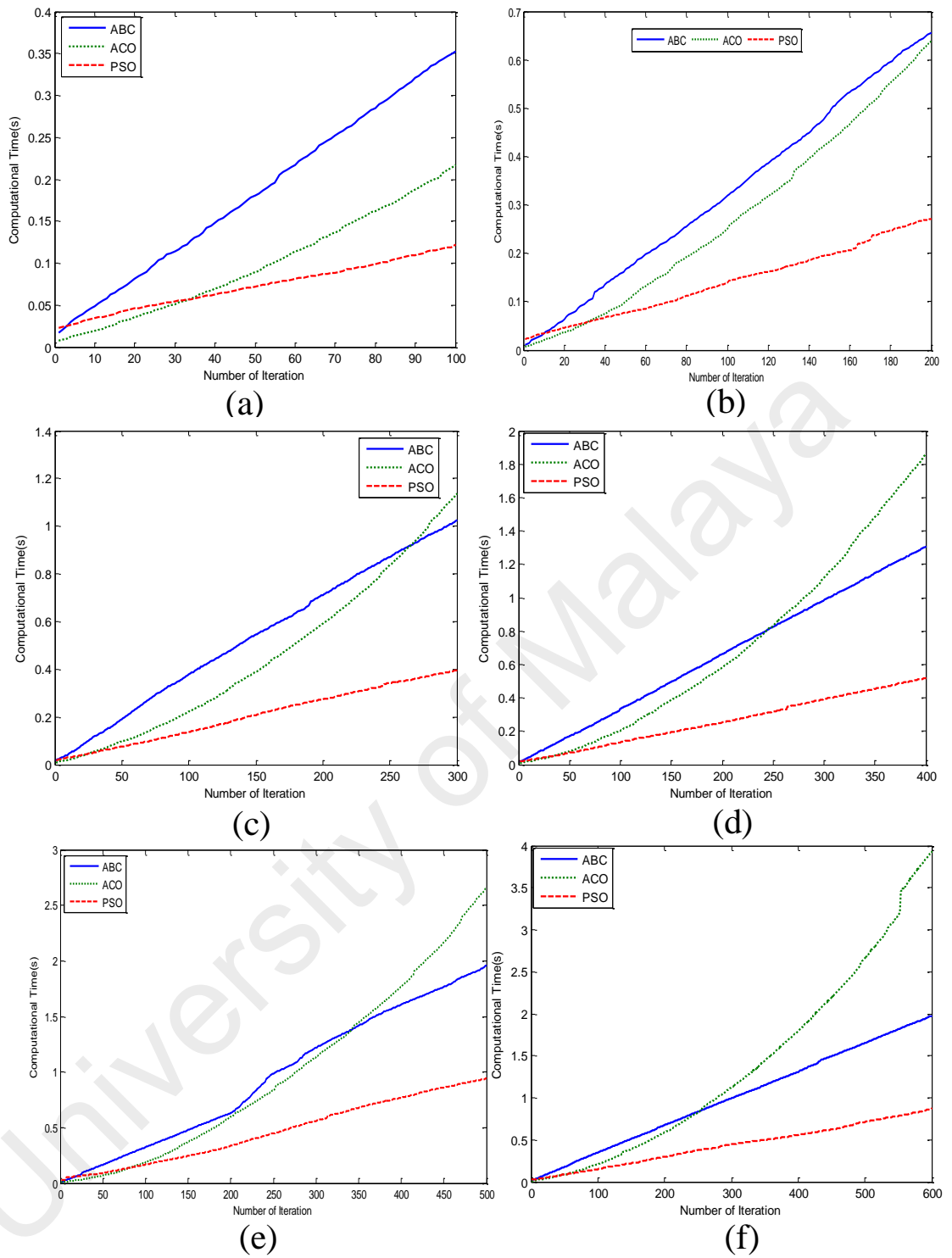


Figure 4-4: The computational time in seconds for natural inspired algorithms where number of populations 20 with different iterations.

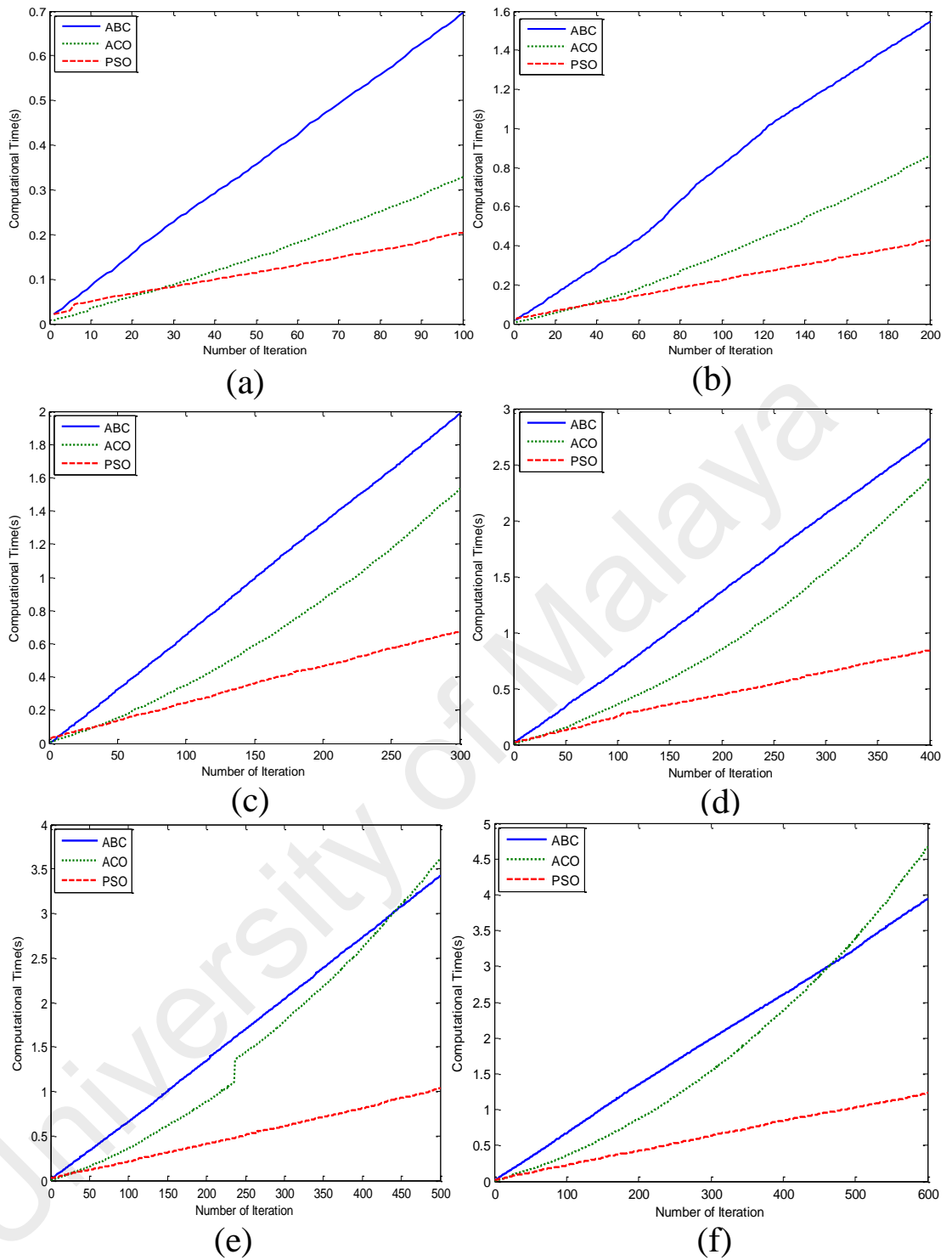


Figure 4-5: The computational time in seconds for natural inspired algorithms where number of populations 50 with different iteration.

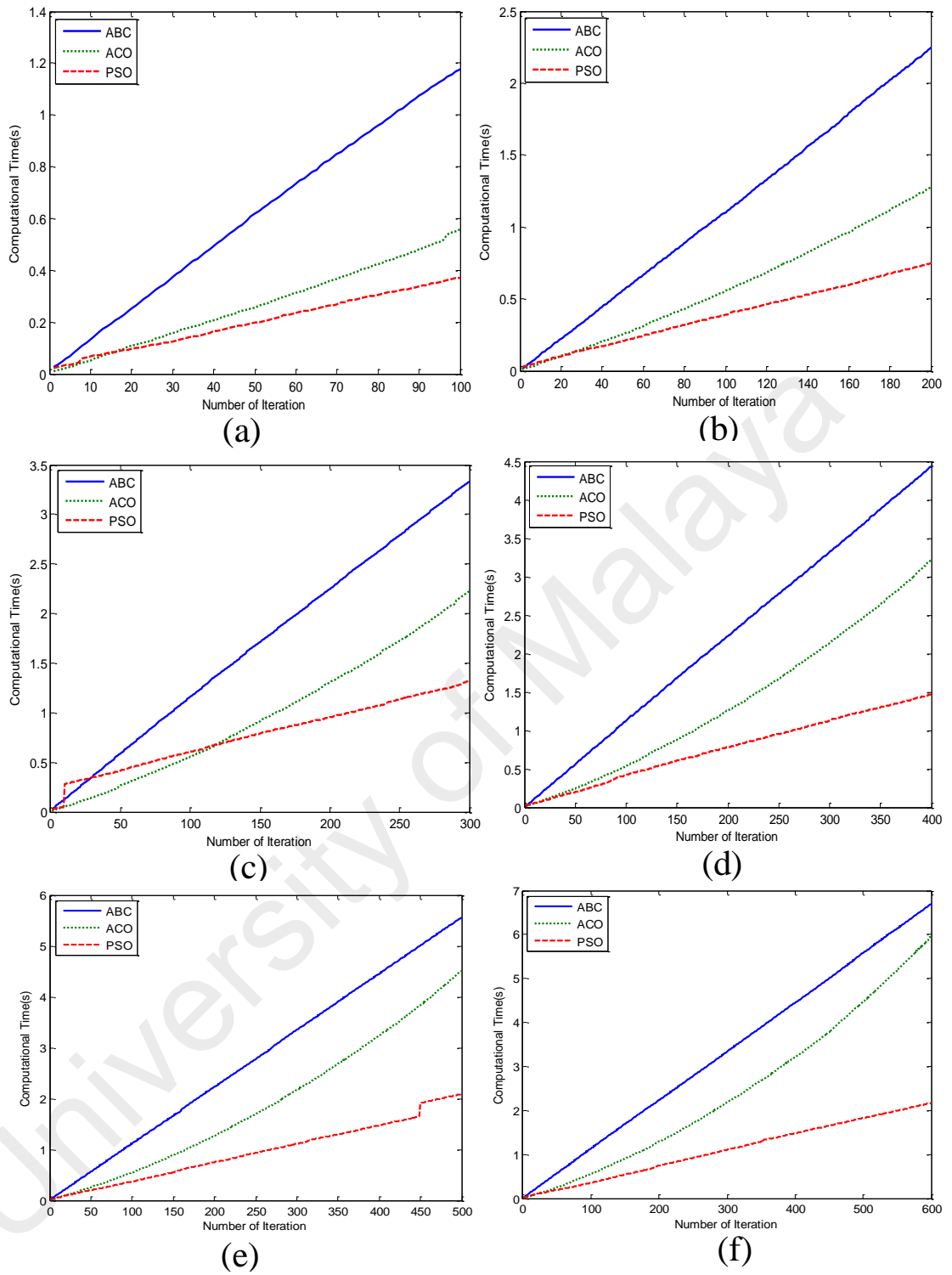


Figure 4-6: The computational time in seconds for natural inspired algorithms where number of populations 100 with different iteration.

Table 4-5: Computation time of different algorithms (ACO, PSO, and ABC) with different population size (20, 50, and 100).

Algorithms	No. of iteration	Computational time(s) for population		
		20	50	100
ACO	100	0.22	0.32	0.59
	200	0.63	0.82	1.25
	300	1.11	1.55	2.25
	400	1.681	2.40	3.25
	500	2.52	3.51	4.50
	600	4.00	4.52	6.00
PSO	100	0.25	0.2	0.39
	200	0.27	0.62	0.75
	300	0.40	0.58	1.25
	400	0.50	0.58	1.5
	500	0.95	1.00	2.1
	600	0.95	1.25	2.1
ABC	100	0.35	0.70	1.19
	200	0.65	1.15	2.25
	300	1.02	2.00	3.40
	400	1.23	2.27	4.50
	500	1.95	3.34	5.50
	600	2	4.00	6.5

4.1.4 Prediction of Power Coefficient Using ANFIS

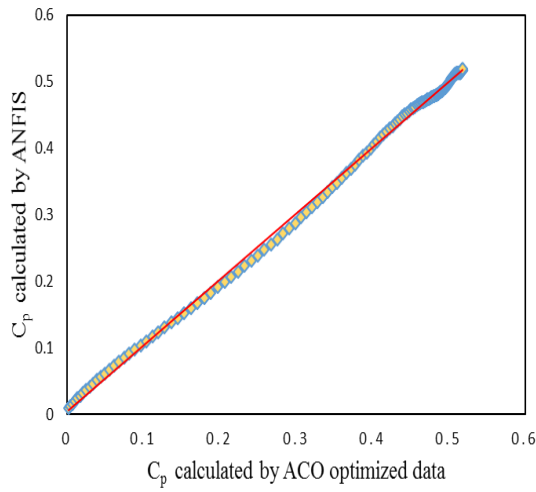
The best input combination of ABC, ACO and PSO algorithms from Table 4-1 to Table 4-3 (highlighted rows) are used in ANFIS for power coefficient prediction. To achieve the goal, 60% data are used for training and 40% data used for testing. The predicted power coefficient training and testing values using ANFIS model for a wind turbine values are presented in Figure 4-7(a) and Figure 4-7(b), respectively. In Figure 4-8(a) and Figure 4-8(b) the training and testing values using ANFIS model for a power coefficient of wind turbine are shown here. Figure 4-9 shows the prediction power coefficient values obtained from ANFIS model and ABC optimization of Eq. (2.13). Figure 4-9(a) provides the results for training data set. It can be noticed that most of the point drop along the diagonal line. Figure 4-9(b) shows the testing data set where most of

the points are very close to diagonal line. It can be concluded that the predicted values ANFIS are very close with the calculated by ABC algorithm.

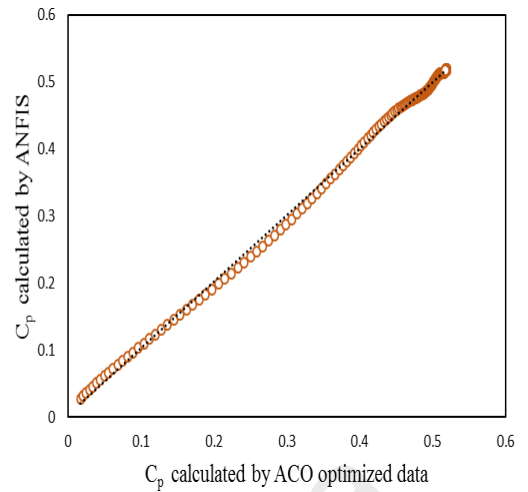
As seen in the Figure 4-7 to Figure 4-9 the coefficient determination (R^2) are very high. Therefore, the ANFIS model used for the study has a promising R^2 with the wind turbine model. Note that the R^2 is higher for the ABC-ANFIS power coefficient' shown in Table 4-6, that translates to a better correlation.

Figure 4-10 illustrate the predicted and measured values of ACO algorithm using ANFIS model for a power coefficient of wind turbine. It can be observed that, the predicted and measured value are almost similar with the value of is 0.5175 and 0.52, respectively. Figure 4-11 shows the predicted by ANFIS and measured values by PSO of 0.5135 and 0.52 respectively. An ANFIS method is very supportive for faster prediction of power coefficient with blades parameters. Figure 4-12 shows the wind power coefficient comparison between predicted and measured values ABC algorithm using ANFIS technique. From Figure 4-12, the measured (optimized) values ($C_p = 0.529$) are very close to the predicted valued $C_p = 0.5215$, i.e. the variation is small.

Figure 4-13 shows the predicted power coefficient comparison between ACO, PSO, and ABC values. The prediction of power coefficient of ABC algorithm value is higher as compared to ACO and PSO algorithms. Thus, the proposed ANFIS model has obtained high accuracy in predicting wind turbine power coefficient.



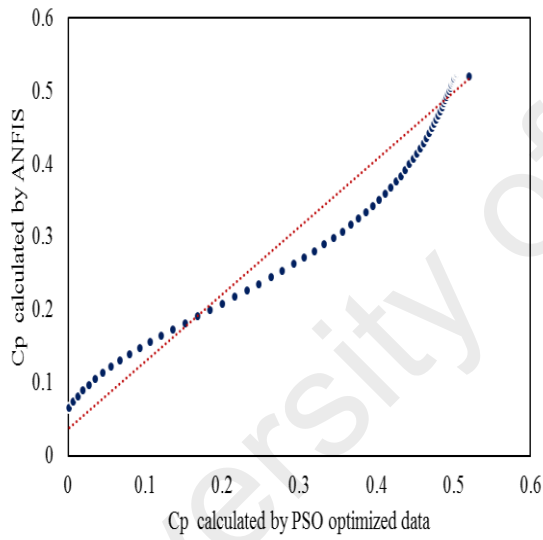
(a) Training data set



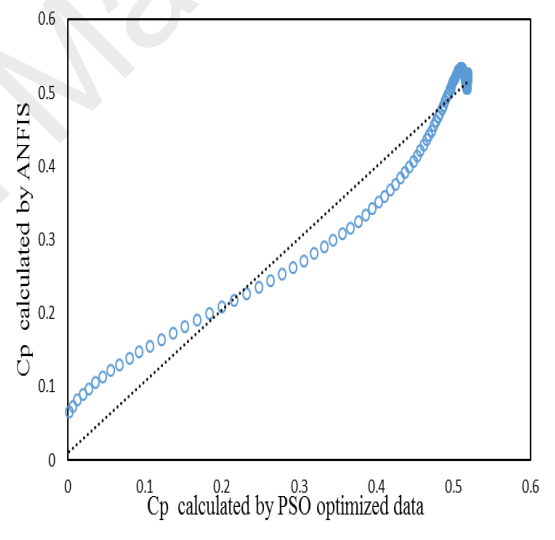
(b) Testing data set

Figure 4-7: Power coefficient prediction by ANFIS and optimized (ACO)

: (a) Training data set and (b) Testing data set.



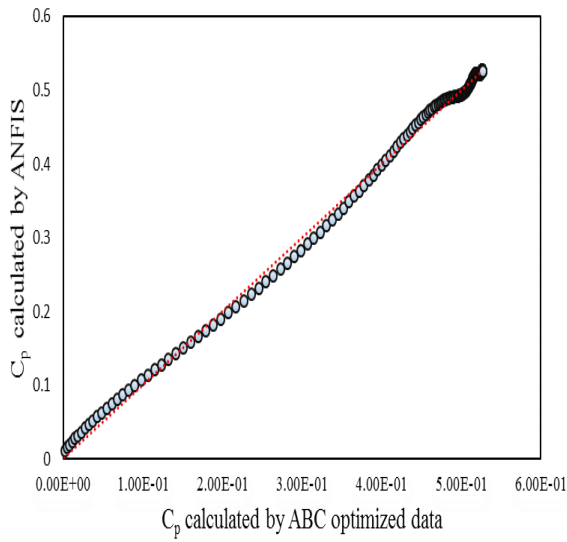
(a) Training data set



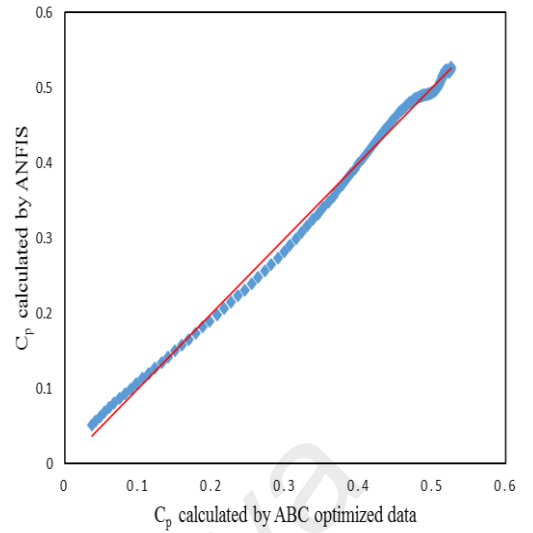
(b) Testing data set

Figure 4-8: Power coefficient prediction by ANFIS and optimized (PSO)

: (a) Training data set and (b) Testing data set.



(a) Training data set



(b) Testing data set

Figure 4-9: Power coefficient prediction by ANFIS and optimized (ABC)

: (a) Training data set and (b) Testing data set.

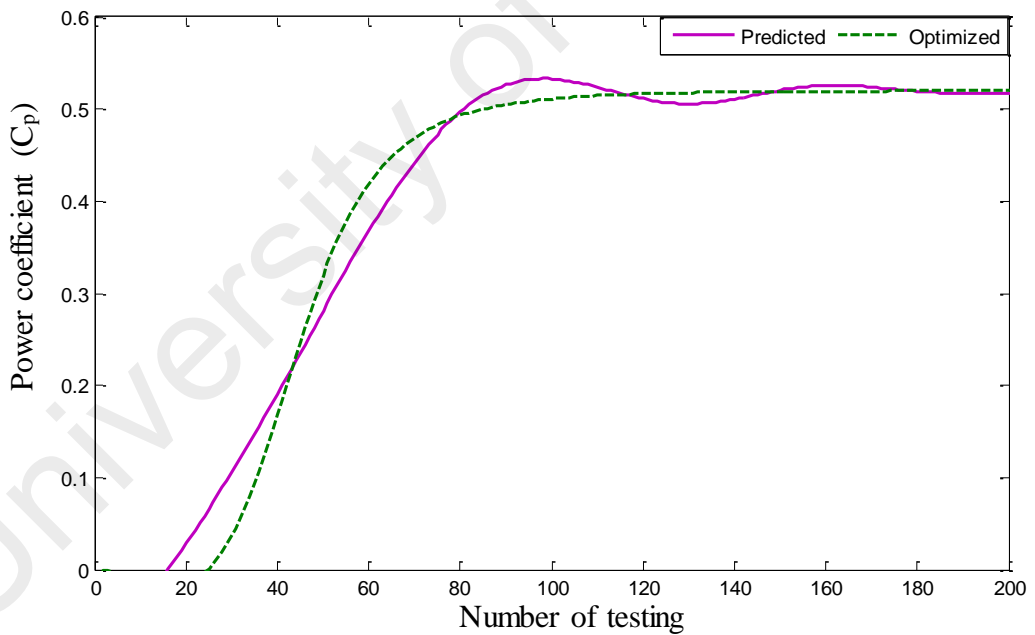


Figure 4-10: Predicted (ANFIS) versus optimized (ACO) of power coefficient.

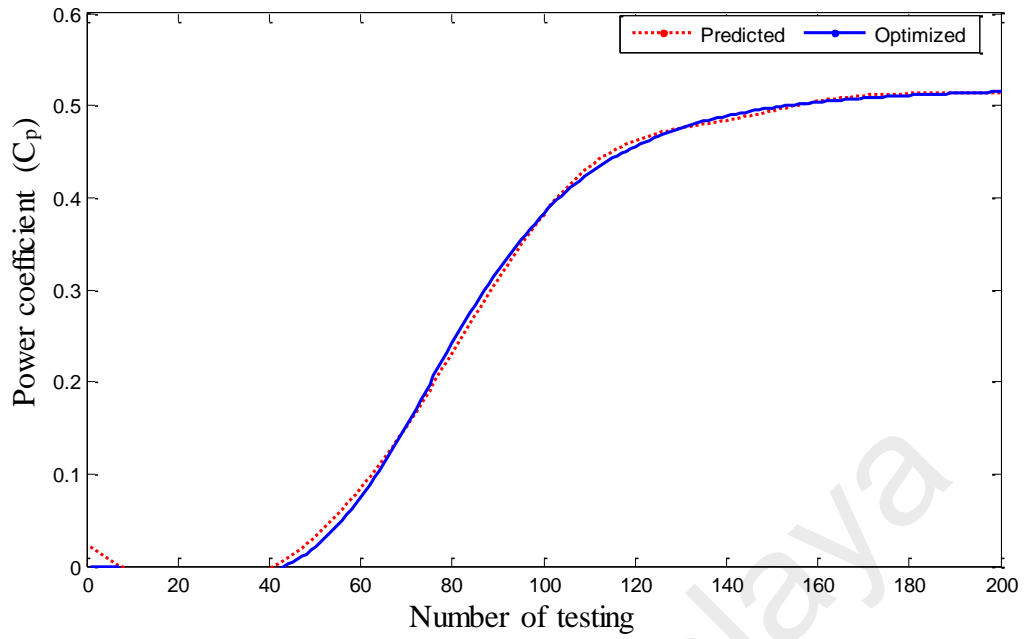


Figure 4-11: Predicted (ANFIS) versus optimized (PSO) of power coefficient.

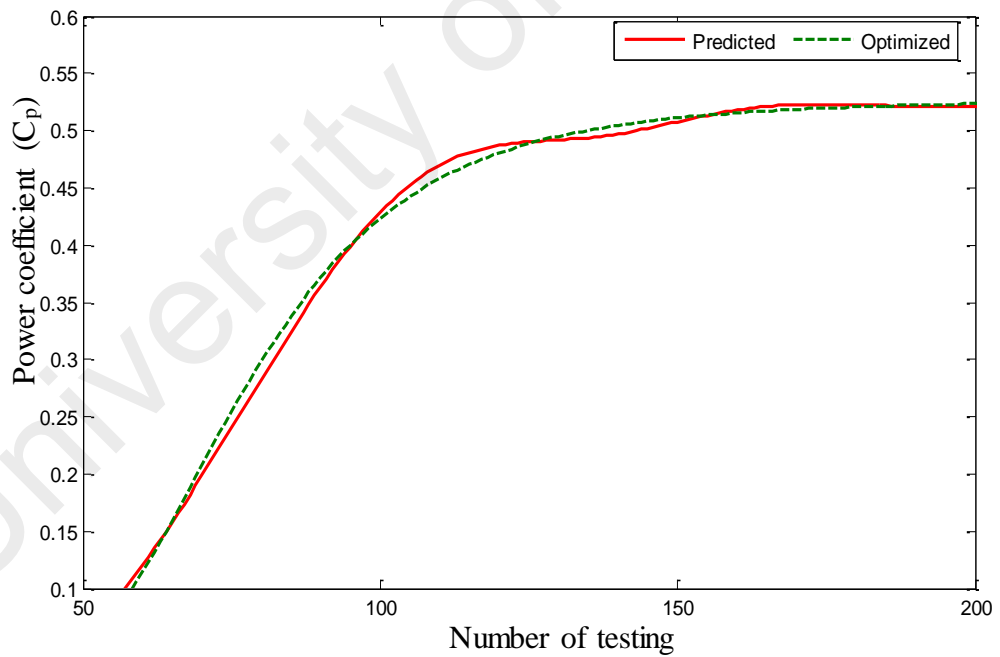


Figure 4-12: Predicted (ANFIS) versus optimized (ABC) of power coefficient.

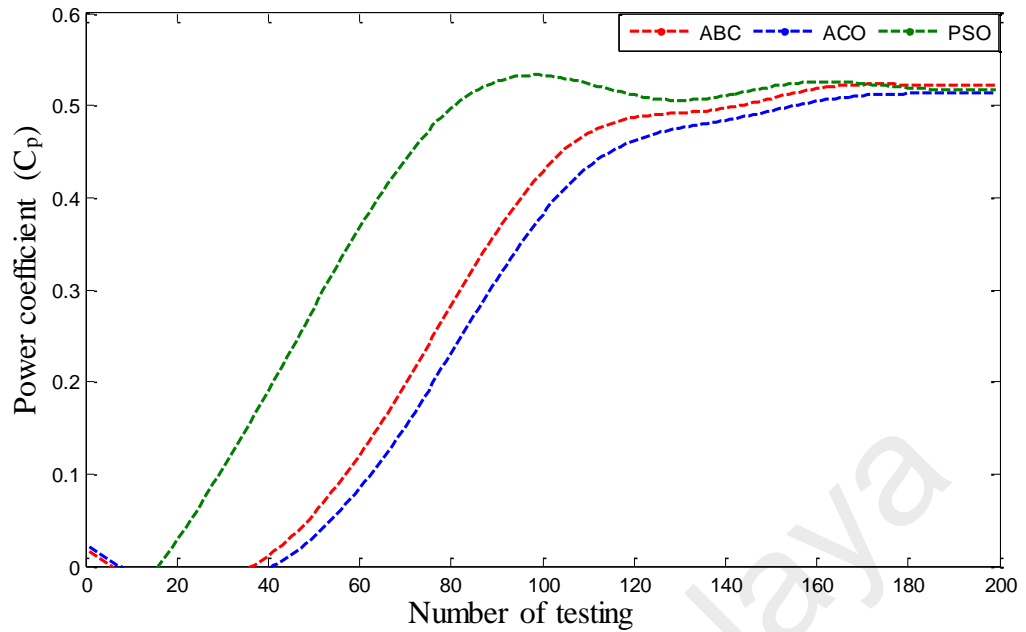


Figure 4-13: Prediction of ACO, PSO, and ABC.

Table 4-6: Performance of the established training and testing of ANFIS models for power coefficient based on statistical indicators.

Model	Training		Testing	
	RMSE(W/m ²)	R ²	RMSE(W/m ²)	R ²
ABC-ANFIS	0.00654	0.999	0.363	0.9985
ACO-ANFIS	0.00544	0.9989	0.814	0.997
PSO-ANFIS	0.235	0.9711	1.911	0.9777

Table 4-6 shows the results of the statistical analysis for proposed ANFIS model for both training and testing values. There are two statistical indicators that have been used to evaluate the proposed model performance, i.e. RMSE and R^2 . Noted that the units of RMSE and R^2 are dimensionless respectively. Based on the results, the difference in RMSE and R^2 values for training and testing are relatively small. Therefore, it delivers additional evaluation and verification on the suitability of proposed ANFIS model to estimate power coefficient. The investigation results recommended that the proposed ANFIS model can effectively be implanted for prediction for all cases of ABC, ACO and PSO algorithms optimization. Based on the ANFIS results, ABC algorithm shows better

accuracy both for optimization and prediction in comparison with ACO and PSO algorithms results. The ANFIS model has very small RMSE (0.363) during testing and the value is slightly higher (0.00654) in training of ABC-ANFIS model for power coefficient. It has been observed that the ANFIS model showed constantly good correlation throughout the testing and training. Therefore, the study results suggested that the proposed ANFIS model can effectively be embedded for prediction of for all cases of ABC, ACO and PSO algorithms optimization. Also, the ABC algorithms shows better accuracy in both optimization and prediction as compared to ACO and PSO algorithms.

4.1.5 Validation of Power Coefficient Optimization and Prediction

Table 4-7 shows that the validation of this present investigation with related literatures. Sedaghat and Mirhosseini (2012) carried out the investigation of 300-kW HAWT for aerodynamic design of province of Semnan. They used the BEMT for the blade "Airfoil is RISØ-A1-18". The power coefficient was found to be 0.51 which was almost similar to my present investigation. Rajakumar and Ravindran (2012) optimized the power coefficient of wind turbine rotor using the blade "Airfoil NACA 4410" and "NACA 2415" by CFD analysis. The C_p of the blade "Airfoil NACA 4410" and "NACA 2415 were found to be 0.48 and 0.45, respectively. The obtained power coefficients of both airfoils were slightly lower than the present investigation. Based on the supervisory control and data acquisition (SCADA) data, Dai et al. (2016) investigated the C_p of wind turbines. They have discovered that the C_p was 0.508 which was almost similar to my present investigation. Table 4-7 shows that the power coefficients of the present investigation are consistent and reliable with the findings of the other researchers. Therefore, it can be concluded that the power coefficient obtained from the literatures supports the results obtained in this research.

Table 4-7: Validation of this present investigation with related literatures.

Subject	Theory	Blade Model	Maximum C_p
Present Investigation	ABC algorithms	Airfoil S822	0.529
	ACO algorithms		0.52
	PSO algorithms		0.52
	ABC-ANFIS		0.5215
	ACO-ANFIS		0.5175
	PSO-ANFIS		0.5135
Validation	BEMT (Sedaghat & Mirhosseini, 2012)	Airfoil is RISØ-A1-18	0.51
	CFD analysis (Rajakumar & Ravindran, 2012)	NACA 4410	0.48
		NACA 2415	0.45
	SCADA system (Dai et al., 2016)	-----	0.508

4.2 Long-Term Wind Speed Forecasting

Figure 4-14 and Figure 4-15 shows WSF of these places when using tansig and logsig transfer function of NAR and NARX respectively. From Figure 4-14 (a) and 4-15 (a) it can be seen that the tansig function results in greater accuracy in WSF (MAE 0.014, MAPE 14.79%, and RMSE 1.102) than logsig function (MAE 0.041, MAPE 16.78%, and RMSE 1.281) for Kuala Lumpur based on Table 4-9. The accuracy of tansig function (MAE 0.025, MAPE 19.27%, and RMSE 1.15) is more than the logsig function (MAE 0.134, MAPE 28.84%, and RMSE 1.788) which can be shown in Figure 4-14(c) and 4-14(d) for Kuantan. As shown in Figure 4-14(e) and 4-14(f), a better precision of tansig function (MAE 0.029, MAPE 10.79%, and RMSE 0.583) is obtained in comparison to logsig function (MAE 0.339, MAPE 11.03%, and RMSE 0.858) for Melaka.

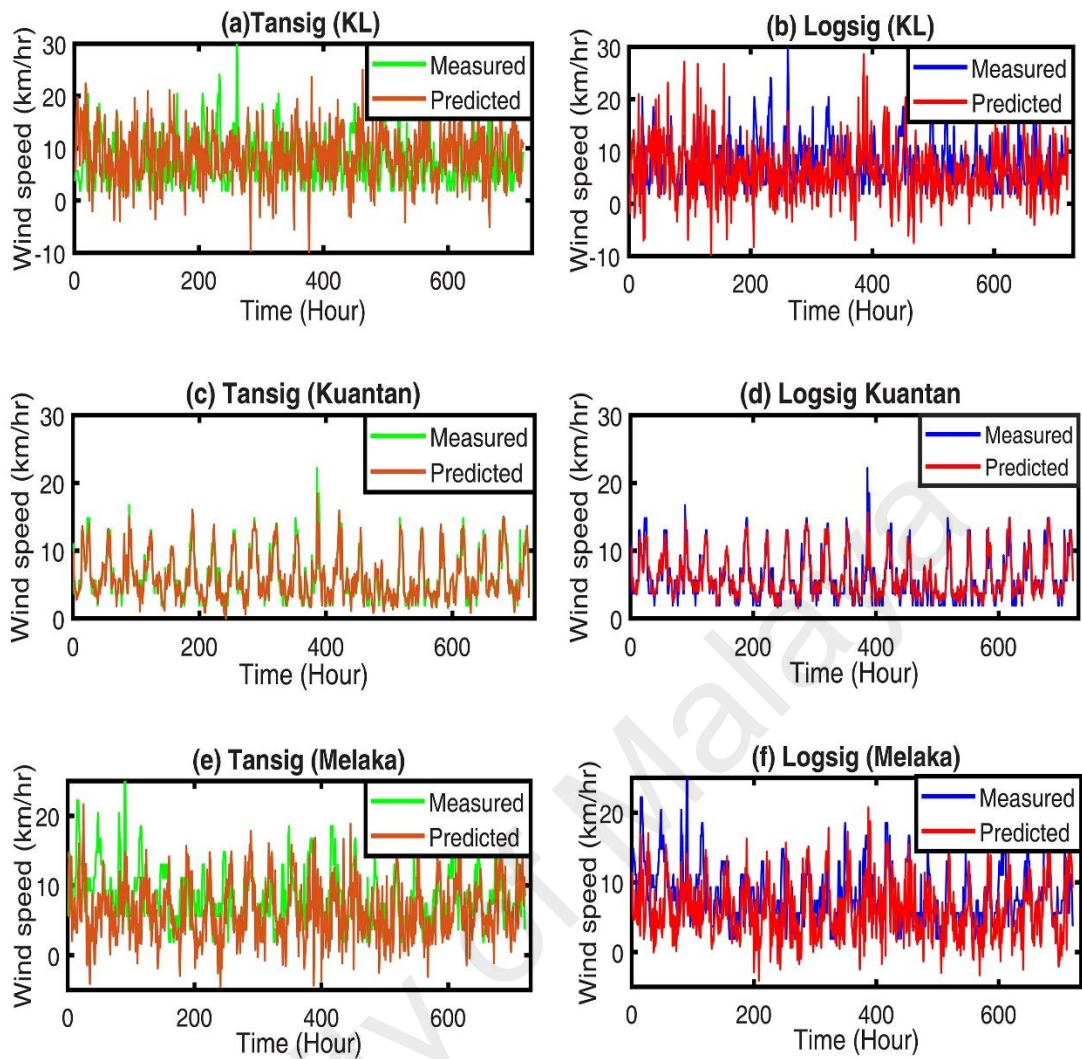


Figure 4-14: Comparison of wind speed forecasting from proposed activation functions of NARNN methods at Kuala Lumpur, Kuantan and Melaka.

Figure 4-15 shows a 1-month-ahead WSF at these places using tansig and logsig functions of NARXNN. For Kuala Lumpur, the performance of tansig function (MAE 0.046, MAPE 14.22%, and RMSE 1.231) is slightly higher than the logsig function (MAE 0.058, MAPE 12.04%, and RMSE 1.028), as shown in Figure 4-15(a) and 4-15(b). For Kuantan, as shown in Figure 4-15(c) and Figure 4-15(d), the accuracy of logsig function (MAE 0.880, MAPE 22.55%, and RMSE 1.485) is lower than tansig function (MAE 0.550, MAPE 20.46%, and RMSE 1.212). For Melaka, the performance accuracy between two activation functions namely tansig and logsig are (MAE 0.434, MAPE 11.23%, and RMSE 0.853) and (MAE 0.180, MAPE 15.15%, and RMSE 1.28),

respectively, with tansig function outperformed logsig function in terms of accuracy, as shown in Figure 4-15 (e) and 4-15(f).

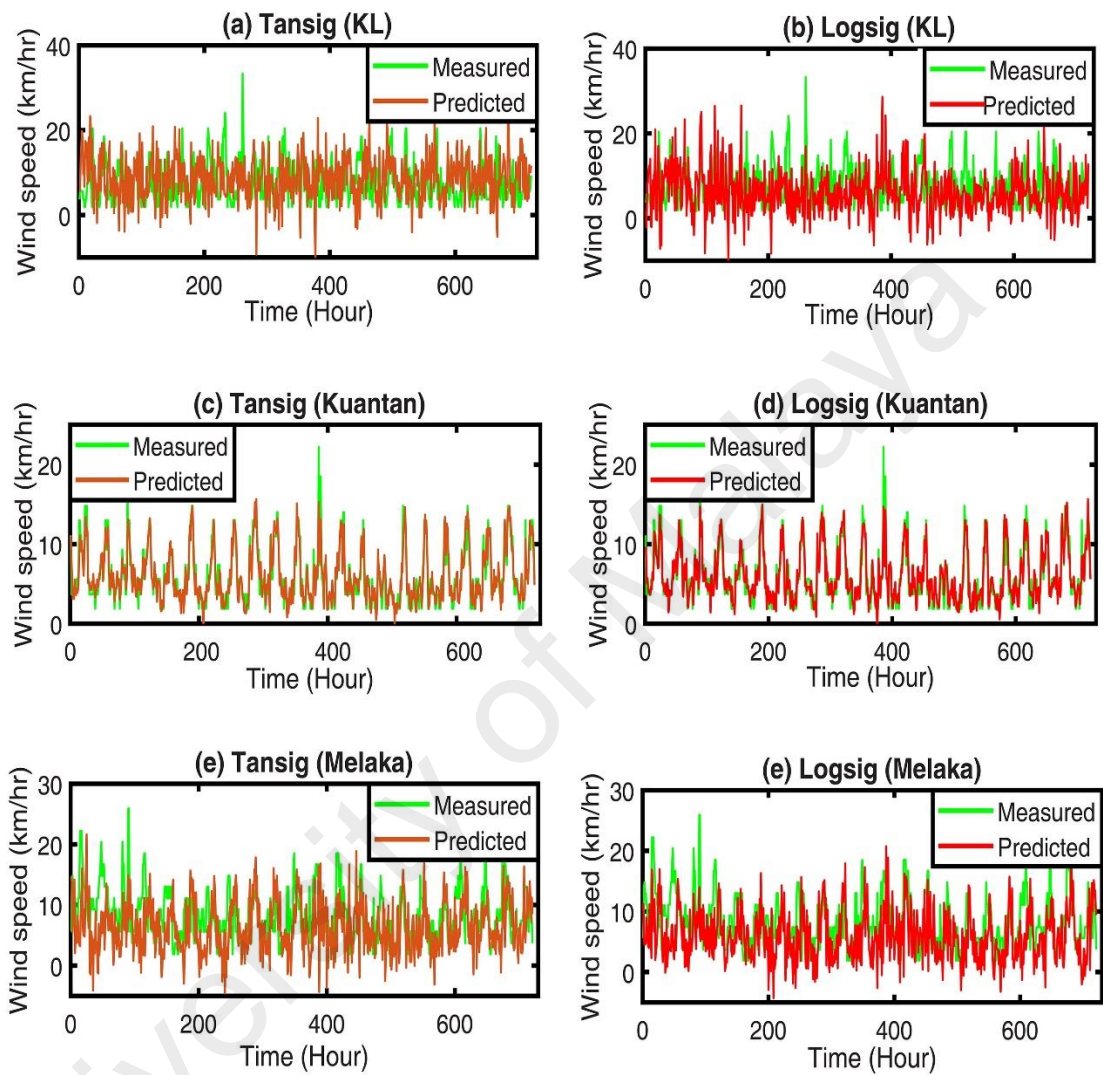


Figure 4-15: Comparison of wind speed forecasting from proposed activation functions of NARXNN methods at Kuala Lumpur, Kuantan and Melaka.

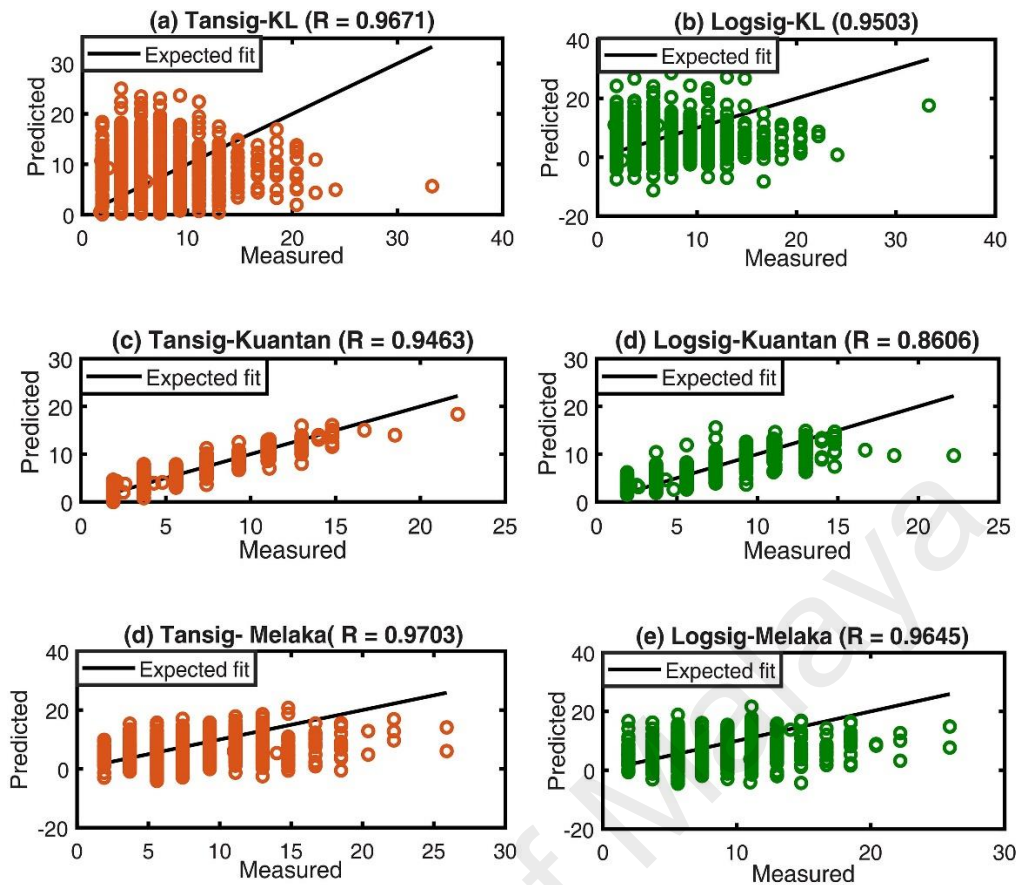


Figure 4-16: Correlation of coefficient of wind speed forecasting at Kuala Lumpur, Kuantan, and Melaka using both activation functions (tansig and logsig) of NARNN.

The ratio of contraposition of predicted and measured values' outcome can be defined as correlation of coefficient (R) which is between -1 and 1. The R is presented as how well a regression model fits the data. The scattered values of predicted and measured wind speed have been shown in Figure 4-16. Two different activation functions of NARNN provides WSF results for these places. As expected, most of the predicted and measured values are around to the diagonal line in all cases. By using tansig function, the correlation coefficient in case of Kuala Lumpur, Kuantan, and Melaka were obtained as 0.9671, 0.9463, and 0.9703, respectively. By using logsig function, the correlation coefficient of Kuala Lumpur, Kuantan, and Melaka were obtained to be 0.9503, 0.8606, and 0.9645, respectively. From Figure 4-17, the correlation coefficients from tansig-NARX function were found to be near value 1 (Kuala Lumpur: 0.9665, Kuantan: 0.9288, and Melaka: 0.9780) whereby for logsig function, the correlation coefficients were more deviated from

value 1 (Kuala Lumpur: 0.9514, Kuantan: 0.9115, and Melaka: 0.9561). Based on above evaluation, the coefficient of correlation values for all cases were found in between 0.85 to 0.97 which are almost near to 1. The tansig- NAR and tansig-NARX both functions display slightly better than the logsig-NAR and logsig-NARX for wind speed forecasting in all those places.

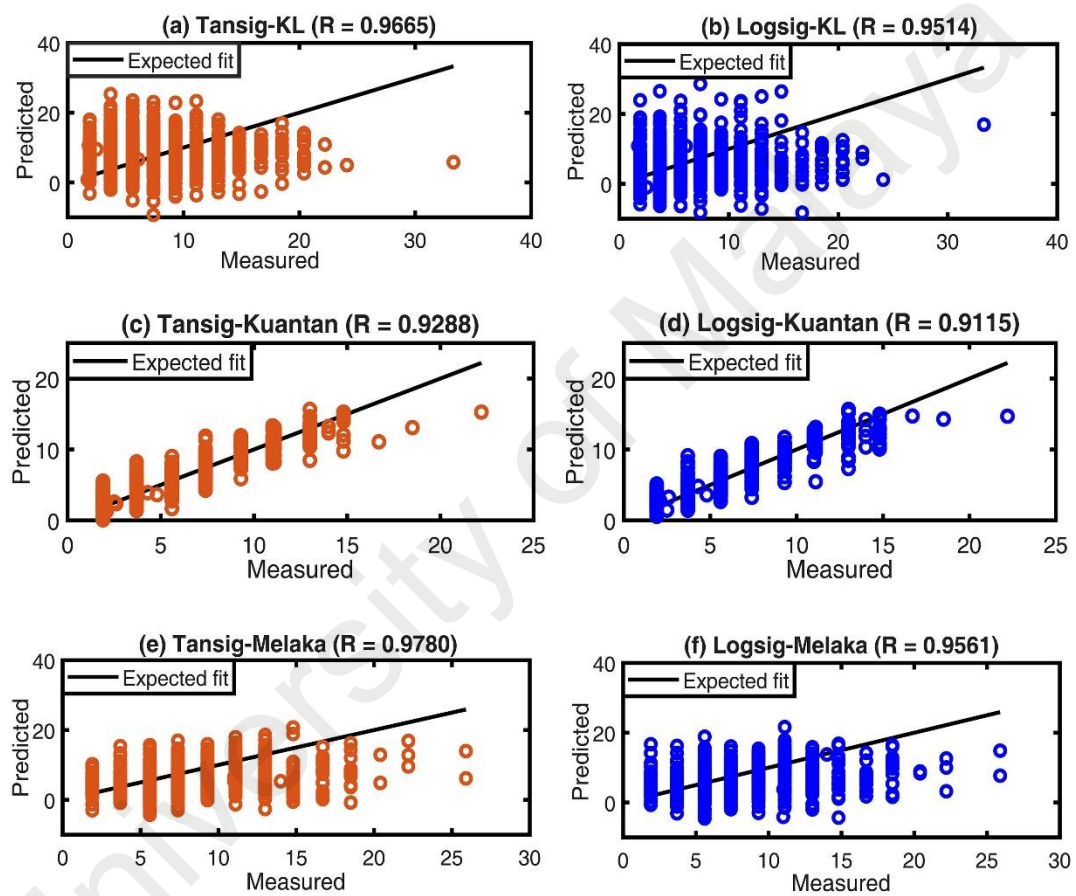


Figure 4-17: Correlation of coefficient of wind speed forecasting at Kuala Lumpur, Kuantan, and Melaka using both activation functions (tansig and logsig) of NARXNN.

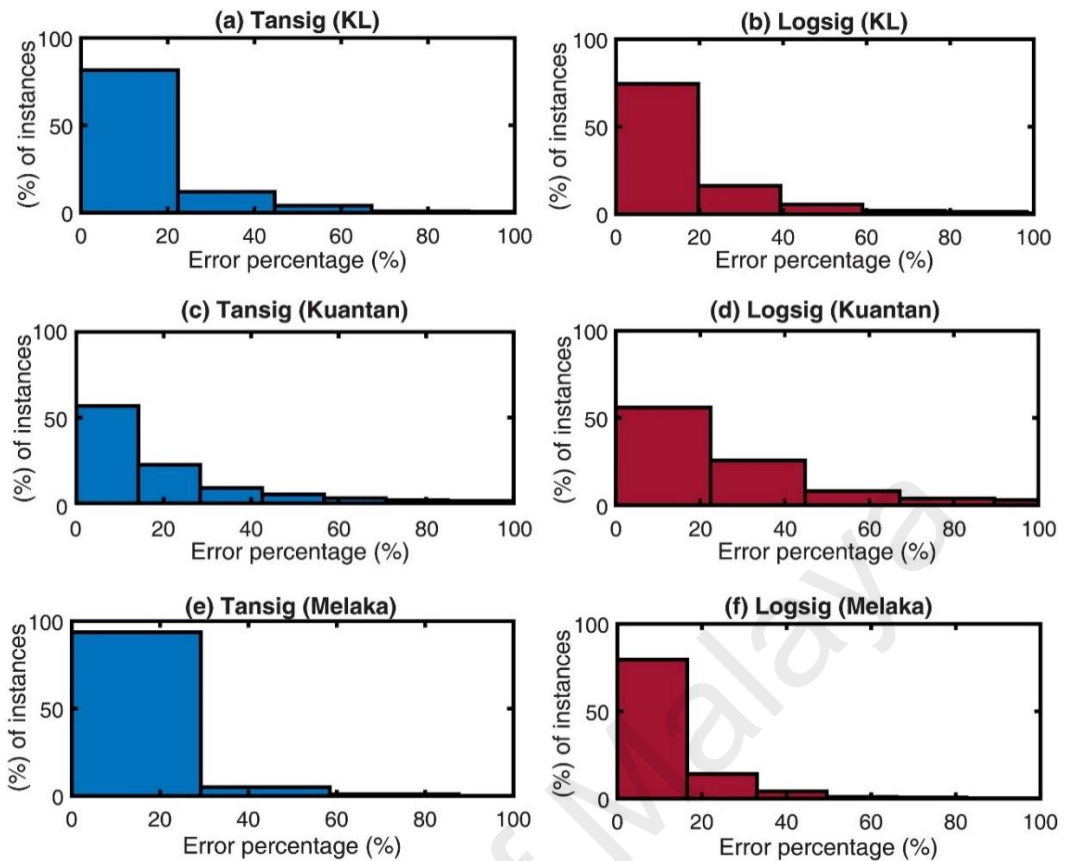


Figure 4-18: Success rate of test wind speed data for Kuala Lumpur, Kuantan, and Melaka using both activation functions (tansig and logsig) of NARNN.

Figure 4-18 and Figure 4-19 show the success rates of the forecasted results where the y axis represents the number of instances i.e. number of test datasets and x axis represents the error in percentage. So, Figure 4-18 and Figure 4-19 mostly show how much test datasets (in percent) resides in low and high error region. It is noticeable that tansig function provides better success rates than logsig function for these places. At Kuala Lumpur, tansig-NAR provides the 85% success rate where the error percentage is 22%. While the logsig-NAR achieves 78% success rate at 20 percentages error. In Kuantan area, the tansig-NAR provide provides around 57% instances at 15% error while the logsig-NAR come around 55 % instances within 22% error. For instance, using tansig, success rates in case of Melaka comes around 95% at 29 percentage error. On the other hand, at 18% error, the instances of forecasting deliver 83%.

Figure 4-19 shows in terms of “percentage of instances” vs. “error bin in percentage”, for two activation functions of NARX. For instance, using tansig, success rates in case of Kuala Lumpur, Kuantan, and Melaka come around 85%, 64%, and 96% respectively. For instance, using logsig, success rates in case of Kuala Lumpur, Kuantan, and Melaka come around 76%, 53%, and 64% respectively. However, logsig-NARX provide the percentage of instance is slightly higher than the tansig-NARX in Kuantan while the error percentage of tansig-NARX shows the better than logsig-NARX. It can be seen that tansig deliveries better success rates than logsig for all three palaces.

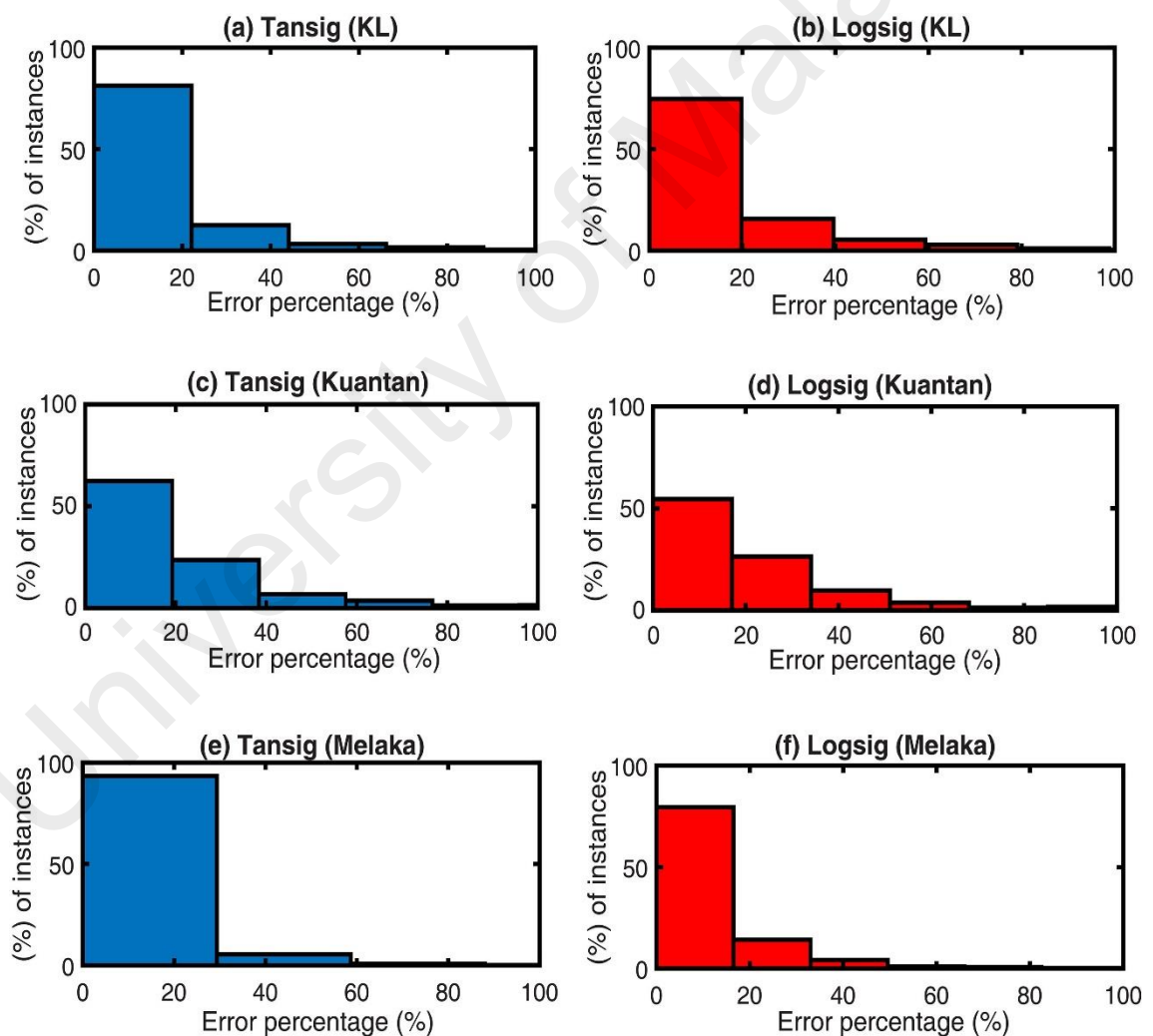


Figure 4-19: Success rate of test wind speed data for three different areas in Malaysia using both activation functions (tansig and logsig) of NARXNN.

Table 4-8: Model parameters of NARNN and NARXNN with tansig and logsig functions.

Areas		NAR and NARX Neural Network							
		Tansig				Logsig			
		Epoch	Time (s)	Performance	Neuron	Epoch	Time (s)	Performance	Neuron
NARNN	Kuala Lumpur	160	58	1.02	20	160	65	1.55	20
	Kuantan	160	55	1.21	20	160	65	1.39	20
	Melaka	161	62	1.34	20	160	71	2.11	20
NARXNN	Kuala Lumpur	160	66	1.24	20	160	70	1.36	20
	Kuantan	160	99	1.09	20	160	112	1.38	20
	Melaka	160	78	1.12	20	160	80	1.29	20

Table 4-8 shows the key four parameters of NARNN and NARXNN namely epoch, time, performance and number of hidden neurons. In this study, epoch and number of neurons were fixed, where other two parameters were varied with input characteristics, i.e. fluctuation of wind speed. For NARNN, the neural network performance of tansig function are 1.02, 1.21, and 1.34 for Kuala Lumpur, Kuantan, and Melaka, respectively. On the other hand, the logsig-ANN shows the higher performance 1.39 at Kuantan while the lower performance 2.11 delivers at Melaka. The tansig training function completed at the shortest time, i.e., 55s. The performance of tansig function has showed the lowest value of 55s for Kuantan in comparison with Kuala Lumpur and Melaka. In terms of the operation time, 65s is needed for logsig function for Kuantan and KL, which is lower than Melaka. For NARXNN, the performance of neural network of tansig function has showed the lowest value at 1.09 for Kuantan as compared with the other two areas. For Kuantan, Kuala Lumpur and Melaka, the neural network performance of logsig function are 1.38, 1.36, and 1.29, respectively. By using tansig function, the operation time taken for Kuala Lumpur, Kuantan, and Melaka are 66s, 99 s, and 78s, respectively. For logsig function, the operation time of the same places are 70s, 112s, and 80s in that order. It can be concluded that based on the above discussion, not only the performance of the tansig

activation function is always made significant contribution assessment to the logsig function, but also at the operation time neural network.

Table 4-9: Performance indicators of WSF.

Areas		NAR and NARX Neural Network					
		Tansig			Logsig		
		MAE (m/s)	MAPE	RMSE	MAE (m/s)	MAPE	RMSE
NARNN	Kuala Lumpur	0.014	14.79	1.102	0.041	16.78	1.281
	Kuantan	0.025	19.27	1.15	0.134	28.84	1.788
	Melaka	0.029	10.79	0.583	0.339	11.03	0.858
NARXNN	Kuala Lumpur	0.046	14.22	1.231	0.058	12.04	1.028
	Kuantan	0.550	20.46	1.212	0.880	22.55	1.485
	Melaka	0.0317	9.53	0.833	0.434	11.23	0.853

Three performance indicators are used to measure the accuracy of WSF for three different regions with two transfer functions of NARNN and NARXNN, as shown in Table 4-9. Firstly, by considering MAE, tansig function shows a better result in terms of MAE, i.e. 0.014 for KL as compared with the other two wind stations. The logsig training function provides the best result with MAE of 0.041 for KL wind station in comparison to Kuantan and Melaka. MAE results of both tansig-NARNN and logsig-NARNN are found to be lower than MAE of 0.8 m/s, which was provided (Azad et al., 2014) for long-term wind speed forecasting at Malaysia. Secondly, considering the MAPE, the lowest MAPE value was found for Melaka when using tansig function (MAPE of 10.79). In addition, the MAPE values of Kuala Lumpur and Kuantan are 14.79 and 19.27, respectively. The lowest MAPE value among these places when using logsig function is 11.03 for Melaka station. Thirdly, by considering the RMSE, the tansig function provides a smaller value (RMSE of 0.583) for Melaka, whereby the other two areas show almost similar values of RMSE of around 1.15. Moreover, the logsig function shows the lowest RMSE value, i.e. 0.858 for Melaka. The RMSE value of Kuala Lumpur is almost similar to Kuantan (RMSE of around 1.788). For NARXNN, three performance indicators namely MAE (0.0317), MAPE (9.53), and RMSE (0.833) have showed lower values for

tansig in comparison to the logsig transfer function as shown in Table 4-9. From the Table 4-9. It can be decided that the tansig function display lower error based on the RMSE, MAE and MAPE indicators for wind speed forecasting.

In support of the above outcome, Table 4-10 shows the outcome of different studies that used both tansig and logsig activation functions for various forecasting tasks. It can be seen that the results of these studies also found tansig to be a better activation function. Therefore, it can be concluded that tansig activation function should be used in NAR and NARX neural networks to obtain a better accuracy on time series forecasting jobs. The primary reason is that logsig function is more prone to neuron-saturation. If an input value is large, logsig function makes the gradient close to zero, whereas tansig function provides much greater gradient. Therefore, for the same number of epochs, logsig function makes NARNN learn lesser than tansig function. This is why for the exact same epochs, topology, initial weights and other similar settings, tansig always provides a better accuracy than logsig function, as presented above. Therefore, it can be said that the outcome of some previous similar studies on time series forecasting which used only logsig such as could have been better if tansig had been used.

Table 4-10: Supportive outcome other studies.

Studies	ANN Model	Objective	Accuracy with tansig	Accuracy with logsig
(Zadeh et al., 2010)	Multi-Layer Perceptron (MLP)	To predict daily outflow	($R^2 = 0.89$ and RMSE = 1.69)	($R^2 = 0.80$ and RMSE = 2.30)
(Vafaeipour et al., 2010)	MLP	To predict Wind velocity	(MAE = 1.48, RMSE = 1.22 and $R^2 = 0.843$)	(MAE = 1.48, RMSE = 1.218 and $R^2 = 0.844$)
(Rezaeianzadeh et al., 2013)	MLP	To forecasting daily outflow	($R^2 = 0.87$ and RMSE = 1.87)	($R^2 = 0.84$ and RMSE = 2.1)
(Musa et al., 2019)	MLP	To identify potential archers of psychological coping skill variables	94% efficiency	84% efficiency
(Aladag, 2017)	ANN	To forecast the number of outpatient visits	(RMSE = 203.06)	(RMSE = 243.28)
(Gomes et al., 2011)	ANN	To forecast financial time series	(MAPE=20%)	(MAPE =25.7 %)

4.3 Pitch Angle Controlling

PID controller parameters have been optimized by ACO algorithm through MATLAB/Simulink for pitch angle controlling of wind turbine to WTG power within rated power. At first, there are some ACO parameters selected for conducting optimization processes namely the number of ants, number of paths and population of PID parameters etc. After starting the process of model, the system evaluates the objective/cost function. The cost function of the system is error between desired power to actual power. After each iteration, optimum values of PID parameters are updated and stopped when maximum iteration number have reached or when the objective function criterion is satisfied. In this study, number of ants and number of iterations were 50 and 10, respectively. The search range for PID parameters K_p , K_i and K_d was selected

randomly between $[-100, 1 \times 10^{-13}, 6 \times 10^{-07}] \sim [100, 1 \times 10^{-03}, 6 \times 10^{-01}]$. The optimum PID parameters of three controllers are shown in Table 4-11.

The calculation of pitch angle that has been sent to servo motor block for adjusting blade pitch by the controller which is shown in Figure 4-21. The output of servo motor is used as pitch angle of wind power conversion system. For controlling pitch angle, the output power will be maintained within nominal power. The Mean Squared Error (MSE) that has been collected from MATLAB workspace, has been sent by error signal using ACO algorithm. The MSE error is shown in Figure 4-20. From the Figure 4-20, after around 5 iteration, the convergence curve reached at lower value 0. The MATLAB/Simulink model of WT has been conducted by PID controller parameters optimization using ACO algorithm.

PID-ACO is carried out the ACO algorithm. But the trial and error process are used for the PID controller parameter tuning. Normal fuzzy technique is used for the Fuzzy-PID. The PID-ACO controller result presents the better result of smoothing output power of WT in comparison with conventional PID controller parameter and Fuzzy-PID controller Figure 4-22(a).

Figure 4-22(b) shows the zoomed figure area. In an analysis of output power of WT with pitch angle controlling, PID-ACO is obtained below 5.01×10^5 kW that is very near to desired output power (5×10^5) of WT. In addition, Fuzzy-PID is also gained 5.05×10^5 kW at time 34s. It can be noticed that the output power of WT with Fuzzy-PID controller is fluctuating at different point that (13s, 17s, 34s and 90s) which are higher than PID controller output power shown in Figure 4-22. On the other hand, the output power with PID controller is obtained 5.25×10^5 kW that is higher than the desired output power of WT. Based on above discussion, it can be concluded that the tuned PID

controller with ACO method can be stabled output power of WT smoothing to compare PID and Fuzzy-PID controllers

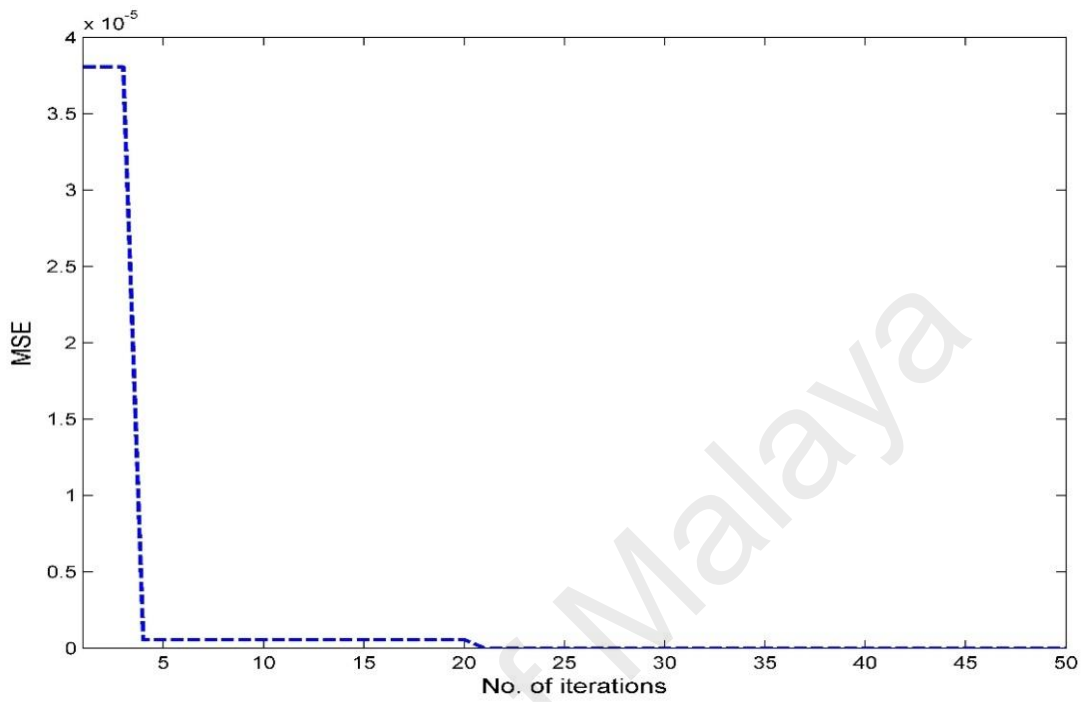


Figure 4-20: Convergence curve of ACO.

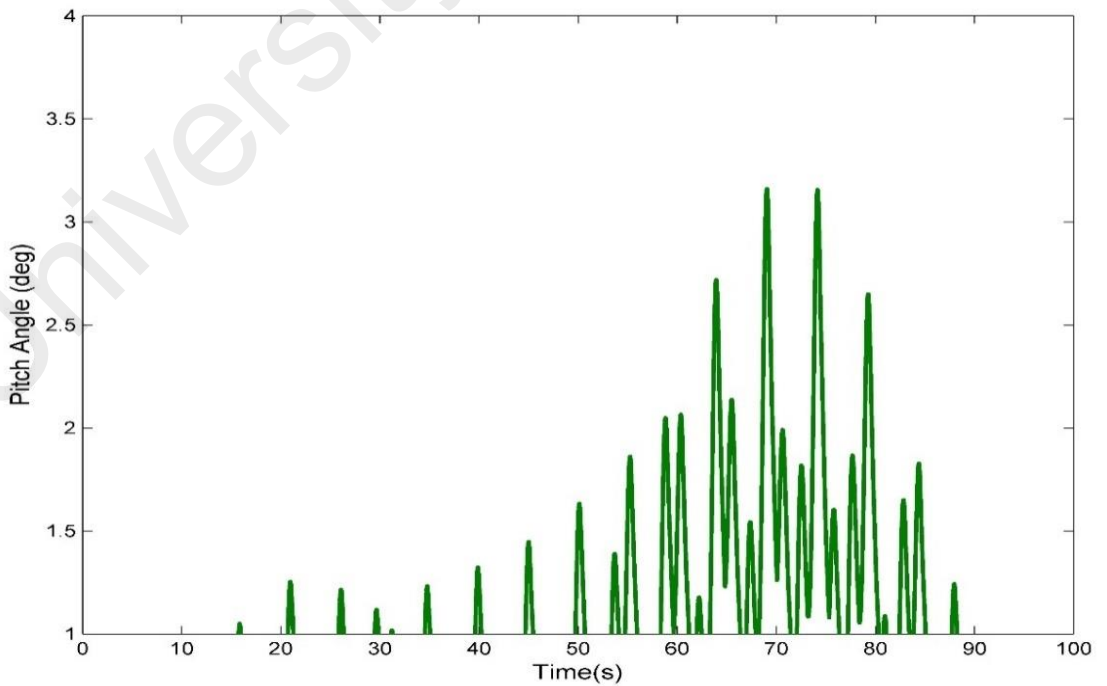
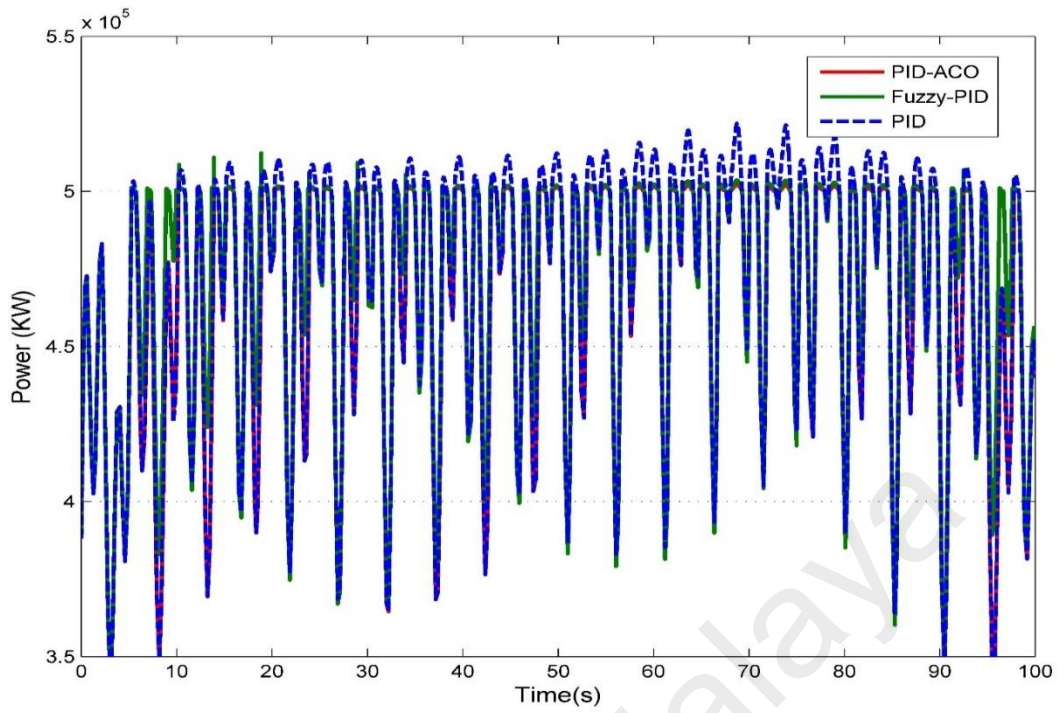
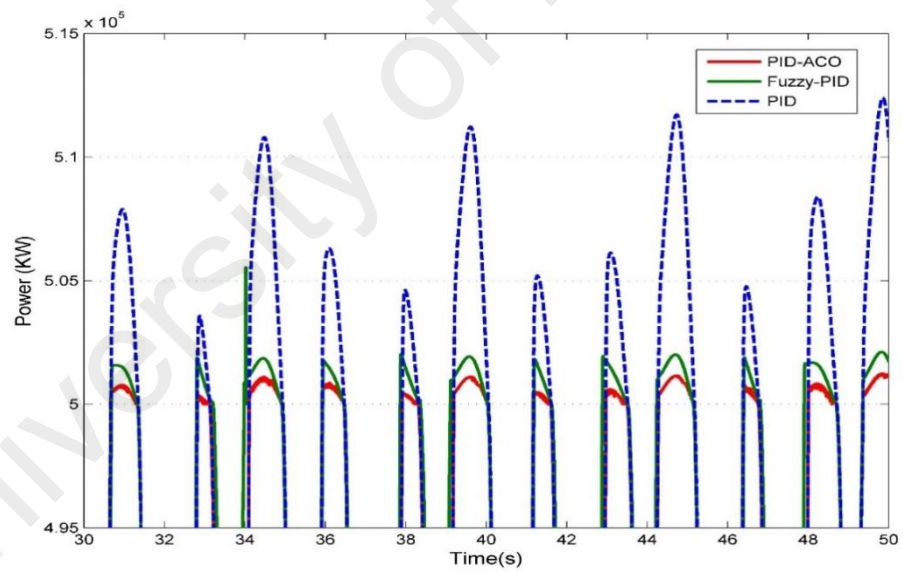


Figure 4-21: Pitch angle of wind turbine blade.



(a)



(b)

Figure 4-22: (a) Optimized wind turbine output power of PID-ACO in comparison with conventional PID and Fuzzy-PID; (b) zoomed figure region.

Table 4-11: K_p , K_i and K_d parameters of conventional PID with Fuzzy logic and ACO.

Controller gain	PID method	Fuzzy logic method	ACO method
K_p	-1.4e-05	-18.4e-01	-11.4e-01
K_i	-2.4e-05	-1.354e-16	-1.354e-11
K_d	6.254e-05	6.254e-05	6.254e-03

Table 4-12: Root mean square error (RMS) error of proposed PID-ACO to compare with PID and Fuzzy-PID.

Methods	Root mean square (RMS)
PID method	0.0044
Fuzzy-PID	0.0013
PID-ACO	0.00036

The comparison is done for the desired and controlled system by comparing the smoothing output wind power. The RMS error calculated between the desired to output power of WT with controllers. The RMS error calculations between three controlling methods are shown in Table 4-12. Based on the error calculation, it can be concluded that the PID-ACO controller is presented the lowest RMS error (0.00035) compared with Fuzzy-PID and conventional PID controller which are 0.0013 and 0.0044, respectively.

CHAPTER 5: CONCLUSIONS AND RECOMMENDATIONS

5.1 Conclusions

The objectives listed in this research have been achieved with promising results. Results depict the following findings of this research:

- I. The forecasting of wind speed plays an important role to produce wind energy and its one of the rapid growing renewable energy sources in the world. To improve and optimize wind power generation; an accurate forecasting of wind speed is important key. Specifically, long-term speed forecast can help us to enable a model predictive manage of wind turbines as well as real time expansion of wind farm operation. Overall, the WSF is important for engineering, number of operations, and financial reasons. In this investigation, accuracy of proposed NARNN and NARXNN with two different activation functions namely tansig and logsig for WSF is increased by using four statistical indicators such as MAE, MAPE, RMSE, and R^2 . It is observed that the most suitable model can be identified with the value of the indicators: MAE, MAPE, and RMSE. The average value of tansig-NARNN has given a promising result (MAE 0.0082, MAPE 11.39%, and RMSE 0.86) than that of the logsig-NARNN (MAE 0.0163, MAPE 15.36%, and RMSE 1.13). In addition, the average value of logsig-NARXNN (MAE 0.10, MAPE 15.40%, and RMSE 1.16) has provided a lower result than tansig NARXNN (MAE 0.06, MAPE 9.06%, and RMSE 0.53). The comparison between tansig and logsig functions were carried out in a standard benchmark by keeping the network settings (e.g. topology, number of epochs, number of hidden neurons and initial weights) fixed. Since tansig function provides better results in both neural network (NAR and NARX) at network settings with same input data, it

is therefore the suitable activation function compared to logsig function. The effectiveness of tansig-NARNN and tansig-NARXNN can be used for long-term wind speed forecasting based on error evolution.

The tansig and logsig methods are compared and investigated for improving the performance of the proposed neural networks. It is to be mentioned that the performance of the ANNs are heavily dependent on the selection of activation functions. Moreover, compared to other activation functions tansig can learn more effectively in the training process and was selected as the best non-linear activation function for both the hidden and output layers of the NAR and NARX neural network to predict nonlinear wind speed environments. This is considered to be one of the most significant findings from this study. Although, this study will help the practitioners to gain valuable knowledge about the ANN over the more widely used conceptual wind speed forecasting.

Apart from the control and optimization of wind farm operation, forecasting the behavior of the wind resources can provide valuable information for energy managers, energy policy makers, and electricity traders. Moreover, forecasting information can also help in times of operation, repair, and replacement of wind generators and conversion lines.

II. The blade design parameters have been obtained through optimization by nature-inspired algorithms (ABC, ACO and PSO) with the objective function to maximize the C_p . The prediction of C_p has also been carried out by using ANFIS approach to satisfy the optimized results. The optimization process is employed on non-linear maximization problem. ACO, PSO and ABC have successfully been implemented to find the C_p for wind turbine. The results have shown that ACO, PSO and ABC have the ability to find the best combination of five inputs HAWT blade parameters in order to get the

optimum value of C_p 0.520, 0.520 and 0.5295 respectively. It can be concluded that ABC algorithm has performed well to find the maximum value of power coefficient as compared to ACO and PSO as shown in Table 5-1. Separately, the maximum evaluation number and population size, a standard ACO has three more control parameters (the information heuristic factor α , the expectation heuristic factor β and pheromone evaporation factor ρ), and a basic PSO has three control parameters (cognitive and social factors, inertia weight). Also, limit values for the velocities t_{max} have a significant effect on the performance of PSO. The ABC algorithm has only one control parameter (limit) apart from Colony Size and Maximum Cycle Number. In the present work, we described an expression for determining the value of “limit” depending on population (colony size) and dimension of problem. Therefore, now ABC has only two common control parameters: maximum cycle number and colony size. Consequently, ABC is as simple and flexible as DE and PSO; and also employs less control parameters.

It can be observed that the predicted values of C_p for ABC = 0.5215, ACO = 0.5175 and PSO = 0.5135 are very close to the objective value (C_p), i.e. ABC – ANFIS = 0.5295, ACO – ANFIS = 0.52, and PSO – ANFIS = 0.52.

Therefore, it can be concluded that the presented prediction (ABC-ANFIS, ACO-ANFIS and PSO-ANFIS) are acceptable based on the RMSE and R^2 .

The values of R^2 are near to the 1 which are suitable for the better prediction results. Based on ANFIS results, the effectiveness of ABC algorithm shows better accuracy for both optimization and prediction in comparison to ACO and PSO algorithms. By using ANFIS, it can be used for more complex problem solution, such as accuracy, identification and prediction of power coefficient of HAWT blades. The results have been obtained by optimization and

prediction results and can be used for further design and prototype horizontal axis wind turbine modelling. The comparison with the similar literatures for the C_p also shows the consistent results which supports our present investigation.

Table 5-1: Optimization of power coefficient using ACO, PSO, and ABC.

Optimal Parameters	ACO	PSO	ABC
Power coefficient (C_p)	0.52	0.52	0.5295
Tip-speed ratio	6.0032	6.00	5.4479
Blade radius	4.3089	4.50	4.016
Lift to drag ratio	109.9935	110.00	109.4848
Solidity ratio	0.0539	0.45	0.3885
Chord length	0.0232	0.0010	0.193

III. The WT model is successfully modelled with conventional PID controller. controller is used to control output power of wind turbine generator by optimizing pitch angle. The PID controller is tuned by using ACO method and the response of the system is able to achieve the result near to the desired output. Comparisons between conventional trial and error tuning method of PID, Fuzzy logic turning method and ACO method show, ACO method is slightly better than Fuzzy-PID. The results of system with ACO tuned PID controller compared to system with PID controller, Fuzzy-PID showed significant reduction of output wind power fluctuating of wind turbine. The root mean square (RMS) error calculated between the desired power and the output power of WT with the PID-ACO is found to be 0.00036 which is smaller among the other two controllers namely Fuzzy-PID and conventional PID controller. The simulation results have shown that when the proposed PID-ACO control system is used, the quality as well as amplitude of output power from the WTG system is improved.

5.2 Recommendations

Based on the methodology and finding of the study, future recommendation can be made as follow:

- a. The NARNN and NARXNN have used in this study with two activation function (*tansig* and *logis*) for effective long-term WSF. So, it is recommended to apply other network types such as GRNN, RBFN and ANFIS which similar in NARNN and NARXNN approximation mechanism, should be investigate for long-term, short-term and very short-term WSF investigations in Malaysia.
- b. As more parameters input are likely to increase to provide more information related to output, it is recommended to develop hybrid algorithms (ACO-PSO, PSO-ABC or ABC-ACO) or combine AI and nature-inspired algorithms (ACO-ANFIS, ABC-ANFIS or PSO-ANFIS) to determine the optimal efficiency.
- c. This study used ACO algorithm to optimize PID controller parameters for pitch angle control of wind turbine. Therefore, future work will include hybrid algorithm for PID controller parameter optimization for pitch angle control and rotor speed control of wind turbine.

REFERENCES

- Abd-Allah, M., Said, A., & Ali, M. N. (2015). Mitigation of lightning hazards at the more sensitive points in wind farms using ant-colony optimization technique. *Int. Electric. Eng. J.(IEEJ)*, 6(4), 1856-1868.
- Ackermann, T., & Söder, L. (2000). Wind energy technology and current status: a review. *Renewable and Sustainable Energy Reviews*, 4(4), 315-374.
- Afroz, Z., Urme, T., Shafiullah, G., & Higgins, G. (2018). Real-time prediction model for indoor temperature in a commercial building. *Applied energy*, 231, 29-53.
- Ahmad, S., & Tahar, R. M. (2014). Selection of renewable energy sources for sustainable development of electricity generation system using analytic hierarchy process: A case of Malaysia. *Renewable Energy*, 63, 458-466.
- Akay, B., & Karaboga, D. (2012). A modified artificial bee colony algorithm for real-parameter optimization. *Information Sciences*, 192, 120-142.
- Al-allaf, O. N., & AbdAlKader, S. A. (2011). Nonlinear Autoregressive neural network for estimation soil temperature: a comparison of different optimization neural network algorithms. *UBICC J. Issue ICIT2011*, 6(4), 43-51.
- Al-Hmouz, A., Shen, J., Al-Hmouz, R., & Yan, J. (2012). Modeling and simulation of an Adaptive Neuro-Fuzzy Inference System (ANFIS) for mobile learning. *Learning Technologies, IEEE Transactions on*, 5(3), 226-237.
- Aladag, C. H. (2017). *Advances in Time Series Forecasting: Volume 2* (Vol. 2): Bentham Science Publishers.
- Albani, A., & Ibrahim, M. Z. (2017). Wind energy potential and power law indexes assessment for selected near-coastal sites in Malaysia. *Energies*, 10(3), 307.
- Amandola, C. A. M., & Gonzaga, D. P. (2007, October). Fuzzy-logic control system of a Variable-speed variable-pitch wind-turbine and a double-fed induction generator. In *Seventh International Conference on Intelligent Systems Design and Applications (ISDA 2007)* (pp. 252-257). IEEE.
- Arifujjaman, M. (2010, August). Modeling and optimization of power coefficient using 2^K factorial methodology. In *2010 IEEE Electrical Power & Energy Conference* (pp. 1-6). IEEE.
- Assareh, E., & Biglari, M. (2015). A novel approach to capture the maximum power from variable speed wind turbines using PI controller, RBF neural network and GSA evolutionary algorithm. *Renewable and Sustainable Energy Reviews*, 51, 1023-1037.
- Azad, H. B., Mekhilef, S., & Ganapathy, V. G. (2014). Long-term wind speed forecasting and general pattern recognition using neural networks. *IEEE Transactions on Sustainable Energy*, 5(2), 546-553.

- Bai, C. J., Chen, P. W., & Wang, W. C. (2016). Aerodynamic design and analysis of a 10-kW horizontal-axis wind turbine for Tainan, Taiwan. *Clean Technologies and Environmental Policy*, 18(4), 1151-1166.
- Bai, Q. (2010). Analysis of particle swarm optimization algorithm. *Computer and information science*, 3(1), 180.
- Beale, M. H., Hagan, M. T., & Demuth, H. B. (2010). Neural network toolbox 7. *User's Guide, MathWorks*.
- Bianchi, F. D., De Battista, H., & Mantz, R. J. (2006). *Wind turbine control systems: principles, modelling and gain scheduling design*: Springer Science & Business Media.
- Boroumand Jazi, G., Saidur, R., Rismanchi, B., & Mekhilef, S. (2012). A review on the relation between the energy and exergy efficiency analysis and the technical characteristic of the renewable energy systems. *Renewable and Sustainable Energy Reviews*, 16(5), 3131-3135.
- Burton, T., Jenkins, N., Sharpe, D., & Bossanyi, E. (2001). Aerodynamics of horizontal axis wind turbines. *Wind Energy Handbook, Second Edition*, 39-136.
- Cadenas, E., & Rivera, W. (2009). Short term wind speed forecasting in La Venta, Oaxaca, México, using artificial neural networks. *Renewable energy*, 34(1), 274-278.
- Cadenas, E., & Rivera, W. (2010). Wind speed forecasting in three different regions of Mexico, using a hybrid ARIMA-ANN model. *Renewable energy*, 35(12), 2732-2738.
- Cao, Q., Ewing, B. T., & Thompson, M. A. (2012). Forecasting wind speed with recurrent neural networks. *European Journal of Operational Research*, 221(1), 148-154.
- Chang, G., Lu, H., Chang, Y., & Lee, Y. (2017). An improved neural network-based approach for short-term wind speed and power forecast. *Renewable Energy*, 105, 301-311.
- Chen, Y. J., & Shiah, Y. (2016). Experiments on the performance of small horizontal axis wind turbine with passive pitch control by disk pulley. *Energies*, 9(5), 353.
- Chong, W., Gwani, M., Shamshirband, S., Muzammil, W., Tan, C., Fazlizan, A., Wong, K. (2016). Application of adaptive neuro-fuzzy methodology for performance investigation of a power-augmented vertical axis wind turbine. *Energy*, 102, 630-636.
- Chong, W. T., Poh, S. C., Fazlizan, A., Yip, S. Y., Koay, M. H., & Hew, W. P. (2013). Exhaust air energy recovery system for electrical power generation in future green cities. *International Journal of Precision Engineering and Manufacturing*, 14(6), 1029-1035.

- Chopade, M. R., & Malashe, A. Vertical axis wind turbines (VAWT) and computational fluid dynamics (CFD): A Review. *vol, 1*, 45-49.
- Civelek, Z., Çam, E., Lüy, M., & Mamur, H. (2016). Proportional–integral–derivative parameter optimisation of blade pitch controller in wind turbines by a new intelligent genetic algorithm. *IET Renewable Power Generation*, *10*(8), 1220-1228.
- Dai, J., Liu, D., Wen, L., & Long, X. (2016). Research on power coefficient of wind turbines based on SCADA data. *Renewable energy*, *86*, 206-215.
- Delgarm, N., Sajadi, B., & Delgarm, S. (2016). Multi-objective optimization of building energy performance and indoor thermal comfort: A new method using artificial bee colony (ABC). *Energy and Buildings*, *131*, 42-53.
- Derakhshan, S., Tavaziani, A., & Kasaeian, N. (2015). Numerical shape optimization of a wind turbine blades using artificial bee colony algorithm. *Journal of Energy Resources Technology*, *137*(5), 051210.
- Di Piazza, A., Di Piazza, M. C., & Vitale, G. (2016). Solar and wind forecasting by NARX neural networks. *Renewable Energy and Environmental Sustainability*, *1*, 39.
- Dorigo, M., Birattari, M., & Stützle, T. (2006). Ant colony optimization. *Computational Intelligence Magazine, IEEE*, *1*(4), 28-39.
- Dorigo, M., & Gambardella, L. M. (1997a). Ant colonies for the travelling salesman problem. *BioSystems*, *43*(2), 73-81.
- Dorigo, M., & Gambardella, L. M. (1997b). Ant colony system: a cooperative learning approach to the traveling salesman problem. *Evolutionary Computation, IEEE Transactions on*, *1*(1), 53-66.
- Dou, Z. L., Cheng, M. Z., Ling, Z. B., & Cai, X. (2010, June). An adjustable pitch control system in a large wind turbine based on a fuzzy-PID controller. In *SPEEDAM 2010* (pp. 391-395). IEEE.
- Dufo-López, R., Bernal-Agustín, J. L., & Contreras, J. (2007). Optimization of control strategies for stand-alone renewable energy systems with hydrogen storage. *Renewable energy*, *32*(7), 1102-1126.
- Duong, M. Q., Grimaccia, F., Leva, S., Mussetta, M., & Ogliari, E. (2014). Pitch angle control using hybrid controller for all operating regions of SCIG wind turbine system. *Renewable Energy*, *70*, 197-203.
- Eberhart, R. C., & Kennedy, J. (1995). A new optimizer using particle swarm theory, paper presented at Sixth International Symposium on Micromachine and Human Science, Inst. of Electr. and Electron. *Eng., Nagoya, Japan*.
- Eberhart, R. C., & Shi, Y. (2000, July). Comparing inertia weights and constriction factors in particle swarm optimization. In *Proceedings of the 2000 congress on evolutionary computation. CEC00 (Cat. No. 00TH8512)* (Vol. 1, pp. 84-88). IEEE.

- Ebrahim, E. A. (2014). Artificial bee colony-based design of optimal on-line self-tuning PID-controller fed AC drives. *Int J Eng Res*, 3(12), 807-811.
- Ekelund, T. (1994, August). Speed control of wind turbines in the stall region. In *Proceedings of the third IEEE conference on control applications* (Vol. 1, pp. 227-232).
- Eltamaly, A. M., & Farh, H. M. (2013). Maximum power extraction from wind energy system based on fuzzy logic control. *Electric Power Systems Research*, 97, 144-150.
- Eriksson, S., Bernhoff, H., & Leijon, M. (2008). Evaluation of different turbine concepts for wind power. *Renewable and Sustainable Energy Reviews*, 12(5), 1419-1434.
- Eroğlu, Y., & Seçkiner, S. U. (2012). Design of wind farm layout using ant colony algorithm. *Renewable energy*, 44, 53-62.
- Foley, A. M., Leahy, P. G., Marvuglia, A., & McKeogh, E. J. (2012). Current methods and advances in forecasting of wind power generation. *Renewable energy*, 37(1), 1-8.
- Fuchs, I., & Gjengedal, T. (2011, September). Ant colony optimization and analysis of time step resolution in transmission expansion computations for wind power integration. In *2011 16th International Conference on Intelligent System Applications to Power Systems* (pp. 1-6). IEEE.
- Gaing, Z.-L. (2004). A particle swarm optimization approach for optimum design of PID controller in AVR system. *IEEE Transactions on Energy Conversion*, 19(2), 384-391.
- Galdi, V., Piccolo, A., & Siano, P. (2008). Designing an adaptive fuzzy controller for maximum wind energy extraction. *IEEE Transactions on Energy Conversion*, 23(2), 559-569.
- Gao, R., & Gao, Z. (2016). Pitch control for wind turbine systems using optimization, estimation and compensation. *Renewable energy*, 91, 501-515.
- Giguere, P., & Selig, M. (1999). Design of a tapered and twisted blade for the NREL combined experiment rotor. *NREL/SR*, 500, 26173.
- Giguere, P., & Selig, M. S. (1997). Low Reynolds number airfoils for small horizontal axis wind turbines. *Wind Engineering*, 21(6), 367-380.
- Gomes, G. S. d. S., Ludermir, T. B., & Lima, L. M. (2011). Comparison of new activation functions in neural network for forecasting financial time series. *Neural Computing and Applications*, 20(3), 417-439.
- Guo, Z.-h., Wu, J., Lu, H.-y., & Wang, J.-z. (2011). A case study on a hybrid wind speed forecasting method using BP neural network. *Knowledge-based systems*, 24(7), 1048-1056.

- Guo, Z., Zhao, W., Lu, H., & Wang, J. (2012). Multi-step forecasting for wind speed using a modified EMD-based artificial neural network model. *Renewable energy*, 37(1), 241-249.
- GWEC. (2013). Global Wind Energy Council. Global Wind Report 2013 - Annual market update.
- Habbi, H., Boudouaoui, Y., Karaboga, D., & Ozturk, C. (2015). Self-generated fuzzy systems design using artificial bee colony optimization. *Information Sciences*, 295, 145-159.
- Hashim, H., & Ho, W. S. (2011). Renewable energy policies and initiatives for a sustainable energy future in Malaysia. *Renewable and sustainable energy reviews*, 15(9), 4780-4787.
- He, Q., & Han, C. (2007). Satellite constellation design with adaptively continuous ant system algorithm. *Chinese Journal of Aeronautics*, 20(4), 297-303.
- Huang, J., & McElroy, M. B. (2015). A 32-year perspective on the origin of wind energy in a warming climate. *Renewable Energy*, 77, 482-492.
- Jang, J.-S. R. (1993). ANFIS: adaptive-network-based fuzzy inference system. *Systems, Man and Cybernetics, IEEE Transactions on*, 23(3), 665-685.
- Jiang, P., Wang, Y., & Wang, J. (2017). Short-term wind speed forecasting using a hybrid model. *Energy*, 119, 561-577.
- Jovanovic, R., Tuba, M., & Voß, S. (2016). An ant colony optimization algorithm for partitioning graphs with supply and demand. *Applied Soft Computing*, 41, 317-330.
- Julai, S., Tokhi, M. O., & Salleh, S. M. (2009, November). Active vibration control of a flexible plate structure using ant system algorithm. In *2009 Third UKSim European Symposium on Computer Modeling and Simulation* (pp. 37-42). IEEE.
- Jureczko, M., Pawlak, M., & Mężyk, A. (2005). Optimisation of wind turbine blades. *Journal of materials processing technology*, 167(2), 463-471.
- Karaboga, D. (2005). *An idea based on honey bee swarm for numerical optimization*. Technical report-tr06, Erciyes university, engineering faculty, computer engineering department. (Vol. 200, pp. 1-10).
- Karaboga, D., & Akay, B. (2011). A modified artificial bee colony (ABC) algorithm for constrained optimization problems. *Applied Soft Computing*, 11(3), 3021-3031.
- Karaboga, D., & Basturk, B. (2007). A powerful and efficient algorithm for numerical function optimization: artificial bee colony (ABC) algorithm. *Journal of global optimization*, 39(3), 459-471.
- Karlik, B., & Olgac, A. V. (2011). Performance analysis of various activation functions in generalized MLP architectures of neural networks. *International Journal of Artificial Intelligence and Expert Systems*, 1(4), 111-122.

- Eberhart, R. C., Shi, Y., & Kennedy, J. (2001). *Swarm Intelligence (Morgan Kaufmann series in evolutionary computation)*. Morgan Kaufmann Publishers.
- Khalfallah, M. G., & Koliub, A. M. (2007). Suggestions for improving wind turbines power curves. *Desalination*, 209(1), 221-229.
- Khor, C. S., & Lalchand, G. (2014). A review on sustainable power generation in Malaysia to 2030: Historical perspective, current assessment, and future strategies. *Renewable and sustainable energy reviews*, 29, 952-960.
- Kim, B., Kim, W., Lee, S., Bae, S., & Lee, Y. (2013). Development and verification of a performance based optimal design software for wind turbine blades. *Renewable energy*, 54, 166-172.
- Kıran, M. S., Özceylan, E., Gündüz, M., & Paksoy, T. (2012). A novel hybrid approach based on particle swarm optimization and ant colony algorithm to forecast energy demand of Turkey. *Energy Conversion and Management*, 53(1), 75-83.
- Kong, Y., Wang, Z., & Yuan, H. (2006). A new fuzzy sliding-mode control for MW variable speed-variable pitch wind turbine. 256-256.
- Lanzafame, R., & Messina, M. (2010). Horizontal axis wind turbine working at maximum power coefficient continuously. *Renewable energy*, 35(1), 301-306.
- Leithead, W., & Connor, B. (2000). Control of variable speed wind turbines: design task. *International Journal of Control*, 73(13), 1189-1212.
- Li, G., & Shi, J. (2010). On comparing three artificial neural networks for wind speed forecasting. *Applied Energy*, 87(7), 2313-2320.
- Lin, T., Horne, B. G., Tino, P., & Giles, C. L. (1996). Learning long-term dependencies in NARX recurrent neural networks. *IEEE Transactions on Neural Networks*, 7(6), 1329-1338.
- Liu, D., Niu, D., Wang, H., & Fan, L. (2014). Short-term wind speed forecasting using wavelet transform and support vector machines optimized by genetic algorithm. *Renewable energy*, 62, 592-597.
- Liu, H., Chen, C., Tian, H.-q., & Li, Y.-f. (2012). A hybrid model for wind speed prediction using empirical mode decomposition and artificial neural networks. *Renewable energy*, 48, 545-556.
- López, M., Valero, S., Senabre, C., Aparicio, J., & Gabaldon, A. (2012). Application of SOM neural networks to short-term load forecasting: The Spanish electricity market case study. *Electric Power Systems Research*, 91, 18-27.
- Lydia, M., Kumar, S. S., Selvakumar, A. I., & Kumar, G. E. P. (2016). Linear and non-linear autoregressive models for short-term wind speed forecasting. *Energy Conversion and Management*, 112, 115-124.

- Madsen, H., Pinson, P., Kariniotakis, G., Nielsen, H. A., & Nielsen, T. S. (2005). Standardizing the performance evaluation of short-term wind power prediction models. *Wind Engineering*, 29(6), 475-489.
- Maleki, A., Ameri, M., & Keynia, F. (2015). Scrutiny of multifarious particle swarm optimization for finding the optimal size of a PV/wind/battery hybrid system. *Renewable energy*, 80, 552-563.
- Mamdani, E. H., & Assilian, S. (1975). An experiment in linguistic synthesis with a fuzzy logic controller. *International journal of man-machine studies*, 7(1), 1-13.
- Manwell, J. F., McGowan, J. G., & Rogers, A. L. (2010). *Wind energy explained: theory, design and application*: John Wiley & Sons.
- Marques, J., Pinheiro, H., Gründling, H., Pinheiro, J., & Hey, H. (2003). A survey on variable-speed wind turbine system. *network*, 24, 26.
- Masseran, N., Razali, A. M., Ibrahim, K., & Zin, W. W. (2012). Evaluating the wind speed persistence for several wind stations in Peninsular Malaysia. *Energy*, 37(1), 649-656.
- MathWorks®. (2016). Choose a Multilayer Neural Network Training Function. Retrieved October 25, 2016 from <https://www.mathworks.com/help/nnet/ug/choose-a-multilayer-neural-network-training-function.html>.
- Men, Z., Yee, E., Lien, F.-S., Wen, D., & Chen, Y. (2016). Short-term wind speed and power forecasting using an ensemble of mixture density neural networks. *Renewable Energy*, 87, 203-211.
- Mohammad, S. (2014, November). The renewable energy status in Malaysia. In *Proceedings of the Universiti Malaysia Terengganu Eastern Corridor Renewable Energy Symposium, Kuala Terengganu, Terengganu, Malaysia* (Vol. 3).
- Musa, R. M., Taha, Z., Majeed, A. P. A., & Abdullah, M. R. (2019). Psychological Variables in Ascertaining Potential Archers *Machine Learning in Sports* (pp. 21-27): Springer.
- Mustafar, M. F., Musirin, I., Kalil, M. R., & Idris, M. K. (2007). Ant colony optimization (ACO) based technique for voltage control and loss minimization using transformer tap setting. In *2007 5th Student Conference on Research and Development*(pp. 1-6). IEEE.
- Nyanteh, Y. D., Srivastava, S. K., Edrington, C. S., & Cartes, D. A. (2013). Application of artificial intelligence to stator winding fault diagnosis in Permanent Magnet Synchronous Machines. *Electric Power Systems Research*, 103, 201-213.
- Ochieng, R. M., Onyango, F. N., & Oduor, A. O. (2010). Physical Formulation of the Expression of Wind Power. *International Journal of Energy, Environment and Economics*, 18(1), 107.

- Oghafy, V., & Nikkhajoei, H. (2008, July). Maximum power extraction for a wind-turbine generator with no wind speed sensor. In *2008 IEEE Power and Energy Society General Meeting-Conversion and Delivery of Electrical Energy in the 21st Century* (pp. 1-6). IEEE.
- Oh, T. H., Pang, S. Y., & Chua, S. C. (2010). Energy policy and alternative energy in Malaysia: issues and challenges for sustainable growth. *Renewable and Sustainable Energy Reviews, 14*(4), 1241-1252.
- Perng, J. W., Chen, G. Y., & Hsieh, S. C. (2014). Optimal PID controller design based on PSO-RBFNN for wind turbine systems. *Energies, 7*(1), 191-209.
- Petković, D., Čojbašić, Ž., & Nikolić, V. (2013). Adaptive neuro-fuzzy approach for wind turbine power coefficient estimation. *Renewable and Sustainable Energy Reviews, 28*, 191-195.
- Petković, D., Čojbašić, Ž., Nikolić, V., Shamshirband, S., Kiah, M. L. M., Anuar, N. B., & Wahab, A. W. A. (2014). Adaptive neuro-fuzzy maximal power extraction of wind turbine with continuously variable transmission. *Energy, 64*, 868-874.
- Petković, D., & Shamshirband, S. (2015). Soft methodology selection of wind turbine parameters to large affect wind energy conversion. *International Journal of Electrical Power & Energy Systems, 69*, 98-103.
- Ponta, F., Seminara, J., & Otero, A. (2007). On the aerodynamics of variable-geometry oval-trajectory Darrieus wind turbines. *Renewable energy, 32*(1), 35-56.
- Pookpant, S., & Ongsakul, W. (2013). Optimal placement of wind turbines within wind farm using binary particle swarm optimization with time-varying acceleration coefficients. *Renewable energy, 55*, 266-276.
- Qi, Y., & Meng, Q. (2012). The application of fuzzy PID control in pitch wind turbine. *Energy Procedia, 16*, 1635-1641.
- Rajakumar, S., & Ravindran, D. (2012). Iterative approach for optimising coefficient of power, coefficient of lift and drag of wind turbine rotor. *Renewable energy, 38*(1), 83-93.
- Rezaeianzadeh, M., Stein, A., Tabari, H., Abghari, H., Jalalkamali, N., Hosseinipour, E., & Singh, V. (2013). Assessment of a conceptual hydrological model and artificial neural networks for daily outflows forecasting. *International journal of environmental science and technology, 10*(6), 1181-1192.
- Ruiz, L. G. B., Cuéllar, M. P., Calvo-Flores, M. D., & Jiménez, M. D. C. P. (2016). An application of non-linear autoregressive neural networks to predict energy consumption in public buildings. *Energies, 9*(9), 684.
- Safaei, A., Vahidi, B., Askarian-Abyaneh, H., Azad-Farsani, E., & Ahadi, S. (2016). A two step optimization algorithm for wind turbine generator placement considering maximum allowable capacity. *Renewable energy, 92*, 75-82.

- Santamaría-Bonfil, G., Reyes-Ballesteros, A., & Gershenson, C. (2016). Wind speed forecasting for wind farms: A method based on support vector regression. *Renewable energy*, 85, 790-809.
- Schubel, P. J., & Crossley, R. J. (2012). Wind turbine blade design. *Energies*, 5(9), 3425-3449.
- Sedaghat, A., & Mirhosseini, M. (2012). Aerodynamic design of a 300kW horizontal axis wind turbine for province of Semnan. *Energy Conversion and Management*, 63, 87-94.
- Selig, M. S., & Coverstone-Carroll, V. L. (1996). Application of a genetic algorithm to wind turbine design. *Journal of Energy Resources Technology*, 118(1), 22-28.
- Shafie, S., Mahlia, T., Masjuki, H., & Andriyana, A. (2011). Current energy usage and sustainable energy in Malaysia: a review. *Renewable and Sustainable Energy Reviews*, 15(9), 4370-4377.
- Shafiullah, G. (2016). Hybrid renewable energy integration (HREI) system for subtropical climate in Central Queensland, Australia. *Renewable Energy*, 96, 1034-1053.
- Shafiullah, G., Oo, A. M., Ali, A. S., & Wolfs, P. (2013). Potential challenges of integrating large-scale wind energy into the power grid—A review. *Renewable and sustainable energy reviews*, 20, 306-321.
- Shaked, U., & Soroka, E. (1985). On the stability robustness of the continuous-time LQG optimal control. *IEEE transactions on automatic control*, 30(10), 1039-1043.
- Shamshirband, S., Petković, D., Saboohi, H., Anuar, N. B., Inayat, I., Akib, S., . . . Gani, A. (2014). Wind turbine power coefficient estimation by soft computing methodologies: comparative study. *Energy Conversion and Management*, 81, 520-526.
- Sharafi, M., & ELMekkawy, T. Y. (2014). Multi-objective optimal design of hybrid renewable energy systems using PSO-simulation based approach. *Renewable energy*, 68, 67-79.
- Shen, Q., Jiang, J.-H., Tao, J.-c., Shen, G.-l., & Yu, R.-Q. (2005). Modified ant colony optimization algorithm for variable selection in QSAR modeling: QSAR studies of cyclooxygenase inhibitors. *Journal of chemical information and modeling*, 45(4), 1024-1029.
- Shi, Y., & Eberhart, R. (1998, May). A modified particle swarm optimizer. In *1998 IEEE international conference on evolutionary computation proceedings. IEEE world congress on computational intelligence (Cat. No. 98TH8360)* (pp. 69-73). IEEE.
- Shi, Y., & Eberhart, R. C. (1998, March). Parameter selection in particle swarm optimization. In *International conference on evolutionary programming* (pp. 591-600). Springer, Berlin, Heidelberg.

- Singh, M., & Chandra, A. (2011). Application of adaptive network-based fuzzy inference system for sensorless control of PMSG-based wind turbine with nonlinear-load-compensation capabilities. *Power Electronics, IEEE Transactions on*, 26(1), 165-175.
- Singh, S., & Kaushik, S. C. (2016). Optimal sizing of grid integrated hybrid PV-biomass energy system using artificial bee colony algorithm. *IET Renewable Power Generation*, 10(5), 642-650.
- Socha, K., & Dorigo, M. (2008). Ant colony optimization for continuous domains. *European journal of operational research*, 185(3), 1155-1173.
- Somers, D. M., & Maughmer, M. D. (2003). Theoretical aerodynamic analyses of six airfoils for use on small wind turbines. *National Renewable Energy Laboratory, Golden, CO, Report No. NREL/SR-500-33295*.
- Song, J., Romero, C. E., Yao, Z., & He, B. (2016). Improved artificial bee colony-based optimization of boiler combustion considering NOX emissions, heat rate and fly ash recycling for on-line applications. *Fuel*, 172, 20-28.
- Song, X., Gu, H., Tang, L., Zhao, S., Zhang, X., Li, L., & Huang, J. (2015). Application of artificial bee colony algorithm on surface wave data. *Computers & Geosciences*, 83, 219-230.
- Sopian, K., Othman, M. H., & Wirsat, A. (1995). The wind energy potential of Malaysia. *Renewable energy*, 6(8), 1005-1016.
- Sovacool, B. K., & Drupady, I. M. (2011). Examining the small renewable energy power (SREP) program in Malaysia. *Energy policy*, 39(11), 7244-7256.
- Tangler, J. L., & Somers, D. M. (1995). *NREL airfoil families for HAWTs* (No. NREL/TP-442-7109). National Renewable Energy Lab., Golden, CO (United States).
- Tasnim, S., Rahman, A., Shafiullah, G. M., Oo, A. M. T., & Stojcevski, A. (2014, December). A time series ensemble method to predict wind power. In *2014 IEEE symposium on computational intelligence applications in smart grid (CIASG)*(pp. 1-5). IEEE.
- Tenaga Nasional Berhad. (2014). *Tenaga Nasional Berhad (TNB) Annual Report 2011*.
- Thomas, B., & Urquhart, J. (1996). Wind energy for the 1990s and beyond. *Journal of Energy Conversion and Management*, 37(12), 1741.
- Tong, C. W. (2006). The design and testing of a wind turbine for electrical power generation in Malaysian wind conditions. *Universiti Teknologi Malaysia*.
- Tran, D.-H., Sareni, B., Roboam, X., & Espanet, C. (2010). Integrated optimal design of a passive wind turbine system: an experimental validation. *IEEE Transactions on Sustainable Energy*, 1(1), 48-56.

- Vafaeipour, M., Rahbari, O., Rosen, M. A., Fazelpour, F., & Ansarirad, P. (2010). An artificial neural network approach to predict wind velocity time-series in Tehran. *nature*, 2005, 1.
- Vuković, N., Petrović, M., & Miljković, Z. (2018). A comprehensive experimental evaluation of orthogonal polynomial expanded random vector functional link neural networks for regression. *Applied Soft Computing*, 70, 1083-1096.
- Vafaeipour, M., Rahbari, O., Rosen, M. A., Fazelpour, F., & Ansarirad, P. (2010). An artificial neural network approach to predict wind velocity time-series in Tehran. *nature*, 2005, 1.
- Vuković, N., Petrović, M., & Miljković, Z. (2018). A comprehensive experimental evaluation of orthogonal polynomial expanded random vector functional link neural networks for regression. *Applied Soft Computing*, 70, 1083-1096.
- Wan, C., Wang, J., Yang, G., & Zhang, X. (2010, June). Optimal micro-siting of wind farms by particle swarm optimization. In *International Conference in Swarm Intelligence* (pp. 198-205). Springer, Berlin, Heidelberg.
- Wang, Y., & Xie, J. (2002). An Adaptive Ant Colony Optimization Algorithm and Simulation [J]. *Acta Simulata Systematica Sinica*, 1.
- Yin, X. X., Lin, Y. G., Li, W., Gu, Y. J., Wang, X. J., & Lei, P. F. (2015). Design, modeling and implementation of a novel pitch angle control system for wind turbine. *Renewable Energy*, 81, 599-608.
- Younsi, R., El-Batanony, I., Tritsch, J.-B., Naji, H., & Landjerit, B. (2001). Dynamic study of a wind turbine blade with horizontal axis. *European Journal of Mechanics-A/Solids*, 20(2), 241-252.
- Zadeh, M. R., Amin, S., Khalili, D., & Singh, V. P. (2010). Daily outflow prediction by multi layer perceptron with logistic sigmoid and tangent sigmoid activation functions. *Water resources management*, 24(11), 2673-2688.
- Zhang, L., Li, H., Chunliang, E., Li, J., & Xu, H. (2008, April). Pitch control of large scale wind turbine based on fuzzy-PD method. In *2008 Third International Conference on Electric Utility Deregulation and Restructuring and Power Technologies* (pp. 2447-2452). IEEE.
- Zhao, W., Wei, Y.-M., & Su, Z. (2016). One day ahead wind speed forecasting: A resampling-based approach. *Applied Energy*, 178, 886-901.
- Zheng, Z., Chen, Y., Huo, M., & Zhao, B. (2011). An overview: the development of prediction technology of wind and photovoltaic power generation. *Energy Procedia*, 12, 601-608.
- Zhu, J., Cai, X., & Gu, R. (2016). Aerodynamic and Structural Integrated Optimization Design of Horizontal-Axis Wind Turbine Blades. *Energies*, 9(2), 66.

LIST OF PUBLICATIONS

a) Scopus-Index Publication

- I. **MR Sarkar**, S Julai, CW Tong, OZ Chao, and M Rahman, *Mathematical Modelling and Simulation of Induction Generator Based Wind Turbine in Matlab/Simulink*. ARPN Journal of Engineering and Applied Sciences, VOL. 10, NO 22, Dec, **2015** ISSN 1819-6608. Published (Scopus-Cited Journal)

b) ISI-Index Publication

- I. **R. Sarkar**, S. Julai, S. Hossain, W. T. Chong, and M. Rahman, "A Comparative Study of Activation Functions of NAR and NARX Neural Network for Long-Term Wind Speed Forecasting in Malaysia," *Mathematical Problems in Engineering*, vol. 2019, p. 14, **2019**. (ISI-Indexed) <https://doi.org/10.1155/2019/6403081> **(Published)**
- II. **Sarkar, M.R.;** Julai, S.; Wen Tong, C.; Toha, S.F. ‘Effectiveness of Nature-Inspired Algorithms using ANFIS for Blade Design Optimization and Wind Turbine Efficiency. ‘*Symmetry* **2019**, 11, 456. (ISI-Indexed) <https://doi.org/10.3390/sym11040456>. **(Published)**
- III. **Md. Rasel Sarkar**, Sabariah Julai, Chong Wen Tong and Mahmudur Rahman, “Design of Optimal Pitch Angle Control System for Stable Wind Turbine Power Using ACO-PID Controller”. **Under Review** (ISI-Cited Journal)